Development of a Test Bench to Study Self-Loosening of Bolted Joints

by

Amir HASRAK

THESIS PRESENTED TO ÉCOLE DE TECHNOLOGIE SUPÉRIEURE
IN PARTIAL FULFILLMENT FOR A MASTER'S DEGREE
WITH THESIS IN MECHANICAL ENGINEERING
M.A.Sc.

MONTREAL, SEPTEMBER 25 2018

ÉCOLE DE TECHNOLOGIE SUPÉRIEURE
UNIVERSITÉ DU QUÉBEC

BOARD OF EXAMINERS

THIS THESIS HAS BEEN EVALUATED

BY THE FOLLOWING BOARD OF EXAMINERS

Prof. Hakim Bouzid, Thesis Supervisor
Mechanical Engineering Department at École de Technologie Supérieure

Prof. Anh Dung Ngo, President of the Board of Examiners
Mechanical Engineering Department at École de Technologie Supérieure

Prof. Mohammad Jahazi, Member of the jury
Mechanical Engineering Department at École de Technologie Supérieure

THIS THESIS WAS PRENSENTED AND DEFENDED

IN THE PRESENCE OF A BOARD OF EXAMINERS AND PUBLIC

SEPTEMBER 7th, 2018

AT ÉCOLE DE TECHNOLOGIE SUPÉRIEURE

ACKNOWLEDGMENT

DÉVELOPPEMENT D'UN BANC D'ESSAI POUR ÉTUDIER L'AUTO-DESSERAGE DES JOINTS BOULONNÉS

Amir HASRAK

RÉSUMÉ

Les méthodes courantes pour étudier l'auto-desserrage des assemblages boulonnés sont la théorie, les simulations numériques et l'expérimentation. Les méthodes théorique et numérique, utilisant principalement la méthode des éléments finis, sont utilisées pour comprendre, évaluer et quantifier ce phénomène, tandis que la méthode expérimentale est surtout utilisée à des fins de validation et de vérification.

La plupart des études expérimentales précédentes sur l'auto-desserrage des assemblages boulonnés ont été réalisées avec une machine d'essai connue sous le nom de Machine Junker qui utilise une cellule de charge conventionnelle et un capteur de rotation qui modifient la géométrie de l'assemblage et les conditions de charge. L'insertion d'un capteur de force ou d'un capteur de rotation modifie la longueur de serrage et la rigidité de l'assemblage, qui sont tous deux des facteurs importants pour l'intégrité du système et le comportement d'auto-desserrage. La non-utilisation de ces capteurs peut grandement simplifier l'étude des assemblages boulonnés et des principaux paramètres. Il est important de ne pas modifier la longueur de serrage et la rigidité de l'assemblage lorsqu'elles sont le sujet principal de l'étude. Dans la conception du banc d'essai actuel, la géométrie de l'assemblage boulonné est exactement la même que dans l'application réelle et dans l'analyse par éléments finis utilisée pour la validation. Le banc d'essai conçu offre la possibilité d'étudier des assemblages boulonnés de différentes épaisseurs de pièces de serrage en combinaison avec différentes pré-charges et déplacements latéraux imposés. Un système de collecte de données numériques est mis en place pour fournir la possibilité de mesurer et d'enregistrer la charge axiale du boulon (précharge), le déplacement latéral imposé et la force latérale résultante, la rotation relative de la vis par rapport à l'écrou, la température, le temps et le nombre de cycles.

Dans un premier temps, un dispositif de serrage a été conçu pour recevoir l'assemblage boulonné et son instrumentation. Une articulation a été fixée à la plaque inférieure pour minimiser les forces et les moments de flexion indésirables. Une analyse par éléments finis de la nouvelle conception a été effectuée pour s'assurer de l'intégrité structurelle des éléments permettant l'assemblage et l'installation des plaques, qui sont le point le plus faible du mécanisme. Les capacités maximales de toutes les autres pièces mécaniques standards sont définies par leurs fabricants respectifs et sont comparées aux résultats de l'analyse par éléments finis.

Dans la deuxième étape, les engrenages d'entraînement du système bielle-manivelle ont été modifiés afin d'améliorer leurs performances pour s'adapter aux nouvelles connexions. Dans la troisième étape, deux ensembles de pièces ont été conçus pour recevoir le capteur de déplacement latéral et le capteur de rotation. Les deux ensembles ont été conçus pour s'adapter à différents contextes d'essai en utilisant des calles simples et peu coûteux. Un compteur magnétique numérique est ajouté au système pour enregistrer le nombre de cycles.

VIII

Un thermocouple a également été envisagé pour mesurer la température des plaques dans le cadre d'études ultérieures. Comme dernière étape, tous les capteurs ont été connecté à un ordinateur par l'intermédiaire d'une carte d'acquisition et de control de données et une carte PCB. Le système de collecte de données est visualisé et contrôlé par le logiciel LabView.

Pour des fins de validation et des essais préliminaires, une analyse complète 3D par éléments finis de l'assemblage a été réalisée et les résultats ont été comparés à des essais expérimentaux. Dans cette étape, un assemble composé de deux plaques d'acier (d'une épaisseur de 10 mm), de deux rondelles d'acier, d'un boulon et d'un écrou a été évalué. Les résultats montrent que la machine développée est fonctionnelle et peut être utilisée pour la prochaine étape de la recherche.

Mots-Clés: Auto-desserrage, analyse par éléments finis, pré-charges, force latérale, déplacements latérale.

DEVELOPMENT OF A TEST BENCH TO STUDY
SELF-LOOSENING OF BOLTED JOINTS

Amir Hasrak

ABSTRACT

Common methodologies to study self-loosening of bolted joint are analytical, finite element, and experimental. Analytical and finite element methods are used to find, evaluate, and quantify this phenomenon while the experimental method is mostly used for validation and verification purposes. Most of the previous experimental studies on self-loosening of bolted joints have been performed with a test machine known as Junker Machine which uses a conventional load cell and a rotation sensor which change the geometry of the joint and loading condition. Inserting a load cell or a rotation sensor changes the clamping length and joint stiffness, which both are important factors in joint integrity and self-loosening behavior. Their non-use of load cell can greatly simplify the study of bolted joints and the investigation of other parameters. It is important to not alter the clamping length and stiffness of the joint when they are the main subject of study. In the design of the current test rig, the geometry of the bolted joint is maintained exactly the same as in the real application and in the finite element analysis used for validation. The designed test bench provides the possibility of studying bolted joints with different thicknesses of clamping parts in combination with different preloads and lateral imposed displacements. A digital data gathering system is put in place to provide the possibility of measuring and recording of bolt axial load (preload), imposed lateral displacement and resulting force, relevant rotation of the bolt and nut, temperature, time and number of cycles.

In the first step, a clamping device was designed to accommodate the test plate clamping joints and its instrumentation. A universal joint has been attached to the lower plate to minimize undesirable bending force and moments. A finite element analysis of the new design has been carried out to ensure the integrity of the plate attachments which are the weakest point in the mechanism. The maximum capacity of all other standard mechanical parts is defined by their respective manufacturers and are compared with results from the analysis.

In the second step, the driving gears and crank system have been repaired and modified to improve their performance to adapt with the new connections.

In the third step, two mounting assemblies have been designed to hold the lateral displacement sensor and the rotation sensor. Both assemblies have been designed to accommodate different test settings using simple and low cost inserts. A digital magnetic counter is added to the system to record the number of cycles. A thermocouple has also been considered to measure temperature of plates in further studies.

As the last step, all sensors have been connected and synchronized to a computer via a PCB. Data gathering system is visualized and controlled by LabView software.

As the first phase of the project, a full 3D FE analysis of the joint has been performed and results have been compared to experimental test. In this step, a clamping joint consisting of

X

two steel plates (with 10 mm thickness), two steel washers, a bolt and a nut has been evaluated.
The results show that the developed machine is functional and can be used for the next step of the research.

TABLE OF CONTENTS

Page

LIST OF TABLES

LIST OF FIGURES

Page

LIST OF ABREVIATIONS

3D	Three Dimensional
ANSI	American National Standards Institute
APDL	ANSYS Parametric Design Language
ASME	American Society of Mechanical Engineers
B.C.	Boundary Condition
CNC	Computer Numerical Control
CPU	Central Processing Unit
Deg.	Degree
ETS	École de Technologie Supérieure
FEA	Finite element analysis
GHz	Giga Hertz
HPC	Hi-performance calculation
ID	Identification
IDLH	Immediately Dangerous to Life and Health
LVDT	Linear Variable Differential Transformer
MAZ	Mettre à Zero (set to zero)
MB	Mega Byte
NIOSH	National Institute for Occupational Safety and Health
OSHA	Occupational Safety and Health Administration
PCB	Printed Circuit Board
Ppm	Parts-Per Notation
R&D	Research and Development
TB	Tera Byte
UNF	Unified National Thread - Fine series
USD	United States Dollar
Vs	Versus

LIST OF SYMBOLS

K_t	Total stiffness
K_j	Joint stiffness
K_b	bolt stiffness,
K_n	nut stiffness
K_m	Member stiffness
K_w	washer stiffness
K_p	plate stiffness
A_d	section areas of the unthreaded portion of bolt
A_t	section areas of the threaded portion,
L_t	effective threaded length
L_d	length of the unthreaded portion
E	Young Modulus
A	area
S_y	Yield strength
d_x	Deformation in axial direction
$\vec{R}$	Rotation vector
L	Length
P_L	Preload
D	Applied displacement
d	Circumferential displacement
β	Pitch angle
α	Half-apex angle
μ	Friction coefficient
t	Transverse displacement

INTRODUCTION

0.1 Description of a bolted joint

Bolted joints are the most common non-permanent clamping method in the world because of their short assembling and dissembling time and low fabrication and maintenance costs. They are widely used in many industries like automobile, petroleum, power and energy and construction. The demand for bolted joints and fasteners use in equipment is growing all the time. According to Shish "The global industrial fastener demand will grow 30% to USD 93.8 billion by 2018, among which global automotive fastener demand accounts for 27.8% (USD 26 billion)" (Shih, 2015).

A basic bolted joint includes at least two mating parts or clamping plates, one bolt and one nut. In the tightening process of a bolted joint, the helical geometry of the threads converts the relative angular movement of the bolt and nut to an axial elongation in the bolt. The elongation in the bolt creates a force in the bolt called preload or axial load. This force is responsible for the integrity of the joint assembly. Designers might decide to add other elements to the design of the joint to improve its performance (e.g. washer, spring washer, lock-washer and lock-nut), but the general behaviour of the joint will remain the same.

Several factors affect preload, such as thread pitch, thread friction, thread angle, stiffness of the joint, etc. Many studies have been conducted to identify and improve these factors to increase the efficiency and endurance of bolted joints but there are still many unknown factors.

0.2 Problems associated to bolted joints

The most important problem associated with bolted joints is the loss of preload. "The key issue as far as bolt life and integrity are concerned is, however, the tension in it" (Bickford, 2008). In order to keep the integrity of the joint, minimum preload has to be maintained in the bolt. Problems associated with bolted joints are divided into two categories; a) problems causing material failure or fracture and b) problems causing loss of preload without material failure.

Fatigue, creep, and over-load are the most important causes of material failure in bolted joints. Many studies have been conducted to increase bolt life in vibration and high temperature applications. Although transverse lateral movement can cause fatigue and self-loosening, the failure process is quite different in each case. Even though mechanical rupture is a severe failure in a system, self-loosening is, statistically, the most considerable and major problem in bolted joints. The sources of such problems will not be studied throughout this research.

When a joint is subjected to transverse lateral movement, depending on the preload magnitude and other joint parameters, preload might drop with or without relative rotation of bolt and nut. This phenomenon is called self-loosening. "Self-loosening is the gradual loss of the clamping force in the bolted connections under cyclic external loading, especially transverse loading" (Zhang, Jiang, & Lee, 2007). This problem is pervasive in automobile, aerospace, petroleum, and energy industries. A significant portion of customer service claims in the automobile industry are caused by the loosening of bolted connections which come at a significant financial cost to the industry. The most important bolted joint in the petroleum and energy industries are flanged connections. Any preload drop in flanges increases the chance of leakage which is problematic in sour, flammable, and explosive services. The importance of sealing performance is greater when 20ppm of Hydrogen Sulfide (H2S) is present as the general industry ceiling limit and 100ppm as NIOSH IDLH (Immediately Dangerous to Life and Health) (OSHA, 2013).

Many parameters can affect preload loss and despite the many pieces of research conducted to discover and quantify them, there are still many unknown factors in self-loosening. Friction between threads, between the nut/bolt head and mating parts, and between mating parts are of the most important factors in self-loosening. The pitch and angle of the threads also play a large role in the self-loosening of bolted joints. The friction of pitch and angle of the threads are the determinant factors in self-locking of bolts. The effective factors for self-loosening will be enumerated in the literature review chapter in greater details.

Some solutions, like adding a nut-lock, spring-nut, or spring washer have been suggested and evaluated to prevent self-loosening. However, no definitive solution has been found up to now. Some researchers have found and suggested a safe design zone to avoid self-loosening, but it does not cover all types of bolted joints and as such, the design of joints out of this range remain in the danger zone.

0.3   Overall aim of the present study

The overall aim of this study is to develop a test rig to evaluate the effect of joint stiffness on the self-loosening of bolted joints. Stiffness is a dependent variable which depends on the thickness of plates and material modulus of elasticity of the clamping parts. Both variables have been studied separately before but their effects have not been studied in term of stiffness.

The first important study in self-loosening was carried out in 1969 by Junker who invented a machine to test joints under transverse loads. Some modifications have been applied to his original design of the machine, known as a Junker machine, to improve its performance, but the concept remains the same. The basic concept of all self-loosening test machines is the same; a power source and a linkage mechanism, which serves to convert and transfer power, usually from an electrical motor, exert lateral movement on the tested bolted joint.

Because commercial self-loosening machines are expensive, which does not fit in this project budget, and do not fulfill the required conditions, an in-house instrumented bolted joint system (designed and installed in the lab) is mounted on a simple tensile machine to make a self-loosening test bench.

The overall aim of the first phase of this research is to develop an instrumented test bench that can be mounted on a tensile machine which provides cyclic movement to test samples with different thicknesses. This machine must be able to test a bolted joint consisting of a bolt, a nut, two plates, and two washers. Studying a bolted joint with different plate thicknesses will allow us to evaluate the effect of joint stiffness and joint clamping length.

In order to study the self-loosening phenomenon, a machine with the following capabilities is needed:

- Measuring the relative rotation of bolt and nut;

- Measuring the preload;

- Measuring lateral force in mating parts;

- Measuring the relative movement of plates;

- Measuring the test time;

- Counting the number of cycles during the test time;

- Integrating and correlating the above-mentioned parameters.

Most of vibration and repeated loads in nature and in industry are displacement control; this point obliges all designs to be conducted based on a displacement control. To do so, lateral displacement can be provided by an electrical motor and displacement amplitude can be adjusted via a gearbox or variable linkage mechanism. These systems are easier to drive, but are high in integrity failure risk and stress level control. As a small displacement can cause high stress, it is very important to find and evaluate the most critical point of the system in test rig design to avoid any risk of rupture and danger. To make sure that the test bench works well and the measuring devices are accurate enough, one bolted joint has been analyzed with FE and the results have been compared to experimental tests done by test bench.

0.4   Description of the thesis content

In the second chapter, previous research on self-loosening will be reviewed to clarify problems and methodologies. Different methods and their advantages and disadvantages are reviewed and discussed and their results are compared.

The steps taken in test bench design are discussed and explained in detail in chapter three. The general overview of the system, requirements, simplifications, and limitations in the design process are mentioned. Some of the detailed calculations used in the design and fabrication of parts are also shown. Detailed drawings of all parts are given in the related appendices and their functionality is discussed.

In chapter four, the performed finite element analysis is explained in detail. The simplifications and assumptions of the geometry and boundary conditions are also detailed and the meshing and high-performance calculation information is presented. The tools used for post-processing and the mesh convergence criteria are discussed as the last subjects in this chapter.

Chapter five contains all results from the experimental and finite element analysis. The experimental results are compared to their finite element counterpart and all disparities are discussed. The experimental and finite element comparison is used to justify the accuracy and suitability of the test rig.

Chapter six gives the overall conclusion of the performed study and chapter seven presents some recommendation to improve the rig and future work to be conducted on the study of self-loosening.

CHAPTER 1

LITERATURE REVIEW

1.1   Introduction to previous work studies

The self-loosening phenomenon is related to bolt load drop and has been identified to happen in two stages. Stage I involves the gradual clamping force reduction with no relative rotation of nut and bolt. Cyclic plastic deformation and the resulted stress redistribution and ratcheting deformation in the bolt are responsible for this first stage of self-loosening (Figure 1-1). Stage II is related to the backing-off of the nut and is associated to the relative motion of the nut and bolt causing drastic clamp force reduction. Researchers have studied these two stages using different methods that can be categorised into finite element, analytical, and experimental studies. Each method has advantages and disadvantages depending on the parameters of interest.
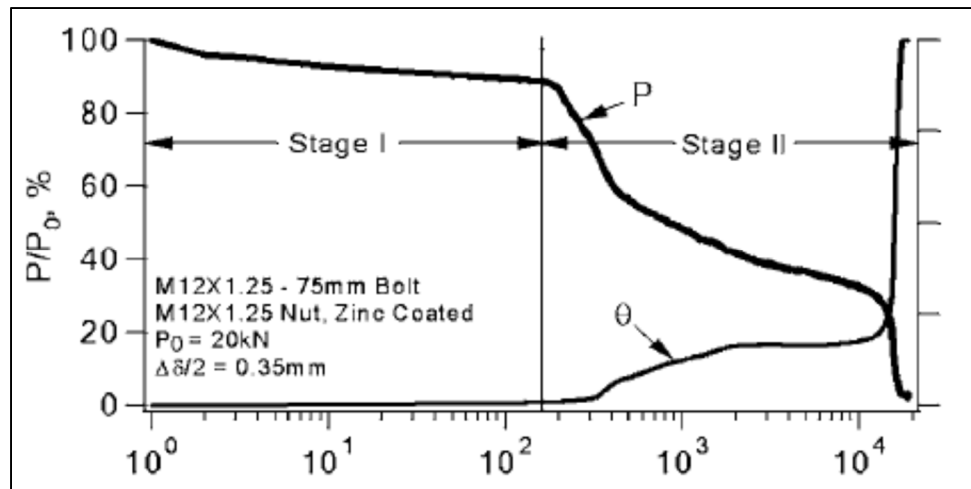
Figure 1-1 Self-loosening process (Jiang, Zhang, & Lee, 2006)

Analytical methods to treat self-loosening involve complex mathematical equations. The bolted joint is a statically indeterminate structure that requires the development of a system of complex equations based on the free body diagrams of the individual joint members and

the compatibility equations of the displacements and rotations that exist between them. Assumptions must be made to simplify the system geometry and equations in order to solve the problem. A lot of time is required to solve the problem because of the many iterations involves, but once completed, all the considered variables can be evaluated with reasonable accuracy. The analytical method is time-consuming and a high-performance computer HPC should be considered for most cases to solve the differential equations. However, the analytical model can easily be extended to cover many different applications and other bolted joint cases by changing the geometry, boundary conditions and loads. The basic differential equation formulation is determined by the joint parameters; therefore, new mathematical models must be elaborated for each independent case. Some researchers focused on this method to develop models for different types of bolts and nuts. Parameters such as preload, bolt/nut friction with joint members, friction between nut and bolt threads have been previously studied. Conversely, there have been few theoretical studies about the effect of the different joint element stiffness's on the self-loosening of bolted joints which is one of the purpose for which the rig has been developed.

The finite element method is widely used in all industries. FE modeling of bolted joints is a relatively a simple task to do nowadays, however the simulation of the self-loosening mechanism is not a straight forward task to be conducted by even an experienced design engineer. The modeling is complex and tedious and HPC is still needed. The simplification of the geometry and the boundary conditions causes some deviation from realistic conditions. Due to complicated helical geometry and non-linear contact surface behaviour in bolted joints, special modeling techniques should be used to yield accurate results. Different material behaviors can be studied more easily with FE when compared to analytical methods. Researchers in different universities and R&D institutions are using FEA to study different combination of joint members, materials, material models, and loadings to see how they affect self-loosening behaviour. In previous studies, stage I and II of self-loosening were studied and different parameters were covered, but there has not been a study that combines both stages and the effect of joint stiffness on the self-loosening.

The experimental method is the most realistic and preferred mean to study the behavior of structures in general and the self-loosening of bolted joints in particular. Valuable data can be obtained by using controlled realistic test conditions; however, cost, measurement limitations and equipment capacity are some restraints to name a few. It is almost impractical to simulate certain load cases or joint combinations with laboratory facilities. Experiments are usually used to verify results derived from other methods such as analytical and numerical simulations. Most of experimental tests are conducted using a Junker machine used in conjunction with instruments that may affect the results like the presence of a load cell in a joint. Indeed, a load cell affects joint stiffness and grip length. In order to avoid such interference new settings are required to maintain acceptable conditions to study the effect of joint stiffness. The distinguishing feature of the test rig that was developed for this project is its faithful representation of the physical behavior of a bolted joint. In this chapter, previous studies are grouped and reviewed based on the method of analysis used.

1.2   Analytical modeling

Yang et al. (Yang & Nassar, 2012) developed an analytical model to study different parameters leading to self-loosening of bolted joints. Bolt and nut differential rotational angle, friction and local slippage behaviour, bolt bending deflection and transverse displacement, and clamping force are to name a few the results have been compared with experimental ones. Their results confirm that higher preload leads to a higher self-loosening resistance.

Yang et al. (Yang & Nassar, 2011a) have also studied the effect of wedge angle on self-loosening both analytically and experimentally. They proposed a model to predict the self-loosening and validated their model experimentally using tests on a modified Junker machine. This model shows that a sufficiently large wedge angle of the nut under head surface can reduce considerably self-loosening as shown in Figure 1-2.
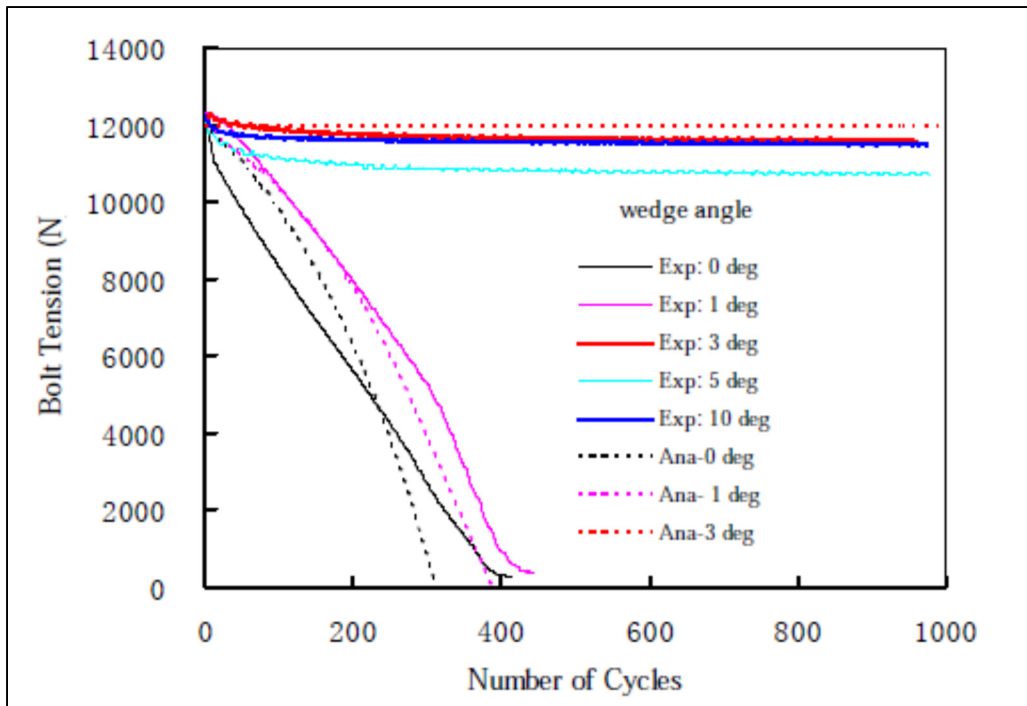
Figure 1-2 Theoretical and experimental comparison of the self-loosening
behavior for the bolt-nut assembly for five wedge angles under a preload of
12000 N (Yang & Nassar, 2011a)

The effect of thread profile angle and the clearance of the thread and hole have been studied using an analytical method (Yang & Nassar, 2011b). They have concluded that increasing the thread and hole clearance reduces the self-loosening resistance of the joint Figure 1-3. It is also concluded that increasing the thread profile angle increases the self-loosening resistance significantly.

A formula to find a preload threshold (minimum initial preload) for self-loosening of countersunk bolts, depending on their bearing friction, thread pitch, and excitation amplitude have been developed (Zaki, Nassar, & Yang, 2011). The authors discussed the effect of grip length, which is an independent factor that joint stiffness depends on. Their results show that decreasing grip length increases the preload threshold non-linearly, such that a joint with a grip length 8% shorter needs a 40% bigger preload in order to not be affected by self-loosening (Figure 1-4). They also confirmed that bearing friction and thread clearance,

respectively, have positive and negative effects on self-loosening. The experimental validation was also conducted on the same machine.
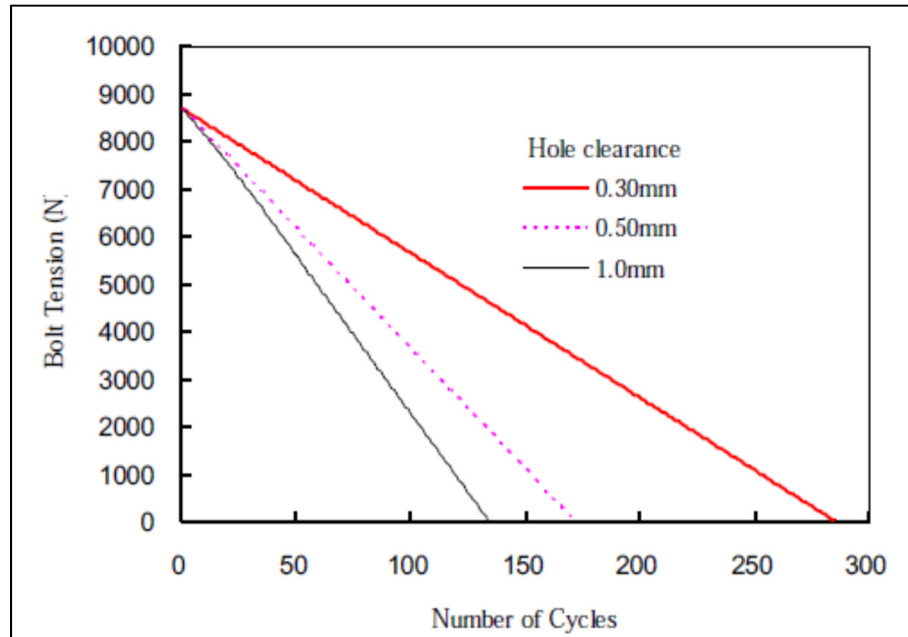
Figure 1-3 Effect of the hole clearance on loosening behavior
(Yang & Nassar, 2011b)

Yang et al. proposed a novel criterion for the self-loosening of threaded fasteners. They developed a new approach to investigate the effect of "bearing and thread friction coefficients, bolt grip length, thread pitch, material, and the cyclic amplitude of the transverse excitation" (Yang, Nassar, & Wu, 2010). The new approach illustrates the true behaviour of the joint in the presence of transversal excitation.

Their results conformed to other research results and confirmed that using fine thread fasteners improves self-loosening resistance, increasing bearing friction and thread friction also increases self-loosing resistance significantly, and excitation amplitude is linearly related to the threshold preload. As illustrated in Figure 1-5, increasing Young modulus decreases self-loosening resistance, and points to the fact that higher preload is required to prevent self-loosening.
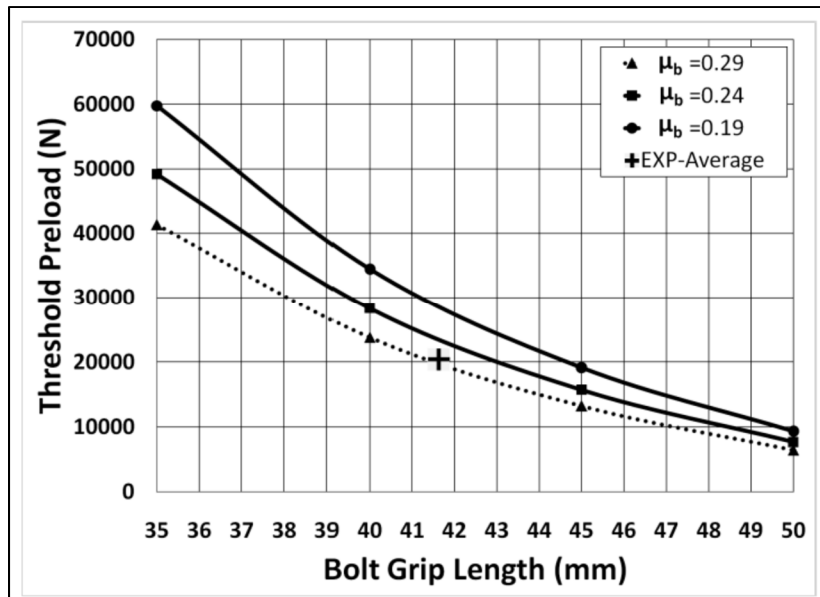
Figure 1-4 Effect of bolt grip length on the threshold preload
for ½"-13 fasteners at 0.365 mm excitation
(A. M. Zaki et al., 2011).
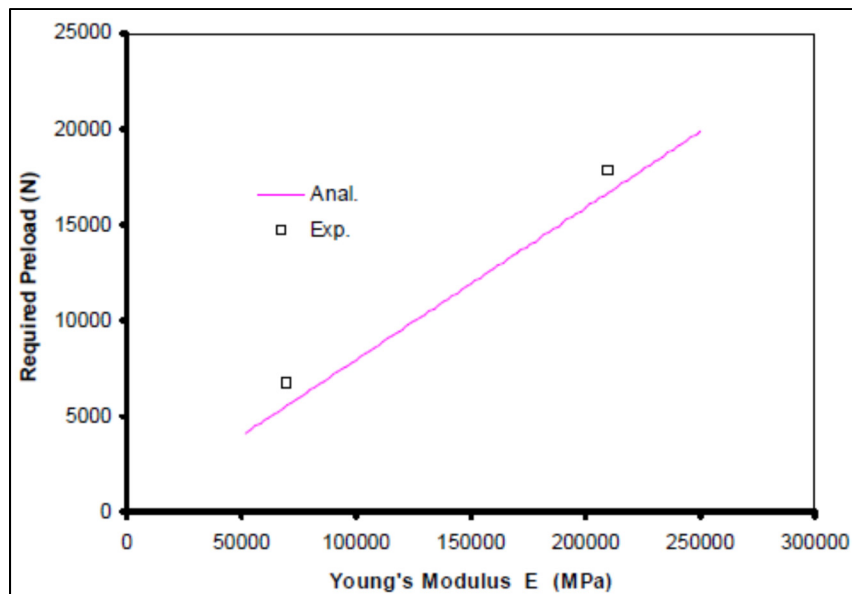
Figure 1-5 Effect of Young's modulus of bolt material on the
threshold preload (Yang et al., 2010)

Nassar and his research team focused on the analytical method and have performed a number of studies to investigate other factors and joint types. They studied the effect of thread fit and hole clearance using analytical and experimental methods (Nassar & Housari, 2007). It was illustrated that preload drops faster and that less cycles are needed for a complete loosening when the hole clearance is increased and the applied displacement is significant enough to slide the bolt all the way through the hole clearance. Thread fit was found to have the same effect on self-loosening resistance, where a tighter thread fit results in a higher loosening resistance. A modified Junker machine was used to perform the experimental test. The experimental and analytical results match well and the deviation between them is justified by the nominal clearance used in the analytical calculations. Clearance has an exact and distinct value for each thread designation in the analytical method whereas it can be defined within a range in the experiment with a max and a min values defined by the standard designation.

In another piece of research, Zaki et al. studied the effects of conical angle and thread pitch on the self-loosening of a bolted joint in the presence of transverse cyclic displacement (A. M. Zaki, Nassar, & Yang, 2012). The different steps for the analytical method including the free body diagram, the compatibility and equilibrium equations, and final solutions are explained and presented. The pitch, which is defined as the distance between the tips of two adjacent threads is found to have an important effect on the loosening. However, increasing conical angle has a direct effect on self-loosening resistance. As illustrated in Figure 1-6, increasing the conical angle improves the loosening resistance of the joint. Like in other studies, a modified Junker machine was used for the experimental tests and preload was measured using a load cell.

Zaki et al. investigated the effect of thread and bearing friction on the self-loosening of countersunk bolts (A. Zaki, Nassar, & Yang, 2010). As the friction coefficient is directly influenced by the coating type and thickness, this study helps predicting the effect of coating on self-loosening. The analytical model they developed was solved using a MATLAB code and the resulting data showed a good correlation with the experimental results. They defined different zones of loosening and no-loosening based on thread and bearing friction. The

bordered zones define the combinations of thread and bearing friction with excitation amplitude, so that a loosening life cycle can be estimated. Alternatively, a desired thread and bearing friction can be found to improve self-loosening resistant in a bolted joint (Figure 1-8). As with the other studies conducted by this research team, the Junker machine was used to perform the experimental tests.
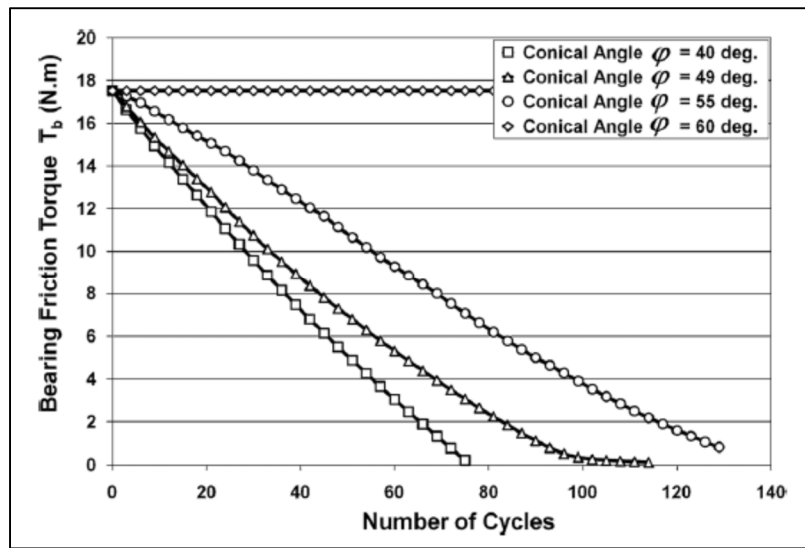
Figure 1-6 Effect of under head conical angle on the self-loosening behavior (A. M. Zaki et al., 2012)

Zhang et al. performed an analytical study to clarify the self-loosening mechanism. Their proposed model is based on a simple block sliding in a double inclined plane (Figure 1-7)(Zhang et al., 2007). This model shows that the back-off of the nut, which is the main reason for preload drop in stage II of self-loosening, is caused by "repeated micro slip between the contact surfaces of the engaged threads and the reversed bending moment exerted on the bolt and the nut" (Zhang et al., 2007).

Many different types of self-loosening resistant bolts and nuts have been invented and are being used in industry. Any combination of bolt and nut makes a different bolted joint that behaves differently when subjected to lateral vibration. The prevailing torque nut (locknut) is currently one of the most popular nuts used in industries to enhance loosening resistance.
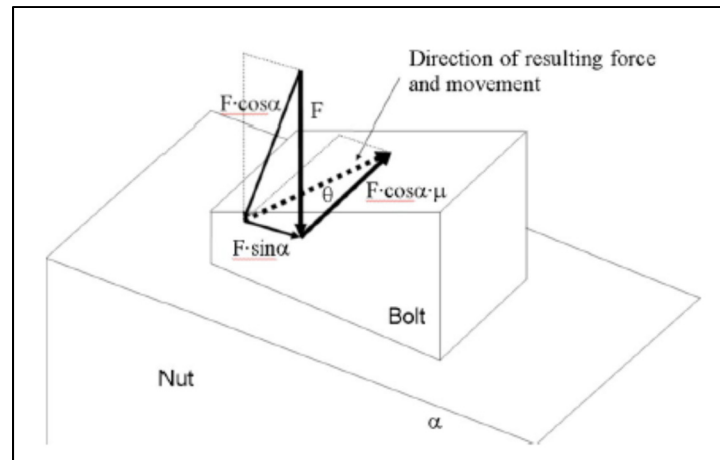
Figure 1-7 Free body diagram of bolt and nut thread
contact (Zhang et al., 2007)
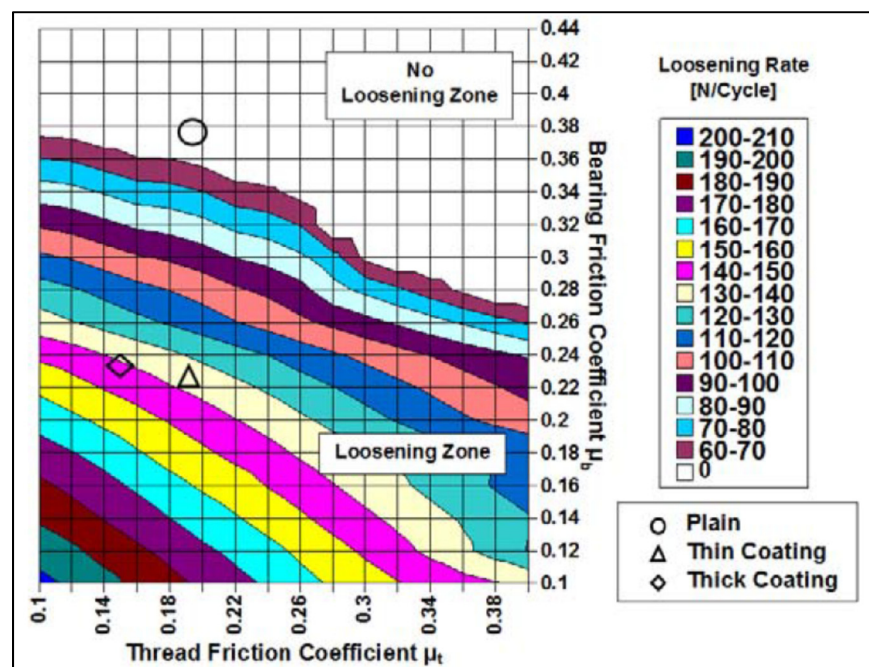
Figure 1-8 Effect of friction combination on the rate of
self-loosening (A. Zaki et al., 2010)

Eccles et al. investigated the self-loosening behavior of joints with a locknut. Their study
showed that although prevailing torque nuts improves self-loosening resistance, they increase
the chance of complete detachment of the joint when axial load and transverse movement are

applied simultaneously (Eccles, Sherrington, & Arnell, 2010). In joints with regular nuts, the rotation of the nut stops when the axial load of the bolt reaches zero, nevertheless the axial load provided by the elastic deformation of a locknut presumes the loosening process to the complete detachment of the nut. The analytical model used in this study is similar to the one used by Zhang et al. A simplified free body diagram of the bolt and nut thread contact is used to explain the loosening mechanism based on slippage.

1.3   Experimental studies

Junker performed one of the earliest experimental studies on the self-loosening of bolted joints. He discussed the theory of loosening and conducted experimental tests with a machine that laid the groundwork for many future experimental studies (Junker, 1969). The basic components of his machine are an electrical motor to provide excitation displacement, a gear and linkage system to control and transfer the displacement, clamps, and sensors to gather information during the test. He used rollers to reduce friction between the mating plates and consequently reduces the required lateral force; however, this creates an unrealistic condition. The displacement control is far from the joint centerline and the displacement values are influenced by the deformation of other parts. Adding a rotation measurement device might be the most important modification to study stage II of self-loosening. This machine is the basic concept for most test rigs although it has been modified to study different cases. Altogether, he is the founder of self-loosening experimental study. The finite element and analytical investigations from the following studies are discussed in the analytical and finite element sections, therefore, only the experimental test rigs are reviewed in this section.

Zhang et al. performed an experimental study using a hydraulic material testing system to evaluate the effect of the thickness of the mating parts and the applied load direction in an M12 bolted joint (Jiang et al., 2006). A load cell is used between the clamp part and the bolt head to measure axial load. It is important to note that the grip length is one of the two main factors studied in this research and that using a load cell to measure axial load changes the

grip length of the joint and deviates the results from realistic conditions (Figure 1-9). On the other hand, because joint stiffness is changed by the load cell, the axial force will be also affected. The investigated joint consists of two plates and two insert plates that serve to change the thickness of the mating parts. An extensometer is installed on the plates to measure the relative displacement between the two mating parts. Unfortunately the captured displacement does not include slippage or the relative displacement of the insert plates and nut/bolt. A rotation sensor is supported on the nut using a fixture in a way that the tip of the sensor touches the end of the bolt. The captured rotation is the exact relative rotation of the bolt and nut. The authors conclude that increasing clamp length and loading angle enhances self-loosening resistance. This research team used the same machine as (Jiang, Zhang, & Lee, 2003) to study the effect of preload and excitation.
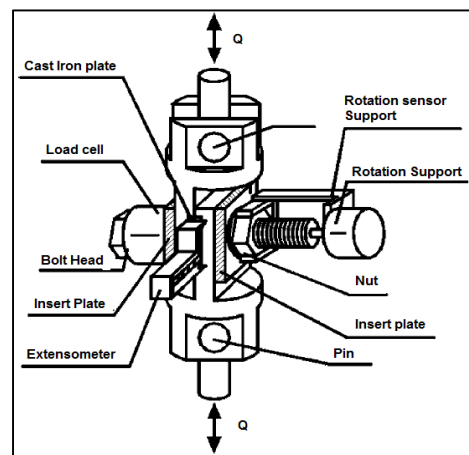
Figure 1-9 Experimental Setup
(Jiang et al., 2006)

Nassar and Housari developed the test setup demonstrated in
Figure 1-10 to study the effects of hole clearance and thread fit using a modified version of the Junker machine.

An electrical motor with a set of pulleys is used to supply the required displacement to the mobile plate using an eccentric mechanism. As in other studies, a load cell is used to measure the axial load of a ½ -13 bolt (equivalent of M14x2). A rotation sensor captures bolt head

18

rotation via a short belt that is connected to a mounted socket cap on the bolt head. Slippage between the belt and cap and the belt and sensor pulley can be a source of error for the rotation measurement. In the current study, the rotation sensor is connected to the bolt directly to avoid such a problem. The eccentric mechanism gives the capability to provide different excitation amplitudes. As previously discussed in section 1.2, the authors concluded that a tighter tolerance in both plate holes and threads increases self-loosening resistance (Nassar & Housari, 2007).
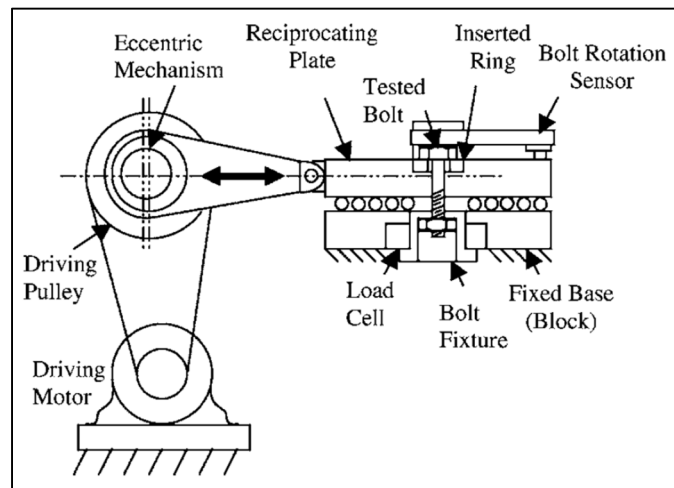
Figure 1-10 Test setup developed by Nassar & Housari (Nassar & Housari, 2007)

Zaki et al. used the same Junker machine to study self-loosening (A. M. Zaki et al., 2012). Lateral cyclic displacement is applied to the upper plate and a load cell is used to monitor preload changes in a ½ -13 bolt (equivalent of M14x2). The same machine is used by Zaki et al. to study the effect of thread pitch, excitation amplitude, and bearing friction (A. M. Zaki et al., 2011) and also to study the effects of thread and bearing friction (A. Zaki et al., 2010) on the self-loosening of countersunk bolts.

Eccles et al. modified the Junker machine (Figure 1-11) to be able to transmit axial load and transverse displacement simultaneously to study the effect of a prevailing torque nut in bolted joints (Eccles et al., 2010). A hydraulic jack is used to provide an independent regulated axial load. Excitation is applied to the upper plate which is in contact with the

lower mating plate via needle bearings to minimize friction between the two parts. A combination of an electric motor and an eccentric cam system is used in this design to generate and adjust the excitation displacement with the axial load of the bolt (M8) that is measured by a load cell. Unfortunately, the complicated joint design and the multiple inserted elements alter the experimental results from actual values. This special design is used to simulate the behaviour of a prevailing torque nut in bolted joints.

Sawa et al. designed a fixture based on the Junker machine to study the effects of the utilization of a double nut, spring plate washer, and hexagon nut with a flange on self-loosening (Sawa, Ishimura, & Nagao, 2012). They studied a joint fastened with an M10 bolt with a load cell inserted underneath the fixed plate. A dial gauge is supported on the far side of the fixed plate while its tip touches the end of the mobile part (Figure 1-12). As the installation point of the gauge is far from the joint centerline, measured values are affected by deformation of the part. Steel bars are used as bearings between the mating parts. Although they decrease the friction and lateral force, they change the grip length and joint stiffness. Valuable information could have been extracted from the test rig had a lateral force and a rotation sensors been incorporated. This machine is also used by Sawa et al. to study the effect of the mating parts inclined bearing surface (Sawa, Ishimura, & Karami, 2010).
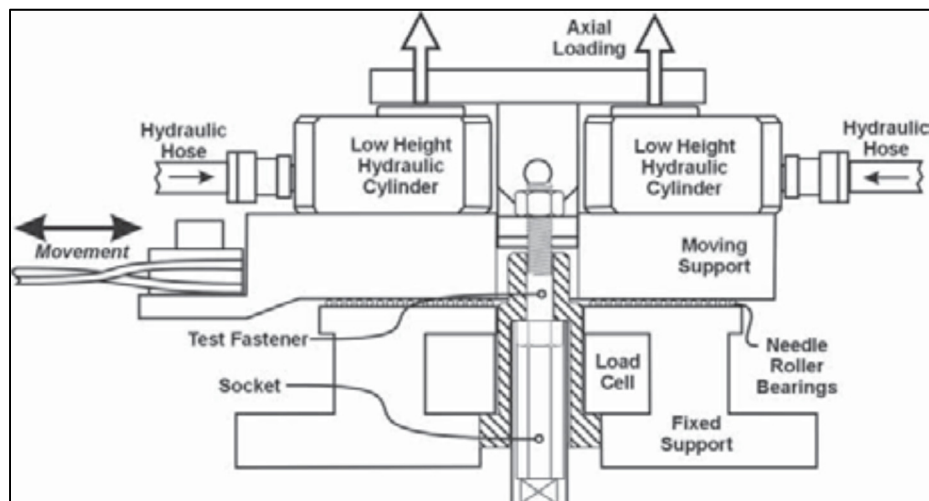
Figure 1-11 Section view of test machine used by (Eccles et al., 2010)
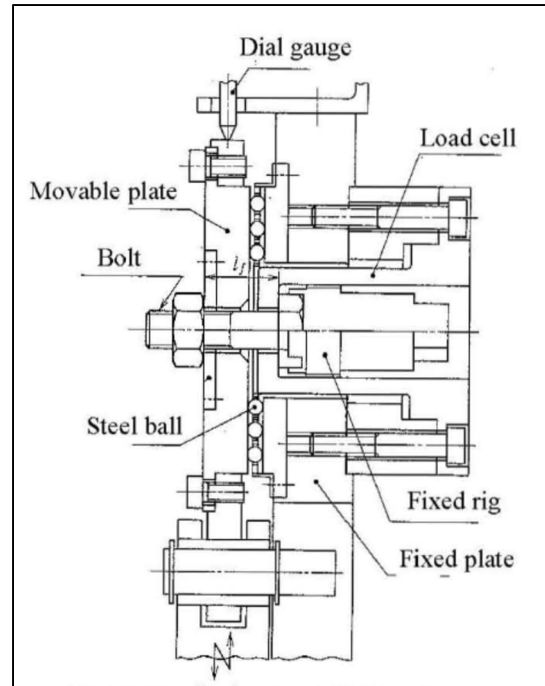
Figure 1-12 section view of test machine
(Sawa et al., 2012)

1.4   Finite Element

Zhang et al. performed a three-dimensional elastic-plastic finite element analysis to study the first stage of self-loosening (Jiang et al., 2003). As rotation is negligible in stage I of self-loosening, they did not consider it and used a symmetric model. The bolt and nut thread connection is modeled as a circumferential groove. These simplifications enhance the CPU performance but unfortunately affect considerably stress distribution on the threads. Local mesh refinement is applied in the first engaged thread with all thread contacts being frictionless, and only sticking behavior is modeled as a restrain with a high critical shear stress. Thermal expansion of the upper mating plate is used to simulate the preload in the bolt. They concluded that "the localized cyclic plastic deformation caused the stresses to redistribute in the bolt, and the result was the gradual loss of clamping force with loading cycles" (Jiang et al., 2003, p. 1). Their results show that lateral displacement is a determinant factor for the preload drop in the first stage of self-loosening whereas friction between the clamping parts does not play an important role.

Zhang et al. conducted another study in 2007 on the second stage of self-loosening using finite the element method (Zhang et al., 2007). Unlike their previous study, due to the importance of the relative rotation of the thread of the nut and bolt the helical geometry of the threads is considered. Because plastic deformation is not a dominant factor in stage II, only the elastic behavior of the material is considered. Due to deformation and displacement occurring in all directions, the researchers were forced to use a full 3D model to study the second stage of self-loosening. An isotropic frictional and infinitesimal-sliding contact is defined in the thread contacts. All other contacts are defined in the same way as the thread contacts with a different friction factor. The thermal expansion method is again used to simulate the preload of the bolt. The plate adjacent to the bolt is fixed and a transverse displacement is applied in four stages to the other mating plate. They concluded that "microslip between the engaged threads and the variation of the contact pressure were identified to be the major mechanisms responsible for the self-loosening of a bolted joint". They also used a simplified FE model of the thread contact to prove their suggested mechanism (Figure 1-13).
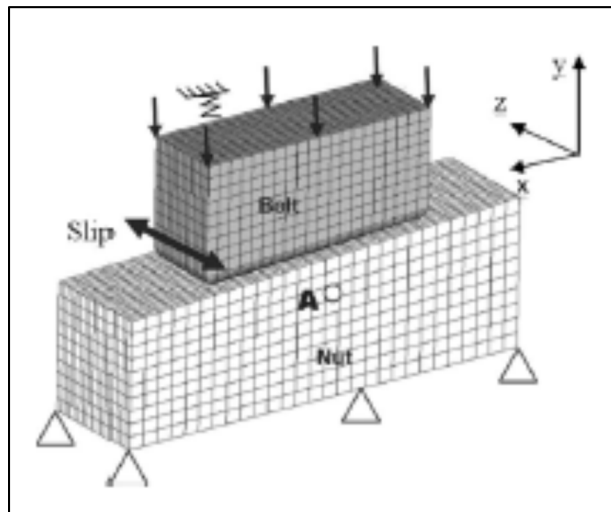

Figure 1-13 Simplified model of thread's
contact (Zhang et al., 2007)

Sawa et al. conducted a FE analysis to study conventional methods (e.g. double nut, sprig plate washer and flanged nut) used to reduce the loosening of bolted joints (Sawa et al.,

2012). 8-noded hexahedral elements are used in the analysis with the penalty method for the contact behaviour of the thread contacts (male and female) and the nut and plate contact area. In this research study, just one plate is modeled and the effect of frictional contact between the bolt head and the two mating plates is neglected. All contacts are considered to have maximum possible realistic conditions. Preload is modeled using forced displacement in the axial direction of the bolt which is restrained in all other directions. Transverse displacement is applied to the plate which is constrained in all directions. They concluded that joints with a flanged nut have the highest rate of loosening and that a spring washer improves joint performance the most among the studied methods (Figure 1-14).
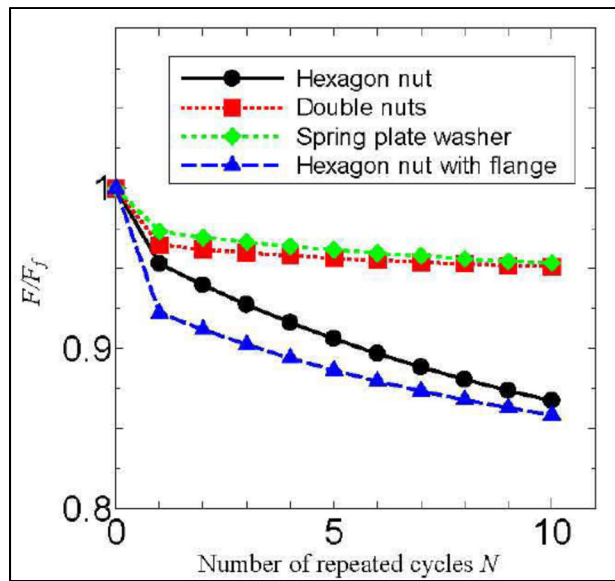
Figure 1-14 Finite element result of studied
joints (Sawa et al., 2012)

Yang and Nassar conducted a study using the FE and analytical methods (Yang & Nassar, 2012). Material behaviour is considered as fully elastic and the frictional contacts are defined in the following connections: bolt to plate, plate to plate, nut to plate, and thread-to-thread. They used the preload feature of the ABAQUS software as in the current study to facilitate and accelerate preload modeling. One side of the lower plate is restrained in one direction and a triangular displacement excitation with time is applied to the opposite side of upper

plate. The FE model is not explained in detail nevertheless it was used to validate a proposed analytical equation to prevent self-loosening of bolted joints.

Sawa and Ishimura conducted a study to research the effect of inclined bearing surfaces and eccentric nuts on loosening, using the FE method (Sawa et al., 2010). Like in their previous research, only one plate is considered in the FE model and the contact between the bolt head and the two mating parts is neglected. 8-noded hexahedral elements are used in the analysis and the penalty method is used for contact behaviour, which is located at the thread contact area (male and female) and the nut and plate contact area. Contact between the convex surface of the lower nut and the concave surface of the upper nut is neither mentioned nor described. The tightening procedure and the inclined surface effect is explained as "After tightening the lower nut, the upper nut is tightened. At this time, a gap and continuously applied lateral clamping force which prevent loosening is occurring" (Sawa et al., 2010). Preload is modeled using a forced displacement in the axial direction of the bolt which is restrained in all directions. Transverse displacement is applied to one of the plates and it is constrained in the other directions. Figure 1-15 shows the described FE model. Different inclined plate angles of 0, 2, and 3 degrees are evaluated with this FE model.
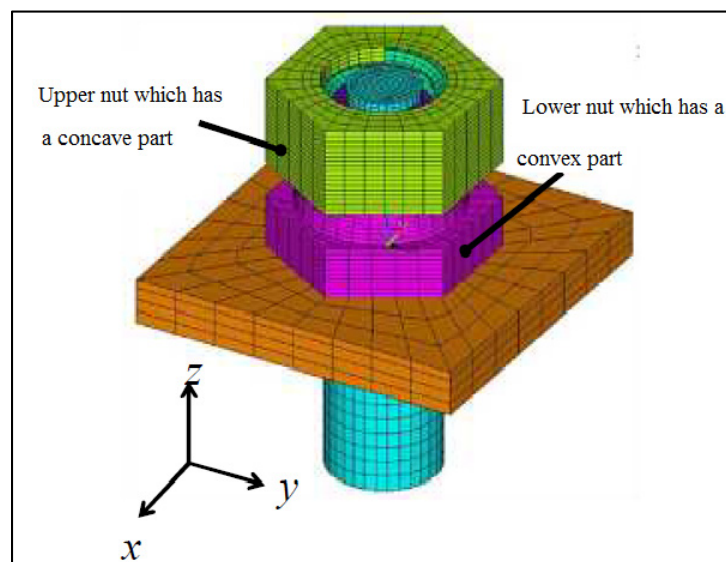

Figure 1-15 FEA model of the eccentric nut (Sawa et al., 2010)

Material behaviour is considered as elasto-plastic. Sawa and Ishimura concluded that "the reduction in axial bolt force with large angle of the incline is larger than that with small angle of the incline" (Sawa et al., 2010).
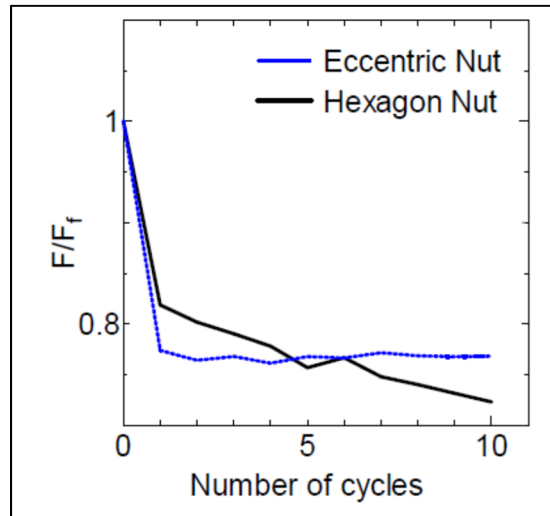
Figure 1-16 Comparison of loosening in

joints with hexagon and eccentric nut

(Sawa et al., 2010)

1.5   Objectives of the current study

The objective of the current study is to develop a test machine to study the effect of plate stiffness and thickness on self-loosening. As mentioned before, very little research has been conducted with experimentally representative test rig. One of the general targets defined in the beginning of the project was the improvement of the measurement systems to avoid problems and disadvantages that test machines used in previous researches suffered from. Reviewing papers and reports from different researchers gives us a good idea about the requirements and expectations of the target test rig. The final machine must be able to test a bolted joint with different plate thicknesses and materials. It should also be able to measure bolt preload, lateral load, lateral displacements, number of cycles, temperature, time, and nut rotation continuously while the real bolted joint geometry and stiffness is not altered. A finite

element analysis will be conducted to unsure that the design of feasible and that the measured parameters are realistic.

With the developed test rig, bolted joint behavior will be studied under different load cases and the experimental results will ultimately be compared with finite element and theoretical results. The results will be also compared with results from previous studies.

The specific objectives are:

1- Design a test fixture to be used with a tensile compression machine to study the self-loosening of bolted joints.

2- Design the clamping plates with variable thickness and bolts with variable length and their adaptors to be able to study the effect of assembly stiffness on the self-loosening.

3- Incorporate all necessary instrumentation to measure bolt load, transverse load, displacement, rotation, temperature, number of cycles and time.

4- Write an interface program in Labview to monitor and record the data in a computer through a data acquisition system.

Conduct preliminary testing of self-loosening of a bolted joint and compare the result using numerical FEM.

CHAPTER 2

EXPERIMENTAL TEST RIG

2.1 General description of the developed test rig

As discussed previously, the general and essential requirements for a self-loosening machine are providing cyclic lateral displacement and the ability to measure preload and the studied parameters. Development of a test rig to study the effect of stiffness and grip length is the ultimate objective of the test rig. The stiffness of a bolted joint is a function of the material and the geometry of the bolt, mating parts, washers, and nut. Any changes in the material of the mating parts only change the stiffness whereas changes to thickness change stiffness and clamping parts simultaneously. Hence, the machine should be designed to also be able to measure other parameters so that they can be compared to the parameters that are influenced by grip length. To do so, the target machine should be able to measure at least rotation, lateral force, lateral displacement, and the number of cycles.

The design is based on an existing fatigue machine as the source of power to minimize the time and cost of the project. The original machine includes the following parts (See Figure 2-1):

- Holding structure,
- Electrical motor,
- Adjustable crank system,
- Basic control panel for start-stop and frequency adjustment,
- Cycle mechanical counter with precision of 10 cycles,
- Lever with three loading point and spring end fulcrum,
- Mobile mounting structure,
- Grips and universal joint,
- Adjustable stem.

The holding structure, electrical motor, lever, mobile mounting structure, and adjustable stem are unmodifiable. The adjustable crank system is repaired and the cycle counter is bypassed

and replaced by a magnetic digital counter. A basic control panel is connected to the designed control system and its outputs are transferred to the control and monitoring program. Speed control is directly connected to the electrical motor and the frequency can be adjusted manually.
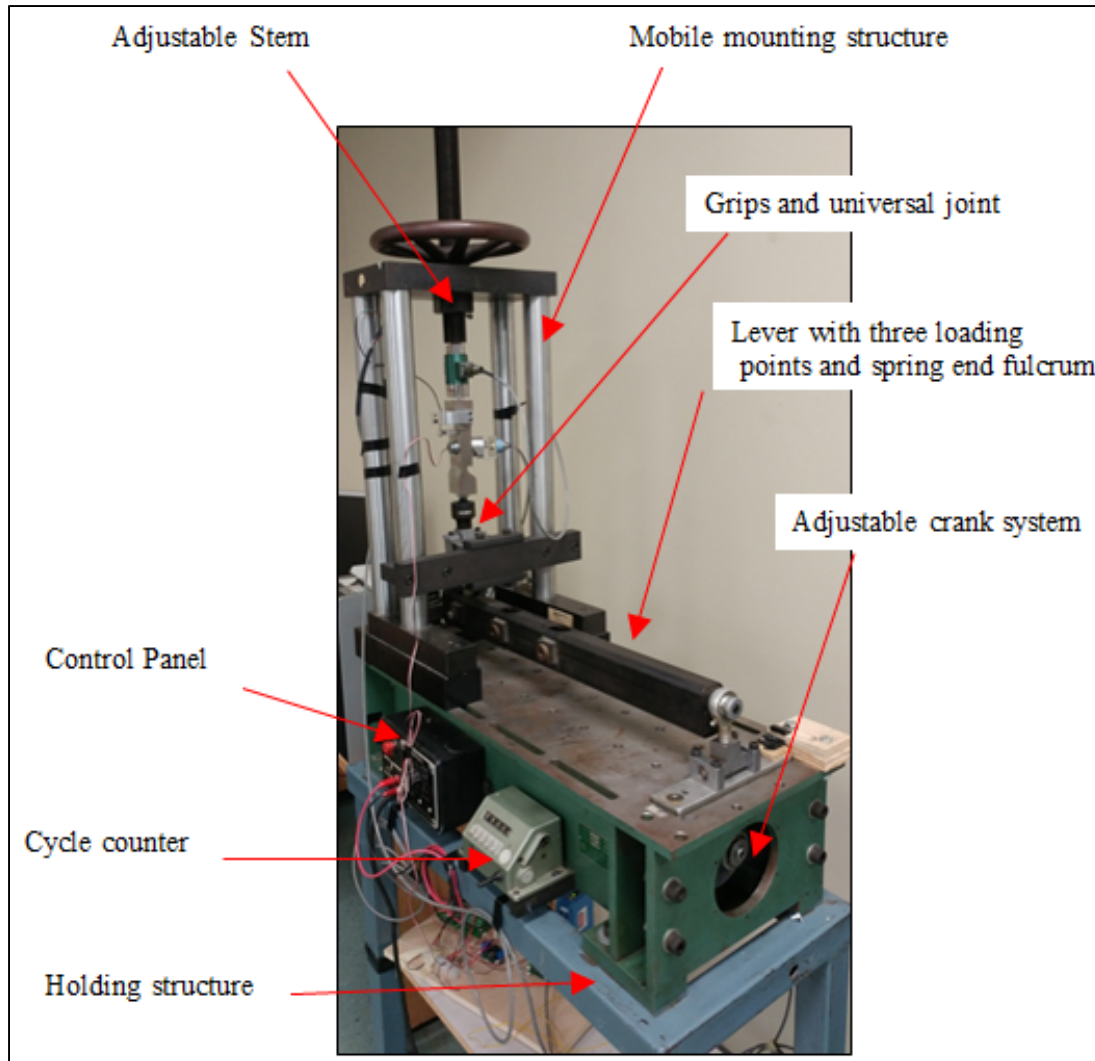

Figure 2-1 Fatigue and endurance testing
machine (Systems Integrators LLC, 2011)

The grips and universal joint section has been completely replaced with a new design that will be explained in next sections.

The lever of the test rig is essentially a "class 2 lever". The displacement provided by the electrical motor and crank system is applied to one end of the lever to produce the load and the test specimens can be installed between the universal joint and the load cell. According to work and energy law, with a certain amount of effort, the maximum load can be reached with the lowest displacement; hence, the closest point to the fulcrum point of the machine is used to install the test specimens in order to have the highest load capacity. The developed test rig is able to apply a lateral displacement from zero to 0.25 (inches) with a maximum frequency of 5000 cycles per minute. The maximum lateral force is 2000 lbs, which is a function of lateral displacement and stiffness of the joint in the lateral direction.

Instrumentation has been centralized via a PCB that is used as the main board to connect all of the measuring devices to a computer. (See Figure 2-2)
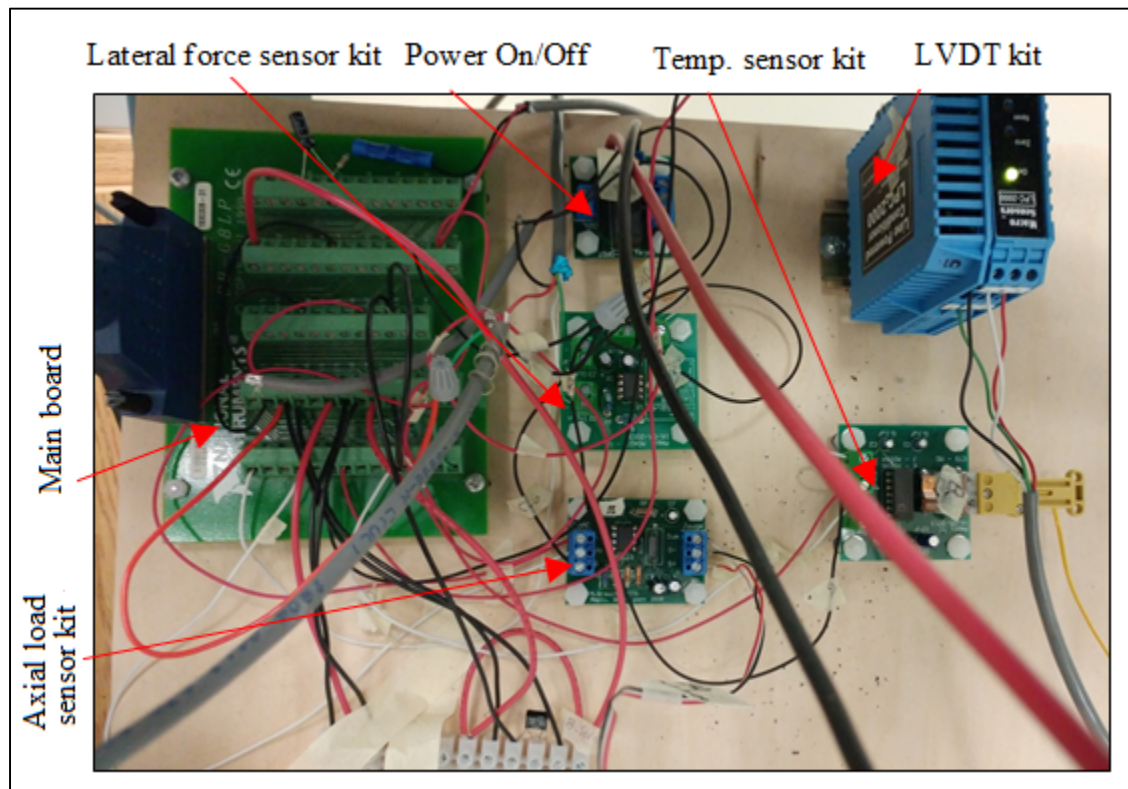

Figure 2-2 Main board and electrical kit assembly

30

The control program is written in Lab View (Laboratory Virtual Instrument Engineering Workbench). This control and monitoring program can continuously display and record lateral displacement, lateral force, axial force, rotation, number of cycles, time and temperature. For safety reasons, the machine can be switched off via software or the control panel on the machine, but it can only be switched on from the control panel.

2.2 Requirements and limitations

Like in all experimental researches, measuring essential variables is the basic requirement of a test rig. Axial force, displacement, and rotation are the essential variables for the self-loosening test. Besides precision and measurement range being crucial factors for sensor selection, compatibility with the control system and measurement devices can be a limiting factor. Finding a feasible combination of available sensors is a challenge in the design of the measurement and control step.

The ability to test different plate thicknesses and bolt sizes is one of the desired specifications of the final test machine, which is limited by machine capacity. Increasing bolt size requires a higher transverse load to reach the same lateral to axial force ratio at the same bolt tightening stress ratio. Matching measurement accessories with different diameters and thicknesses limits the machine design with regards to feasibility, cost, and fabrication equipment. Limitations and their applied solutions are discussed in detail in each section.

In order to have realistic results, the joint geometry has to be kept, as much as possible, in conditions close to industrial applications. This requirement renders many measurement methods and devices ineffectual. As mentioned in the previous chapter, using a load cell to measure axial load affects grip length and joint stiffness directly and creates significant changes in the results when studying joint stiffness. In the current study, the bolted joint is subjected to transverse load conditions, hence, the test rig has to be designed to avoid undesirable loads, such as bending while keeping pure transverse excitation.

When the stiffness of the joint is the subject of a study, it is very important to minimize the modifications made to the parts. Any excessive weakening or reinforcement will affect the properties of the joint and the test results. To meet this requirement, the coaxiality of the plates (mating parts), the fixed point, and the excitation point are considered as determinant factors. These geometrical restraints must be respected in all design modes (different plate thicknesses and their combinations).

The instrumentation fixtures, the maximum capacity of machine, the possibility of performing tests with different frequencies, and the above mentioned geometrical restraints form the major challenges for the design of the grips.

The test rig must be designed and fabricated in such a way that all load cases can be performed safely to both protect the operator and to insure the durability and performance of the machine. The applied safety provisions in the design and programing are as below:

- "General force limit"; Because the maximum force capacity of the machine is defined in the manufacturer manual as 8000 lbs, the program is set to terminate the test if the lateral force is higher than 7000 lbs.
- "Adjustable force limit"; In each test, a value smaller than "General force limit", which is dependent on the load case condition, can be set in the interface panel to terminate the test.
- "Number of cycles limit"; an adjustable limit can be set for each test in the interface panel.
- "Mechanical cycle counter limit"; the count down cycle counter can be set to a value close to the limit entered in interface panel as a backup safety parameter in case of a program malfunction or error.
- "Excitation amplitude limit"; this can be set for each test in the interface panel to control the displacement.

As with all other projects, the available fabrication equipment should be considered in the feasibility of the design to minimize the budget.

2.3   Preload sensor

Preload keeps the mating parts together and decreases in preload can lead to serious problems, such as structural integrity and leakage failures; hence, the integrity of a bolted joint is usually assessed by its capacity to maintain the bolt axial load.

The objective of all research on self-loosening is to evaluate and quantify the effects of different parameters that prevent self-loosening or to estimate the number of cycles before self-loosening occurs in order to help create a safe and effective maintenance program. Hence, finding an accurate measurement method that matches the whole design and causes the least possible deviation from the actual joint properties (standard industrial set up) is one of the most important points of the design.
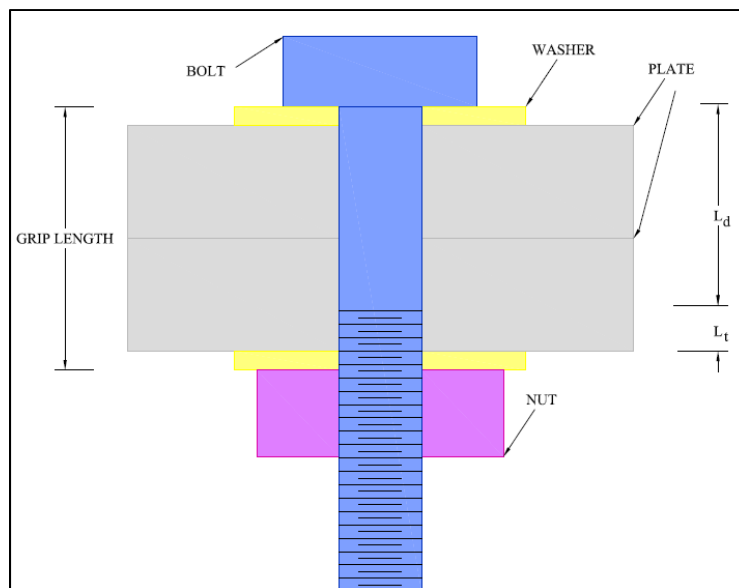
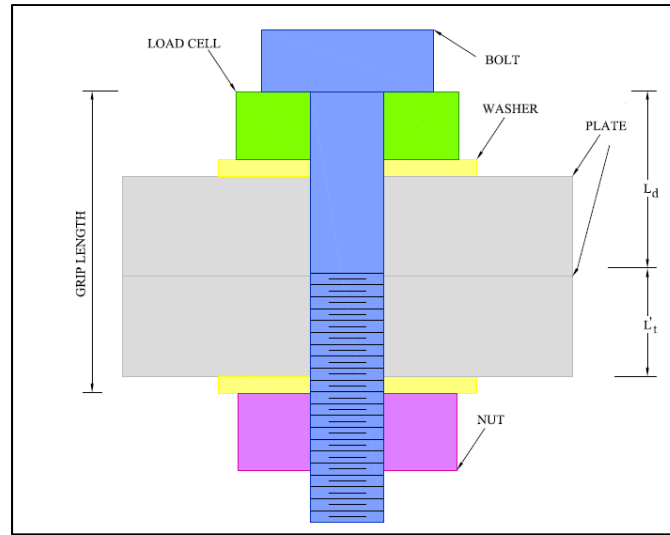Figure 2-3 Grip length before inserting load cell

Figure 2-4 Grip length after inserting load cell

As mentioned above, in most previous studies researchers used load cells to measure preload. The advantages of using a load cell are easy replacement, maintenance, and set-up. However, the biggest disadvantage of this is a significant change in the geometry of the joint. To measure preload, a load cell must be inserted between the bolt head and plate or between the nut and plate. In doing so changes the grip length and stiffness of the joint. (See Figure 2-3).

Grip length is a dominant parameter for both bending moment and stiffness. Yang et al. have shown that a reduction of bending stiffness of the bolt, which is inversely proportional to length, increases resistance to self-loosening. (Yang et al., 2010)

Total joint stiffness before inserting load cell is (Adapted from Budynas & Nisbett, 2008, page 413):

$$\frac{1}{K_t} = \frac{1}{K_b} + \frac{1}{K_n} + \frac{1}{K_{w1}} + \frac{1}{K_{p1}} + \frac{1}{K_{p2}} + \frac{1}{K_{w2}} \tag{2-1}$$

and after inserting load cell will be:

$$\frac{1}{K_t'} = \frac{1}{K_b'} + \frac{1}{K_n} + \frac{1}{K_{w1}} + \frac{1}{K_{p1}} + \frac{1}{K_{p2}} + \frac{1}{K_{w2}} + \frac{1}{K_{cell}} \tag{2-2}$$

$$K_b = \frac{A_t A_d\, E}{A_d L_t + A_t L_d} \tag{2-3}$$

$$K_b' = \frac{A_t A_d E}{A_d L_t' + A_t L_d} \tag{2-4}$$

Where A_d, A_t, L_t and L_d are section areas of the unthreaded portion, section areas of the threaded portion, effective threaded length, and length of the unthreaded portion, respectively. Therefore, adding a load cell to the joint changes joint stiffness directly by adding stiffness to the system and changing bolt stiffness.

Accordingly, when the effect of self-loosening is the objective of the study, using a load cell is not an acceptable method for preload measurement.

To resolve this problem in the current study, a strain gauge that can be installed in the bolt is used as the preload sensor to keep the grip length and bolt's stiffness unchanged. As shown in Figure 2-5, a KYOWA KFG-3-120-C20-11 strain gauge with a cylindrical shape is specifically designed and fabricated to measure bolt strain.
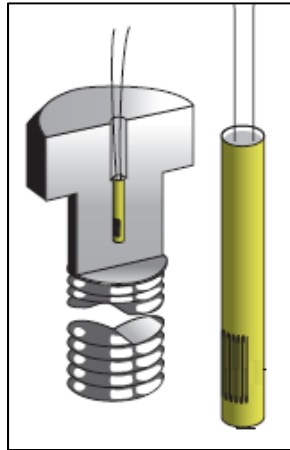

Figure 2-5 Strain gage
(KYOWA Catalog,
See APPENDIX I)

A 2mm diameter hole in the bolt is required to install this gauge (KYOWA Catalog, See APPENDIX I, Strain gage catalog, KYOWA). To compare the stiffness of the bolt before and after installation of the gauge, a simplified calculation for a cylinder with an equal diameter to the bolt is presented below.
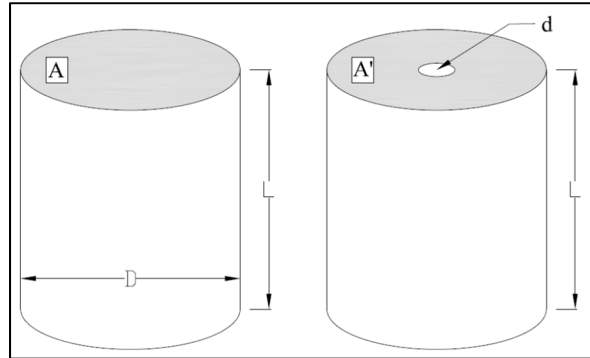
Figure 2-6 Cylinder with and without hole

$$K = \frac{EA}{L} \quad , K' = \frac{EA'}{L} \rightarrow \frac{K'}{K} = \frac{A'}{A} = \frac{(D^2 - d^2)}{D^2} = \frac{(12^2 - 2^2)}{12^2} = 0.97$$

Even if the hole is considered as a thru-hole, it can only change the stiffness of the bolt by about 3%. In order to measure the force more accurately, the strain gauge should be installed as far as possible from the bolt head and nut. Therefore, it has been installed at a depth equal to the average distance of the plate contact surface (14mm from bolt head, see Figure 2-7). The actual length of the hole is about 25mm. As a result, the change in the stiffness of the bolt will be much less than 3% in real conditions for an M12 bolt, which is quite acceptable.
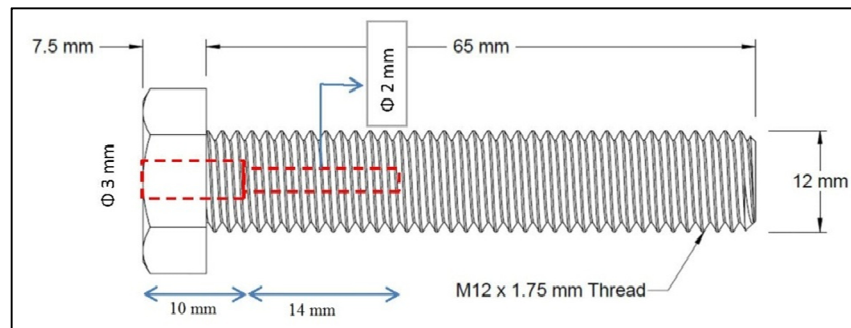

Figure 2-7 Preload sensor position in the bolt

The strain gauge is installed according to the manufacturer manual, using epoxy glue. To make sure that the strain gauge returns correct values, it must be coaxial with the bolt.

Increasing this gap will lead to have an excessive thickness of the glue film and can increase the possible inclination angle (see Figure 2-8).

An automatic CNC machine was used to drill the bolts to achieve a 0.1 mm tolerance. The maximum possible inclination for this sensor will be 0.5°, which is completely negligible.
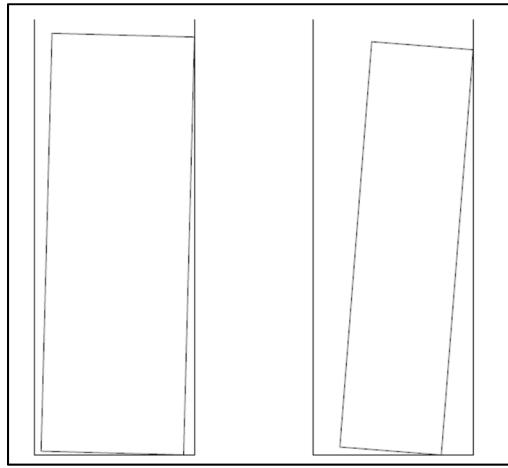

Figure 2-8 Effect of tolerance on
inclination angle

$$Max\ inclination\ angle = arcsin\frac{+\ tolerance}{sensor\ length} = arcsin\ \frac{0.1}{12} \approx 0.5\ degree$$

Essentially, a strain gauge is a sensitive electrical resistor inserted into a very thin, flexible, non-conductive sheet. Usually, the resistor portion is called the grip or coil. The non-conductive sheet is attached to the surface of the object using a suitable adhesive (depending on base material). As the object deforms, it moves the coil and changes its electrical resistance. These changes are translated to strain values using a constant value called "gauge factor". When the adhesive film between strain gage and the object surface is too thick, the measured data is a combination of object strain and shear deformation of the adhesive layer. Hence, it is very important that the layer between the gauge and object surface be as thin as possible. For the strain gauge used in the current design, the hole tolerance affects the glue

layer thickness. The abovementioned effects show the importance of fabrication tolerance and installation accuracy.

To improve the rig performance and to ensure the straightness of the gauge being installed, a vertical rod is used as an installation guide (See Figure 2-9). When the gap between the gauge and the rod is small, the whole fixture works like a sliding guide and does not allow the gauge to tilt. In the installation process, after the positioning of the bolt and guiding rod, the adhesive is applied to the internal surface of the hole. To ensure a successful installation, it is very important to control the movements of the strain gage. If the strain gauge sticks to the wall surface before its final position, it must be removed. If this is repeated many times, the adhesive needs to be removed from the hole surface and the gauge needs to be replaced as it might have eventually be deformed. It is also very important to ensure that the adhesive covers the entire surface of the hole and that it is distributed evenly to maximize the contact surface of the gauge and the bolt. According to the installation manual, the gauge must be dried out at room temperature for 24 hours prior to use. A strain gauge is installed in every of four M12 bolts which are directly calibrated to measure force. The calibration is performed with an MTS 810 tensile machine. Figure 2-13 shows one of the calibration curves as an example. All four SFC Grade 8.8 bolts are calibrated up to 50% of the yield.

For M12 bolt, the max yield force will be: $F = S_y \times A = 640$ (MPa) $\times 84.3$ (mm^2) $= 26976$ N. Figure 2-13 and Figure 2-14 show the results of calibration for one of the bolts. As the grips of the tensile machine are designed to hold parts with standard sections, they cannot hold a bolt directly. Therefore, an adapter must be used to perform the calibration on the MTS 810 tensile machine. As shown in Figure 2-12, the adapter consists of two parts. Part A has, on one end, a notch with a diameter bigger than the bolt stem and smaller than the head width and has a cylindrical shape on the other end. The cylindrical part is made according to the standard specimen dimensions for the tensile machine. The dimension of the notch limits the application range. The adapter is designed to avoid excessive bending at the bolt head. It is not recommended to use Part A for bolts that are more than one size smaller than   the nominal size it is designed for. Part B has a standard section for the tensile machine on one

end and a female threaded connection on the other end. The female thread is unique for each size and therefore a special adapter is needed for each size. All parts have been machined at the ETS machinery workshop.
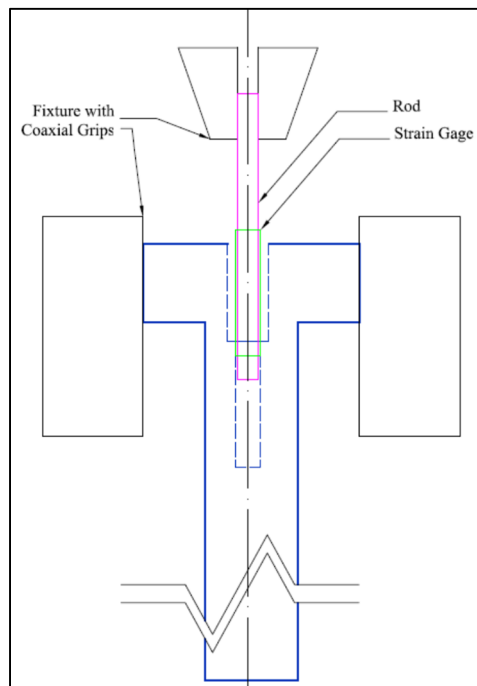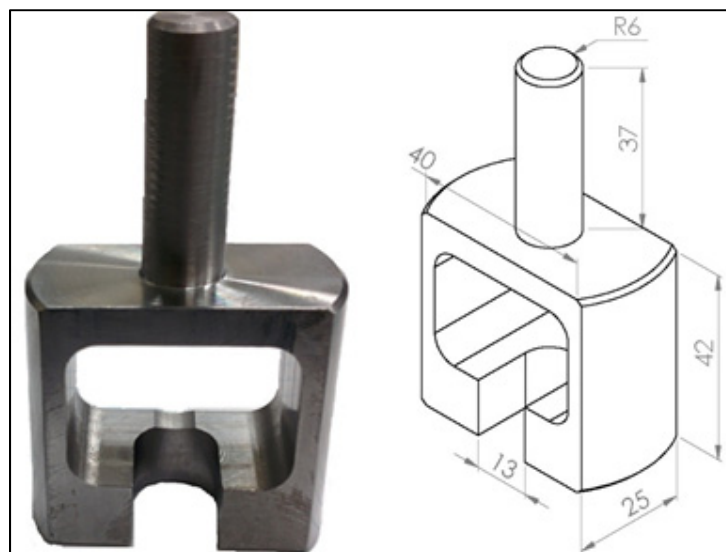

Figure 2-9 Installation fixture
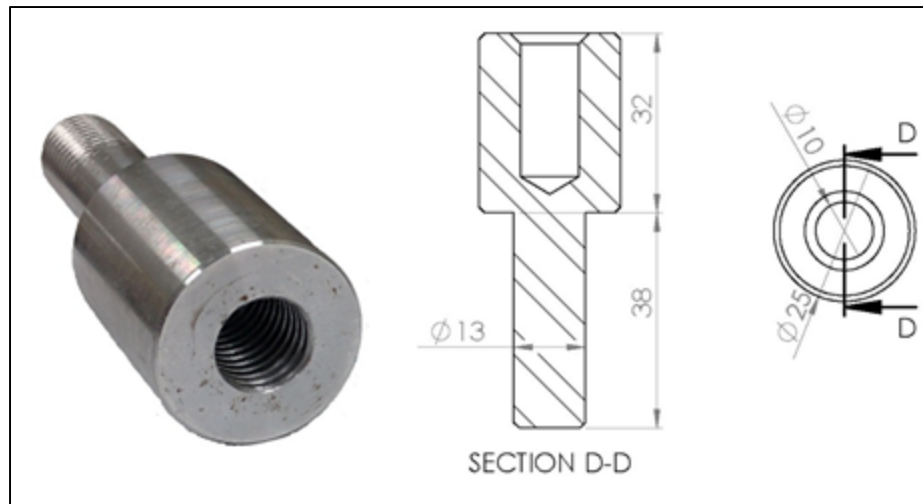

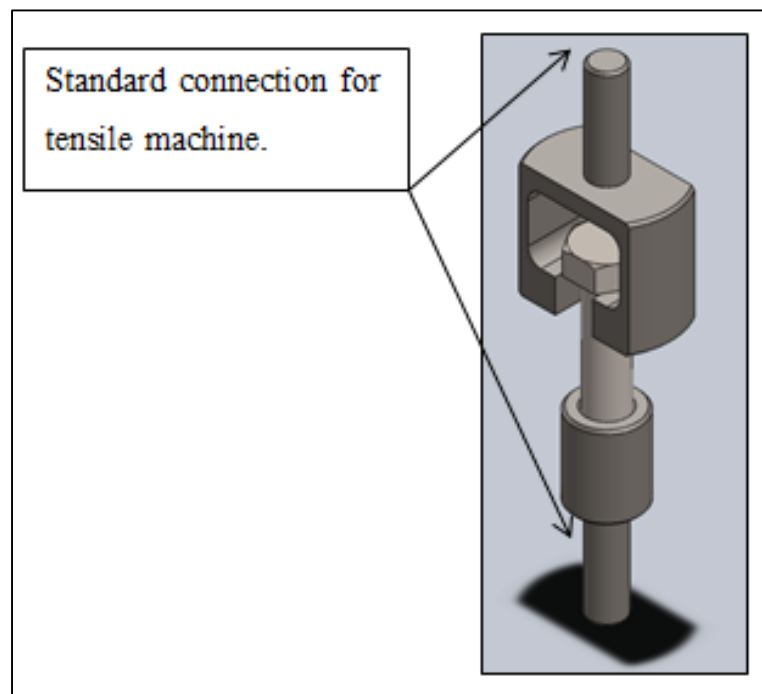Figure 2-10 Adapter, Part A

Figure 2-11 Adapter, Part B
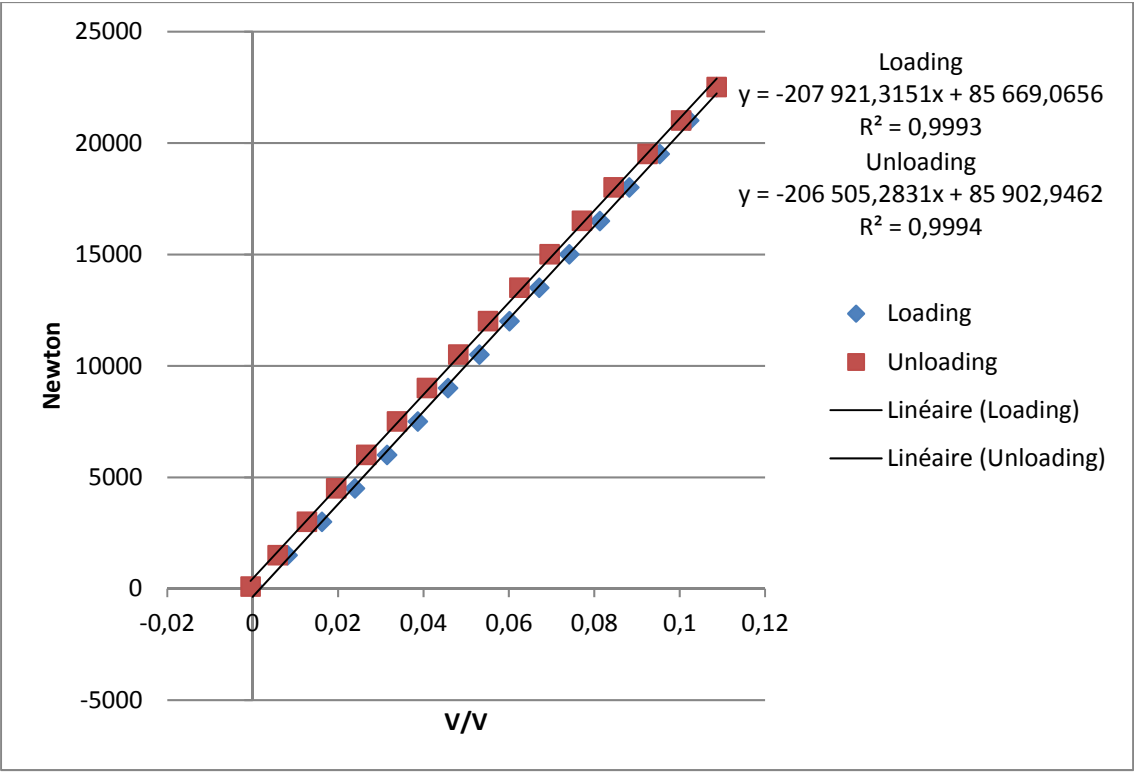

Figure 2-12 Adapter set with bolt
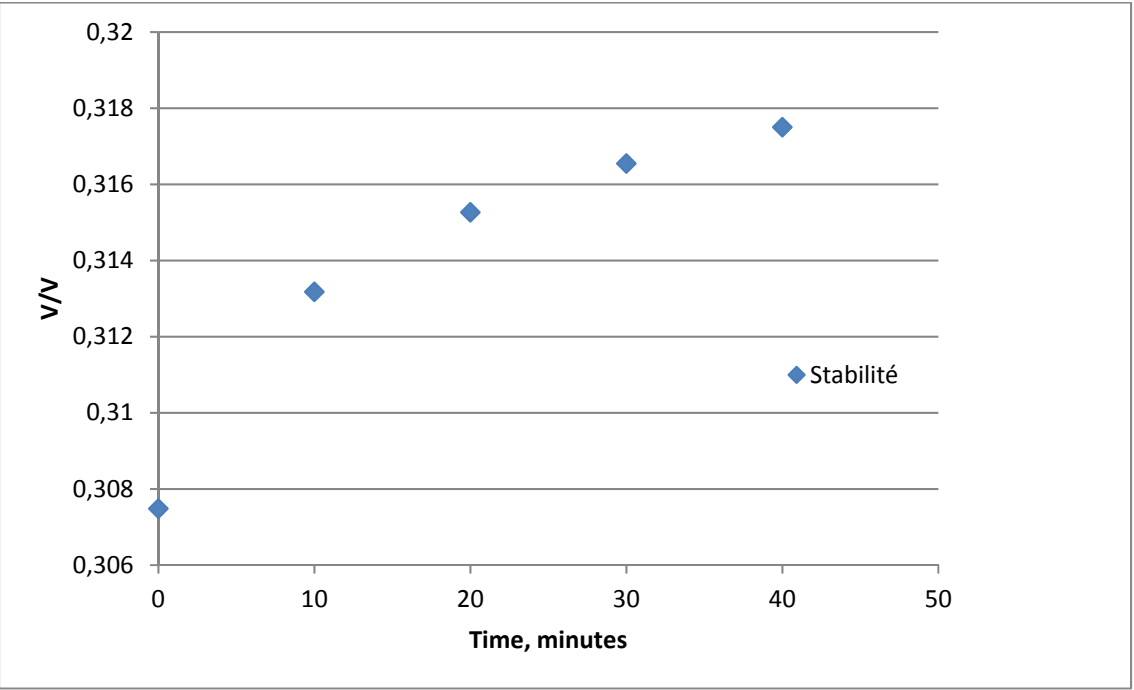
Figure 2-13 Bolt calibration results

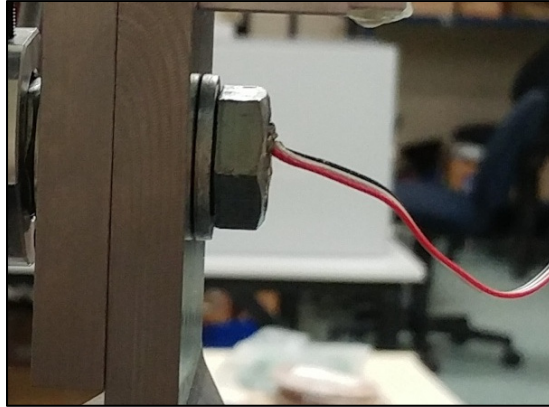Figure 2-14 Bolt strain stability results

Figure 2-15 Strain gage installed in the bolt

2.4   Rotation sensor

The relative rotation of the bolt and nut is one of the indicators of when stage II commences and is an important factor in the study of self-loosening. The relative rotation is the difference between the global rotation of two objects. When one of the object's global rotation is zero, global rotation of the other object will be equal to the relative rotation.

$$\vec{R}_R = \vec{R}_1 - \vec{R}_2 \xrightarrow{\vec{R}_2=0} \vec{R}_R = \vec{R}_1 \qquad\qquad 2\text{-}5$$

A CP-2UT LVRT Linear Velocity Rotation Transformer from MIDORI PRECISIONS is used as the rotation measuring devise (Figure 2-16). This sensor measures the rotation directly and the part under measurement must be connected to its shaft. The general idea of the rotation measurement system is to fix the nut and measure the rotation of the bolt. The rotation measurement assembly consists of a sensor support, nut holder, spacer, and holding bolts (Figure 2-20).

Figure 2-17 shows the sensor support. The rotation sensor is installed on the fixture with two jam nuts; these nuts allow for a slight adjustment of the sensor axial position.
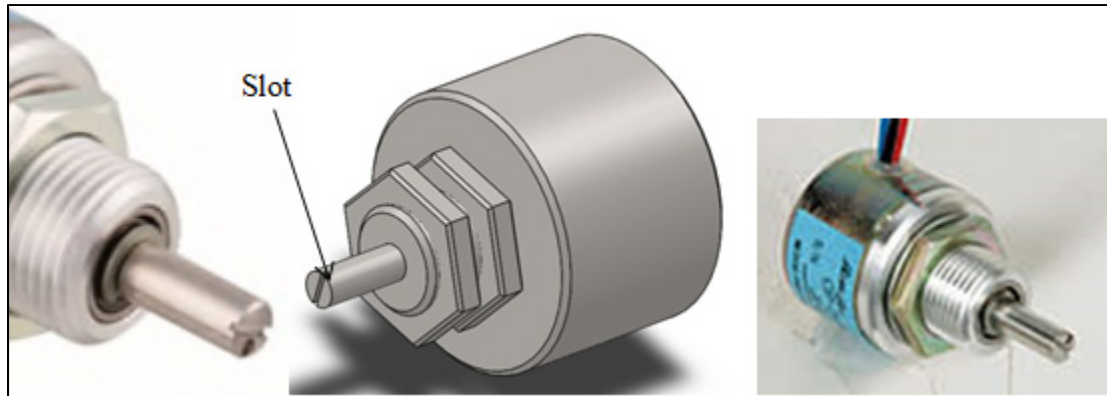
Figure 2-16 Rotation sensor (MIDORI_PRECISIONS, 2009)

To constrain nuts with different sizes, the nut holder shown in Figure 2-18 is used. The three surfaces of the nut (one in between) are fixed with three M3 bolts in the nut holder. As shown in Figure 2-20, the nut holder is fixed to the rotation sensor support via three M3 bolts. The resulting structure forms a rigid body that includes the nut holder, sensor, and sensor support. As the bolt and the nut are free to rotate, their relative rotation can be directly measured.
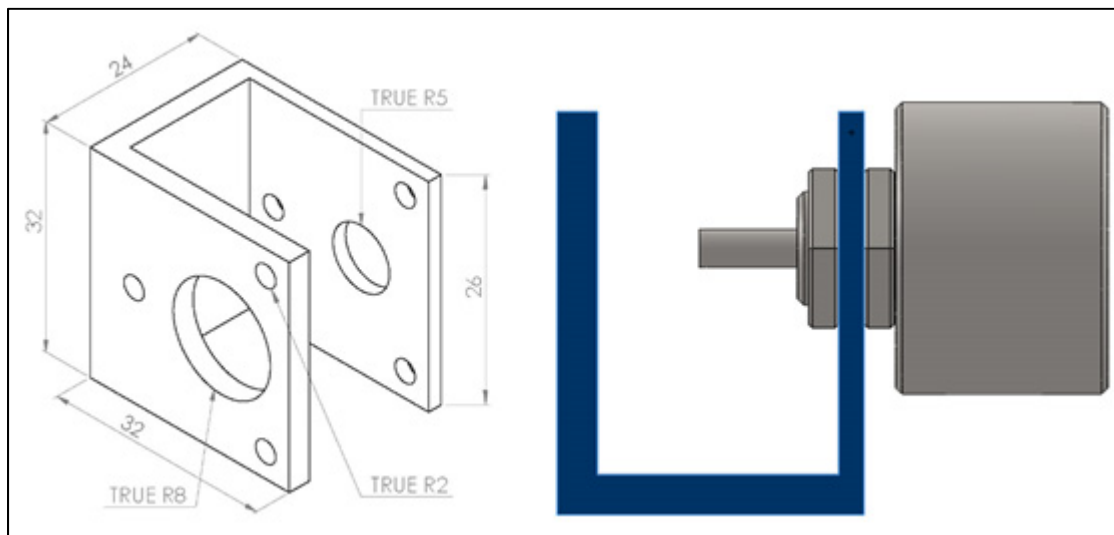

Figure 2-17 Sensor's support

The sensor support can be used for all combinations of bolts and plates in the design range but each bolt size needs a specific nut holder.

In order to be able to use the rotation measurement assembly for all thicknesses in the design range, the distance between the sensor shaft head and the far side surface of the plates has to be fixed. As shown in Figure 2-21, when the plate thickness (L2) changes, the distance between the sensor shaft and the far side plate surface (L1) changes and the bolt cannot touch the sensor shaft. This problem was resolved by making the sensor fixture, nut holders, and bolts of different lengths. Alternatively a spacer with different length is used to adjust this distance. The nut holder and sensor fixture are made for an assembly with two 14mm plates and the thickness of the different spacers is accordingly. Inserting the spacer between the nut holder and the sensor fixture keeps the length L1 fixed. The three bolts that connect the nut holder to the sensor fixture pass through the coincident holes of the spacer. The nut holder and the spacer for the 10mm plates are illustrated in Figure 2-18 and Figure 2-19 respectively.
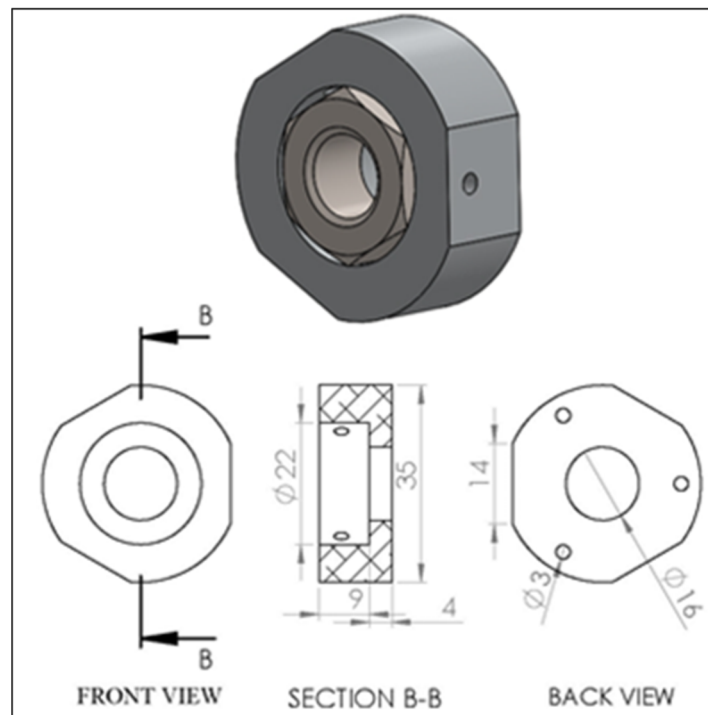

Figure 2-18 Nut holder

The sensor shaft is provided with a slot to create a better contact with the object and reduce sliding between the sensor and the object (See Figure 2-16). As shown in Figure 2-22, the bolt end surface is machined with a recess which goes into the sensor slot to transmit rotation. The less clearance there is between the slot and notch, the more accurate the rotation measurement will be.
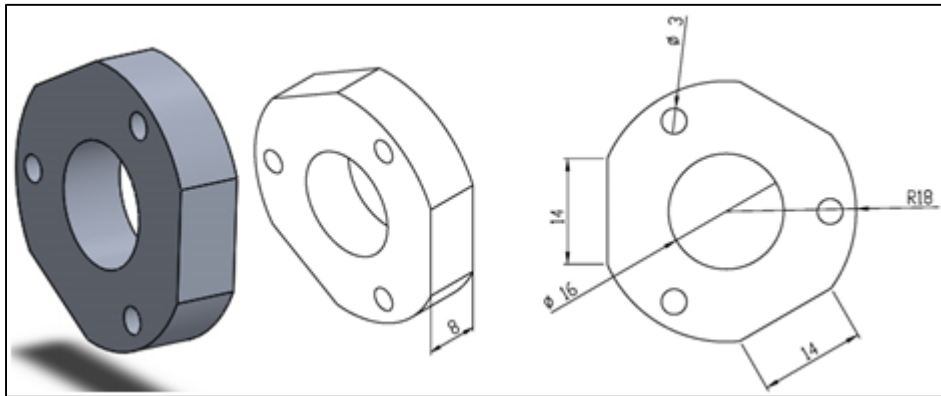

Figure 2-19 Spacer - M12 bolt and 10mm plates assembly

The rotation sensor is calibrated according to the manufacturer's instructions and the results of the calibration are shown in Figure 2-23.
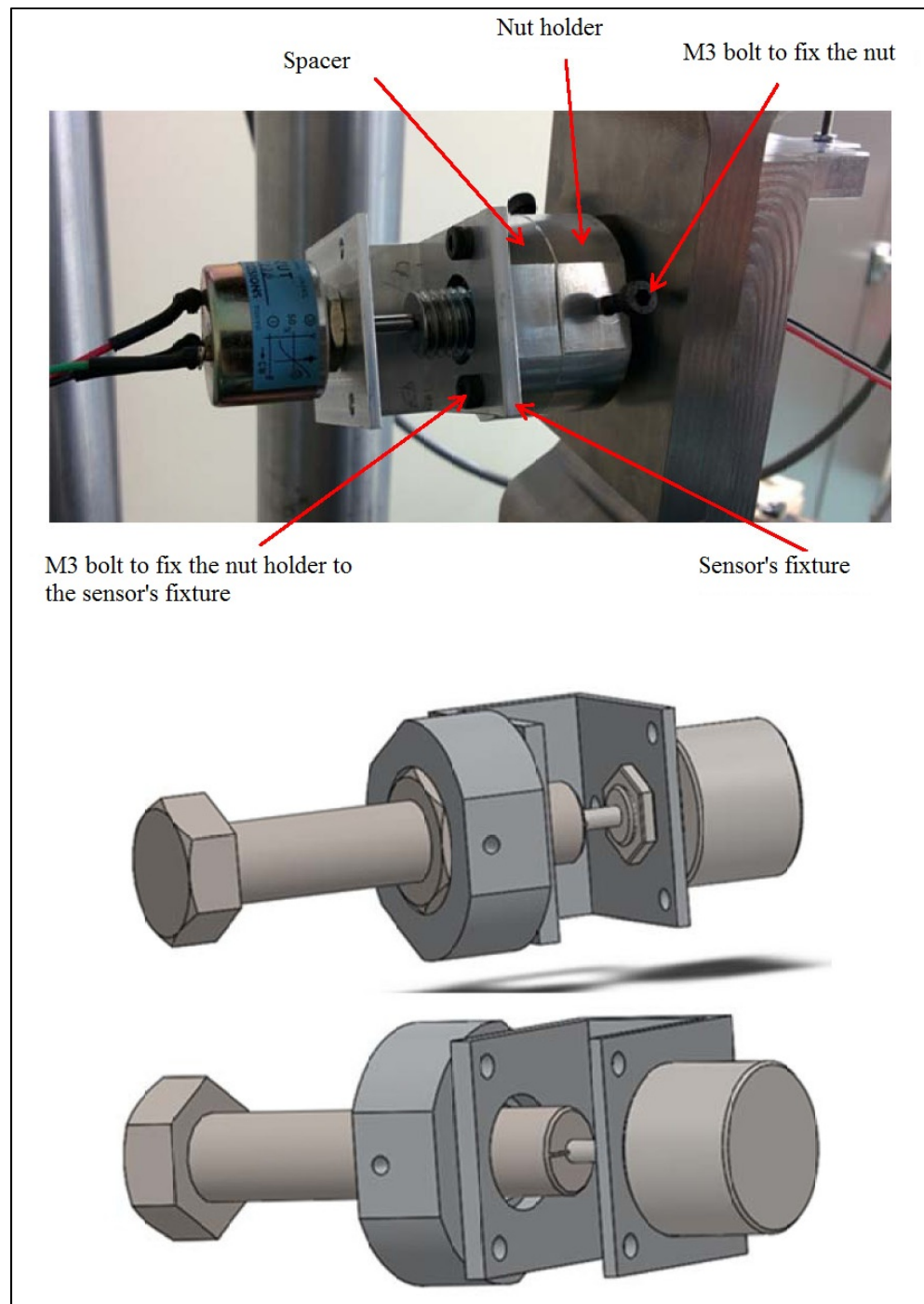
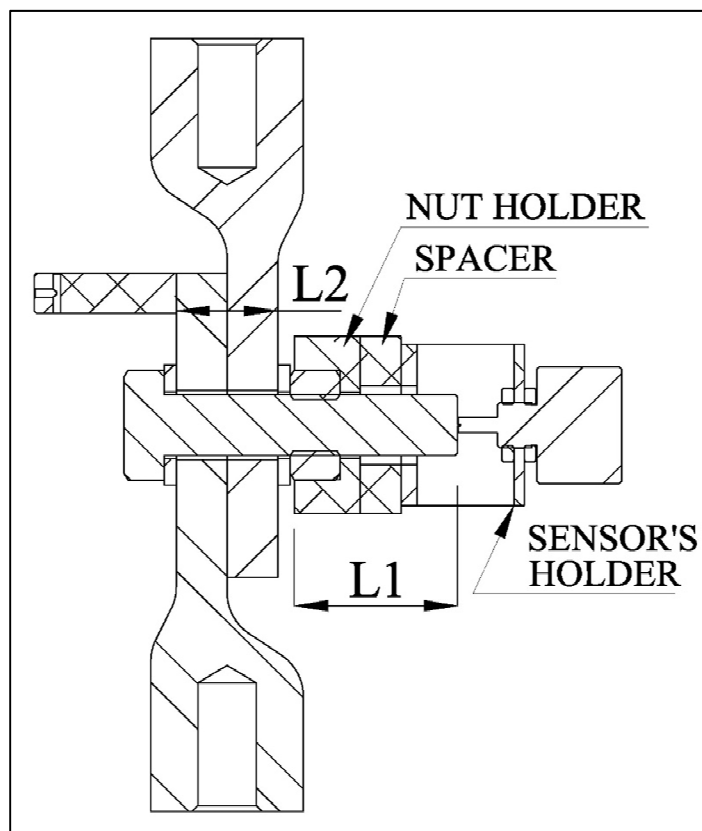Figure 2-20 Fixture of rotation sensor
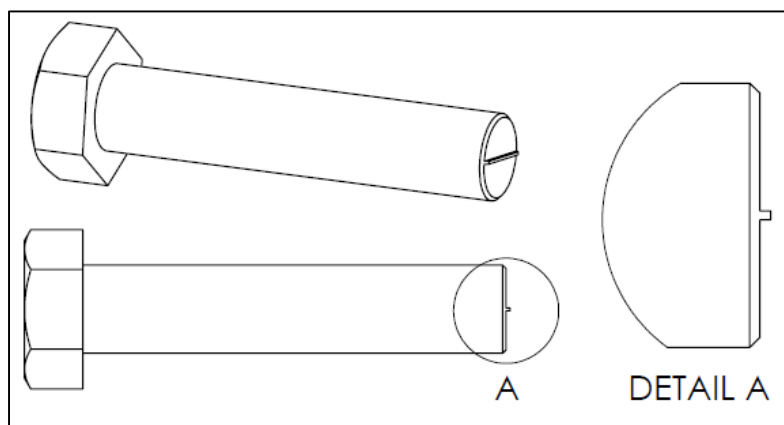
Figure 2-21 Section of rotation fixture

Figure 2-22 Bolt model with notch on the end
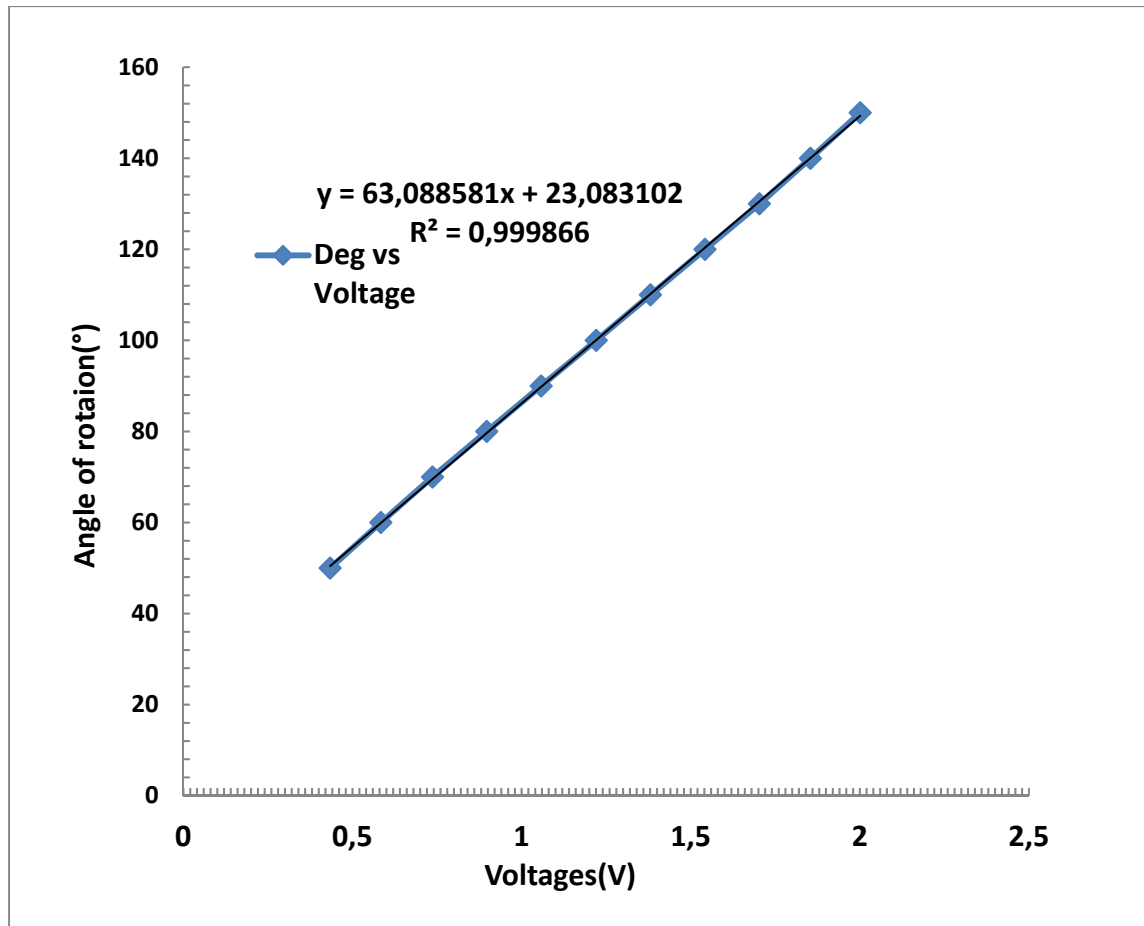
Figure 2-23 Calibration of rotation sensor

2.5 Lateral load cell

Self-loosening tests are performed under force or displacement control. Either the test is performed with a displacement control system or a force control system. Measuring lateral force is very important for the results analysis and safety.

A GSE load cell 5410-8k is used to measure the lateral force. This sensor has a female threaded connection on both ends. As shown in Figure 2-24, the force transducer is connected to the male threaded part of the stem on one side and to the test plate on the other side.

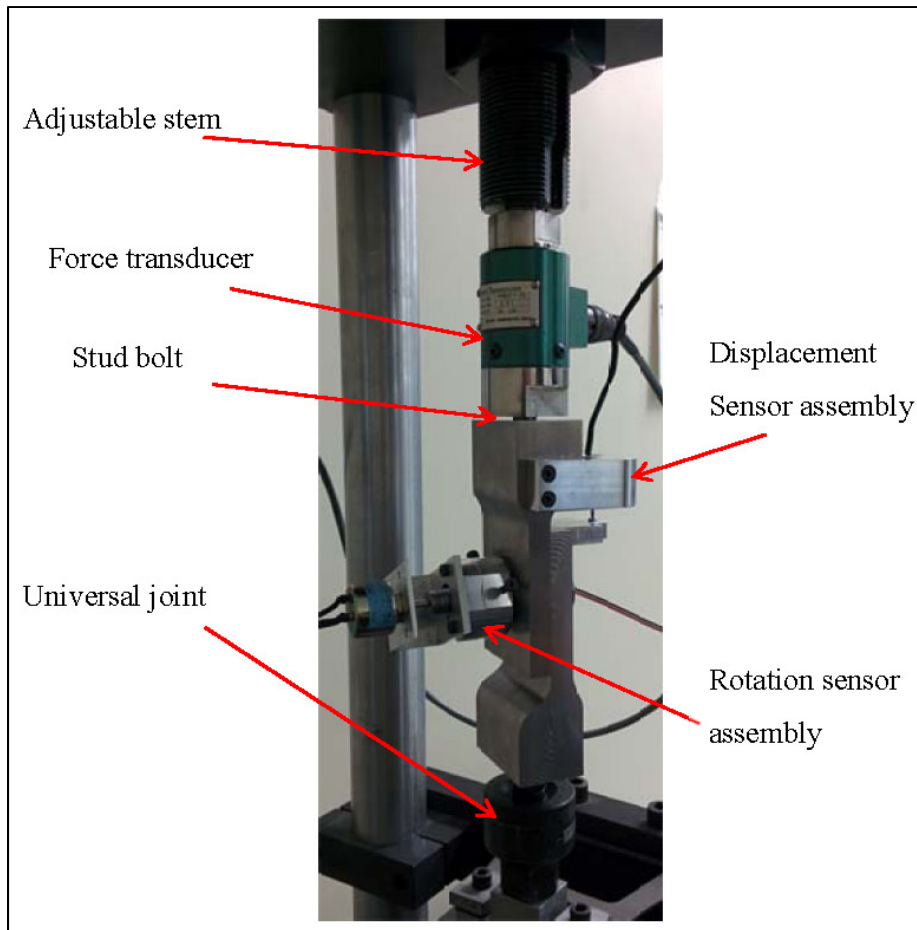Figure 2-24 Test set-up

In the current design, one of the clamping plates is connected to the actuator and the other one is connected to the lateral force actuator. A male threaded connector is required to connect the plate to the transducer but as the connection size of the transducer is ½", it is not easy to make a male connector for all plates. The design range includes plates with a thickness smaller than ½" but connecting a ½" rod to a thinner plate causes many fabrication problems.

To make a female thread in the plate, a thickness bigger than the major diameter of thread is required. The remaining wall of the threaded area (T_1 and T_2) must be thick enough to sustain stresses caused by the lateral displacement (Figure 2-25). These conditions end up requiring a thickness larger than the thickness of the plates to be used in the study. The transition from a

thicker section to a thinner one while also simultaneously respecting the coaxial angles of the plate contact surface and of the axis of the machine, is the resulting challenge of the abovementioned conditions. A sudden change of thickness causes high residual stress and reduces the fatigue life of the plates. Adding a fillet has a notable effect on the stress intensification factor. The fillet radius is limited by the plate dimensions because the contact surface of the plates must be flat and any slope on this surface changes the clamping load during the test.
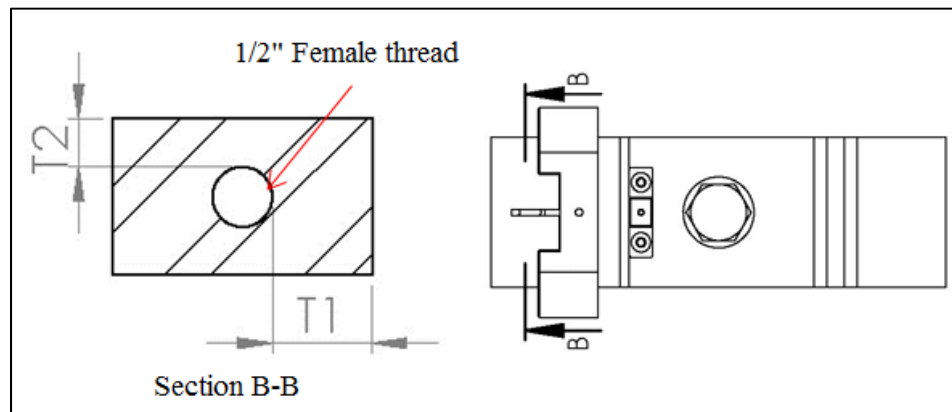

Figure 2-25 Plate section in transducer connection area

A simplified finite element analysis with no thread in the bolt and nut was performed to ensure that the plates are not overstressed. The model includes two plates of 12mm thick each, an M14 bolt, and a nut. A symmetry boundary condition is used to reduce the analysis time (Figure 2-26). Frictional contact is applied between the bolt head, the nut surface, and the corresponding plate surface. However, there remains a gap between the bolt stem and the internal surface of the hole, so a frictionless contact is considered to occur between them to simulate the possible contact. The maximum load capacity of the test machine is 8.9 kN. As explained before, safety measures have been implemented to cut off power in case of an overload (over 6 kN) to protect the actuator and electrical motor. Hence, the assembly is analyzed for three load cases:

- 9 kN of preload, 0.35mm displacement at the pivot point;
- 9 kN of preload , 6 kN force at the pivot point;

- 9 kN of preload, 7.2KN force at the pivot point.

The plates are made from structural carbon steel with S_y=250MPa and the bolt is grade 8.8 with S_y=600MPa.
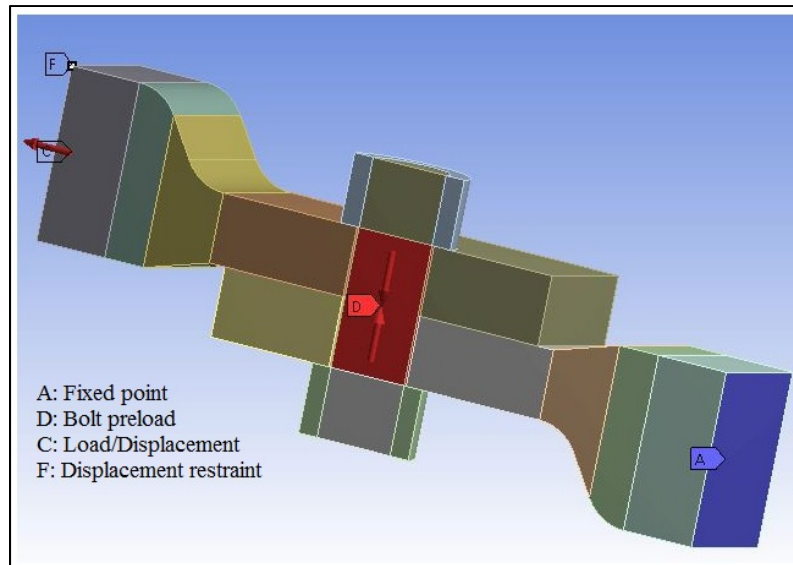

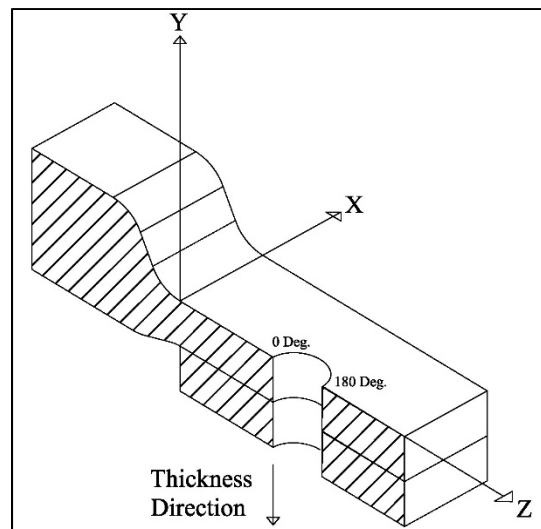Figure 2-26 Boundary Conditions
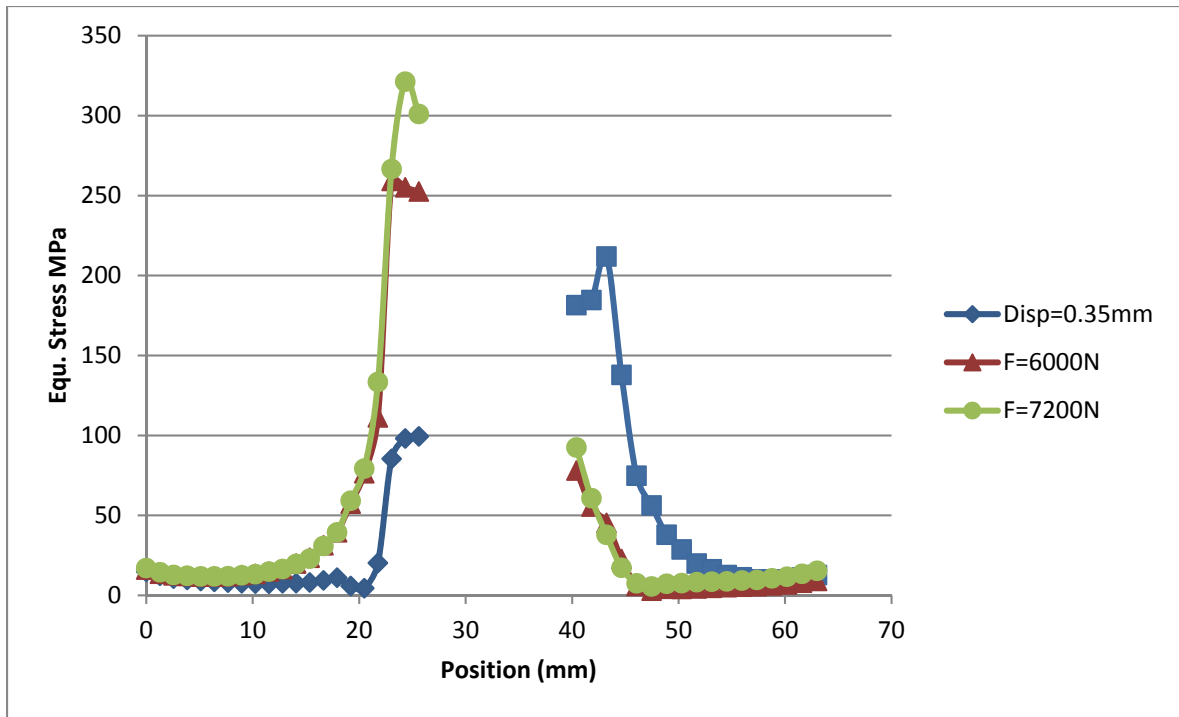

Figure 2-27 Coordinate system used in
FEA results

Figure 2-28 Equivalent stress in axial (Z) direction
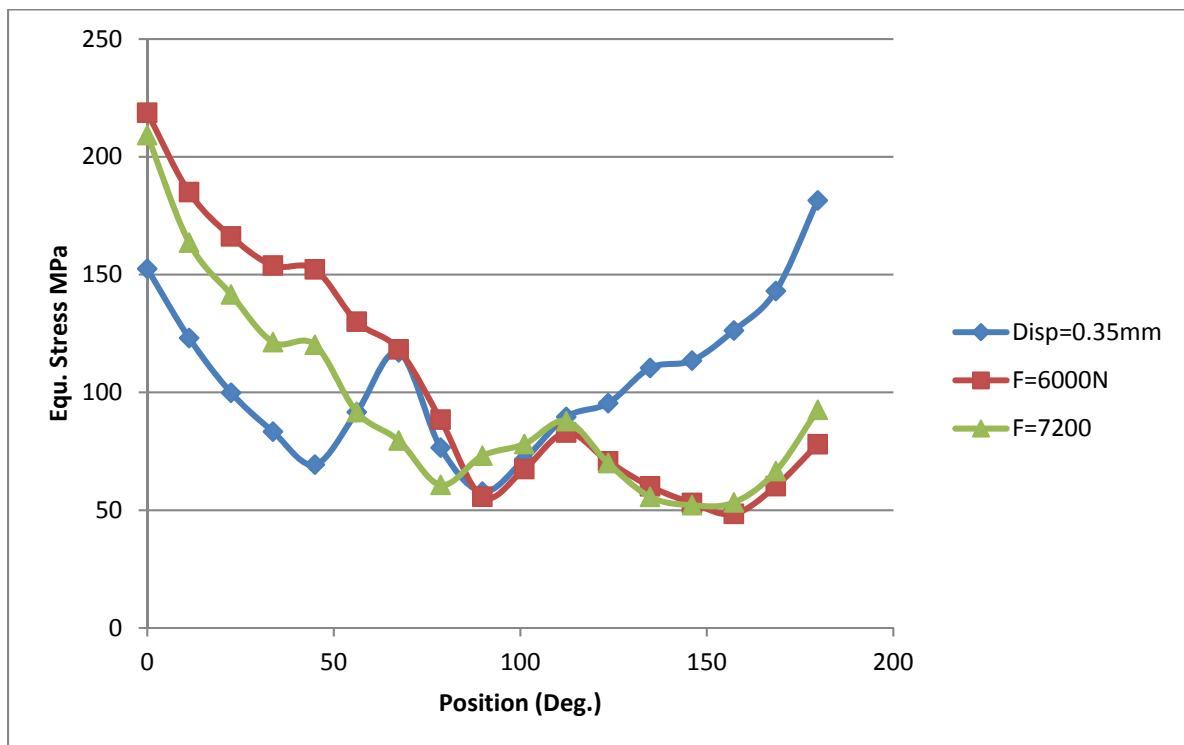
Figure 2-29 Equivalent stress around the hole
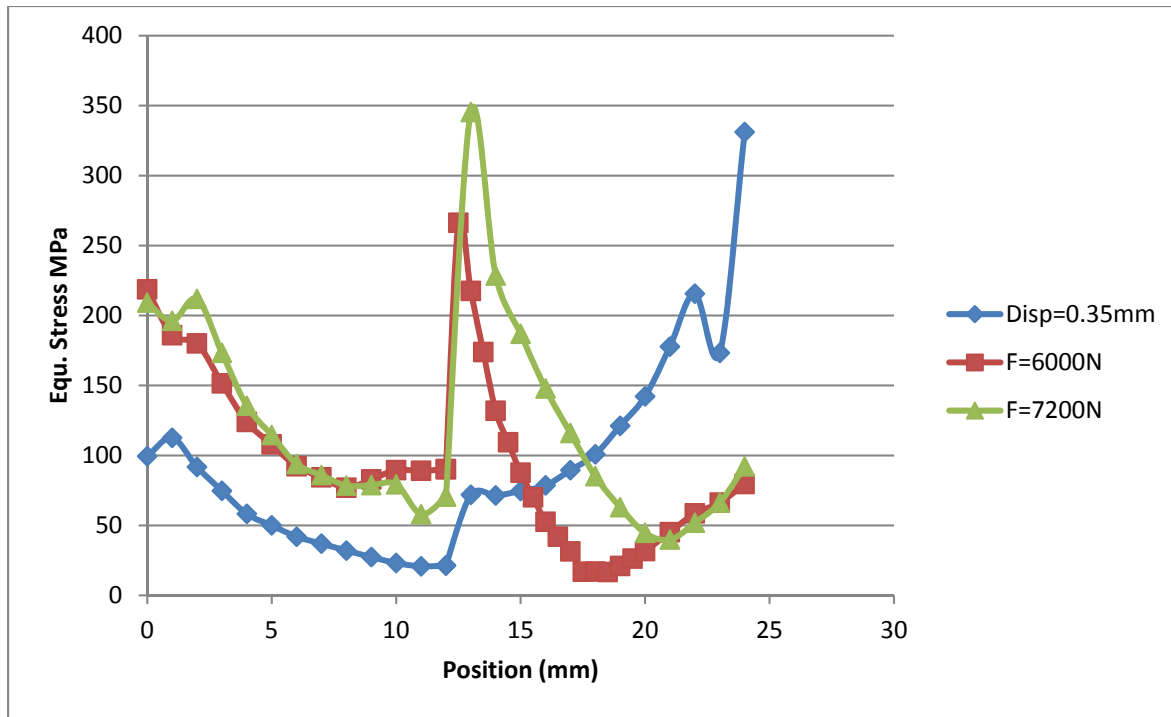
Figure 2-30 Equivalent stress distribution through plate thicknesses

Table 2-1 Boundary condition reaction- relative displacement of plates

Load Case	Reaction in Displacement B.C. (N)	Displacement in Force B.C. (mm)	Relative displacement of plates (mm)
Disp.=0.35mm	2874.8	-	0.0036
F=6000N	-	0.8350	0.0123
F=7200N	-	0.8480	0.0164

The stress at all points, except at the sharp edges which are singularity points, are below S_y, which indicates that the plate design is safe.

As it is shown in Figure 2-24, there are three threaded pieces connected from the lower plate to the actuator lever. If a regular threaded joint were used in all pieces, they could not be fastened together and be adjusted with the upper plate, which is tightened and fixed to the

lateral load cell. When the parts are tightened, their final angular position may be different. The ball and socket joint in the universal joint, which is used to connect lower plate to the actuator, allows this part to rotate in all directions independently. Therefore, the test set-up parts can be tightened and adjusted easily. The ball and socket joint in the universal joint allows free rotation and blocks translation; essentially, it eliminates bending moments on the plates and provides pure lateral displacement.

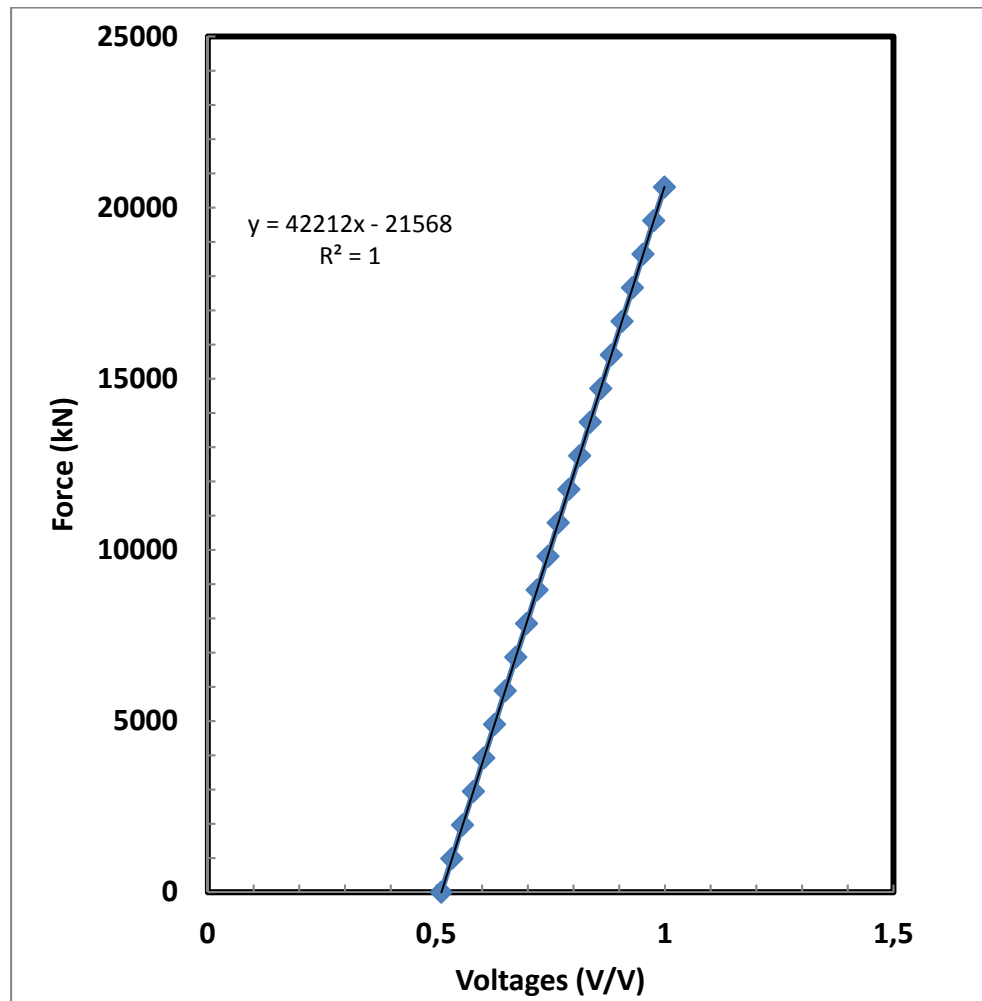The transducer calibration results are shown in Figure 2-31.

Figure 2-31 Results of load cell calibration

2.6   LVDT displacement sensor

A displacement control system is the most popular method to run self-loosening tests and is the method used in the current study. Therefore, it is very important to have a device to measure the displacement between two plates accurately. The test machine has a displacement adjustment system that provides the displacement on the actuator lever, but it is not accurate enough for a self-loosening test. In addition, the displacement at the bolt location is different from the pure relative displacement of the two plates at their free ends. The axial displacement is the sum of the deformation in the universal joint connecting bolts and the axial deformation of the plates. The closer the measuring point is to the bolt, the more accurate the measurement will be. Table 2-1 shows the difference between the displacement at the actuator connection point and the actual relative displacement of the plates and the importance of the displacement sensor location. A 0.835mm displacement of the actuator results in 0.0123mm of relative displacement.

The order of lateral displacement applied to the plates in self-loosening tests is a fraction of a millimeter. Therefore, the displacement sensor (LVDT, Linear Variable Differential Transformer) should be accurate to at least 0.001 of millimeter to be able to measure the displacement during a cycle.

An Macro CD 375-025 LVDT with a nominal range of ±0.63 mm was the selected, which is a magnetic contactless (frictionless) sensor. It consists of two parts: the fixed part is called casing and the mobile part is called the core. This LVDT measures displacement by measuring the electrical current changes caused by magnetic field alternation. Figure 2-32 and Figure 2-33 show the structure of the LVDT and illustrates how it functions. The primary coil (primary winding) is energized with constant amplitude AC current. When the core is in its primary position (midway point), the magnetic flux is coupled equally to both secondary coils and consequently the induced voltage in both coils is the same. When the core moves toward a secondary coil, more magnetic flux will be coupled to that coil and consequently,

more voltage will be generated in it. The difference between the voltage in the secondary coils indicates the core position. (TE_Connectivity_Corporation, 2017)

The manufacturer claims an infinitesimal accuracy. "Since an LVDT operates on electromagnetic coupling principles in a friction-free structure, it can measure infinitesimally small changes in core position. This infinite resolution capability is limited only by the noise in an LVDT signal conditioner and the output display's resolution." (TE_Connectivity_Corporation, 2017). It is very light and does not affect lateral load and as it is a contactless LVDT, it has an unlimited mechanical life.
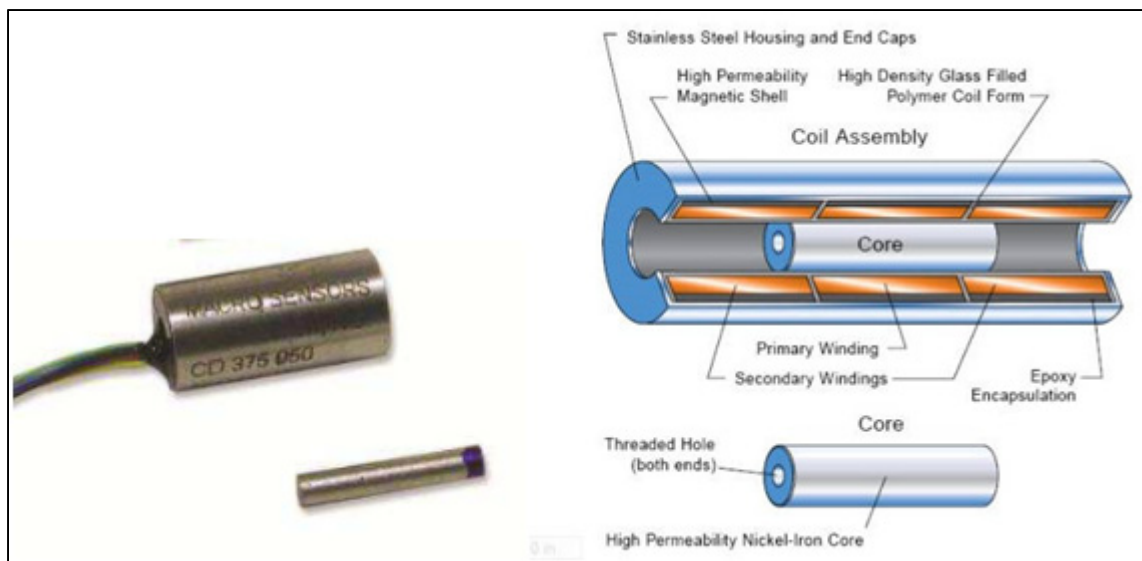

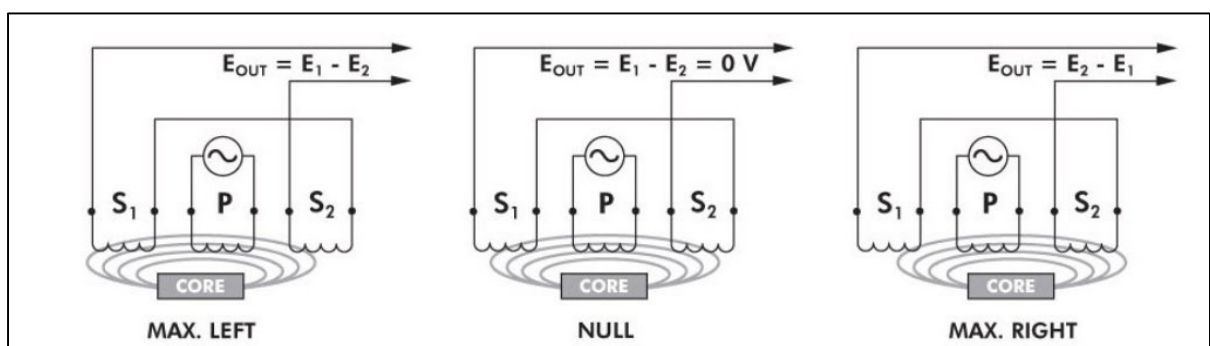Figure 2-32 Macro sensor, CD 375 (TE_Connectivity_Corporation, 2017)

Figure 2-33 Concept of LVDT performance (TE_Connectivity_Corporation, 2017)

To have the best possible measurement of displacement, the LVDT holder is installed on the plates. Because the LVDT wires are connected to the casing, it is better that it is installed on a fixed part. As shown in Figure 2-34, a U-shape holder has been designed for installation on the upper plate (fixed plate) to hold the casing. To make sure that the casing does not move, a hole is made at the centerline of the casing position in the U-shaped holder, which is then fixed in position by an M3 bolt.
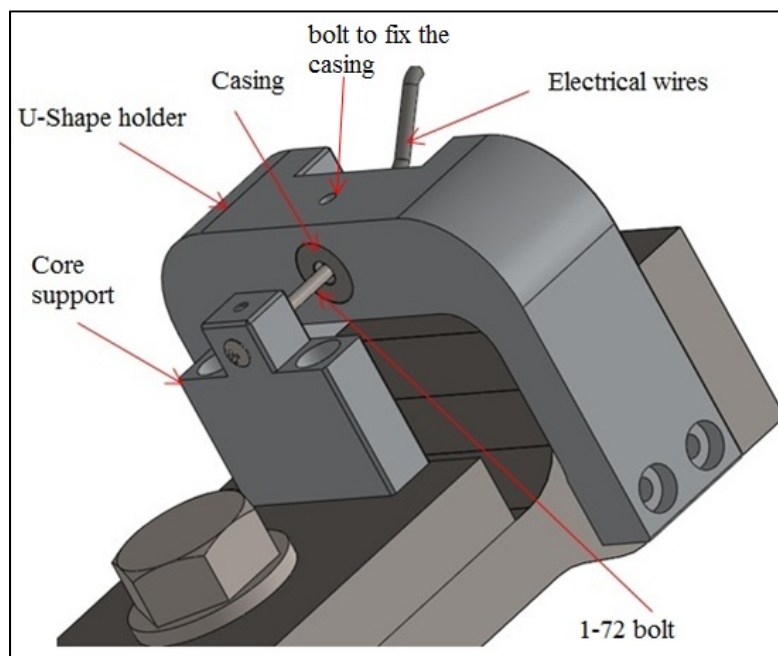
Figure 2-34 LVDT fixture

The core is held with a support on the lower plate (mobile plate). Both holders are connected to the plates with M3 bolts. The core has 1-72 UNF female threads on both ends and is connected to its support with a 1-72 bolt. There are two nuts on both sides of the support to adjust the position of the core in the casing. Figure 2-35 and Figure 2-36 show the position, details, and dimensions of the LVDT holder.

The results of the LVDT calibration are shown in Figure 2-37.

Figure 2-35 LVDT holders, position and details

Figure 2-36 Dimensions of LVDT holders

Figure 2-37 Results of LVDT calibration

2.7 Cycle counter
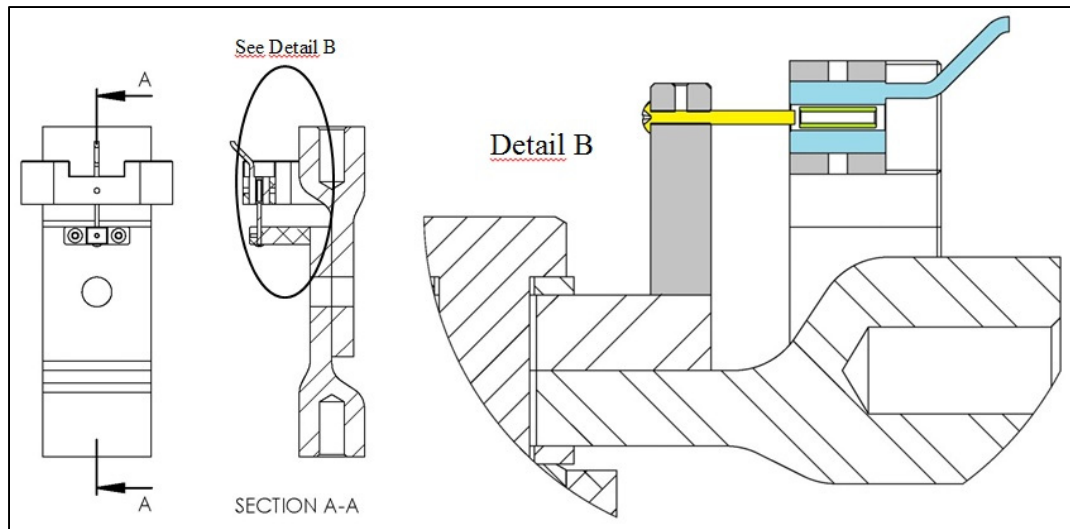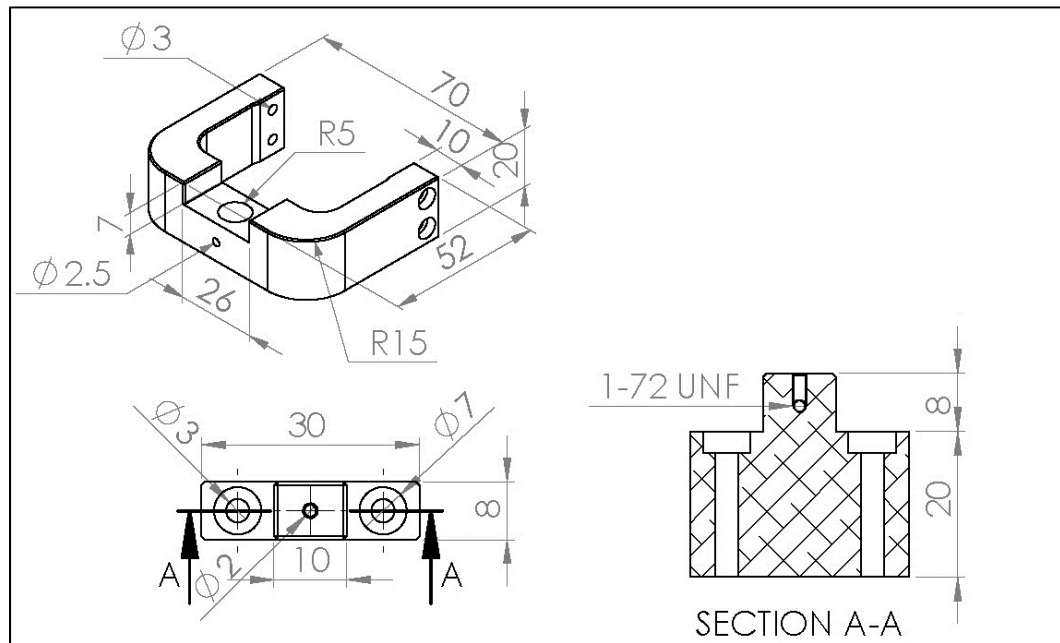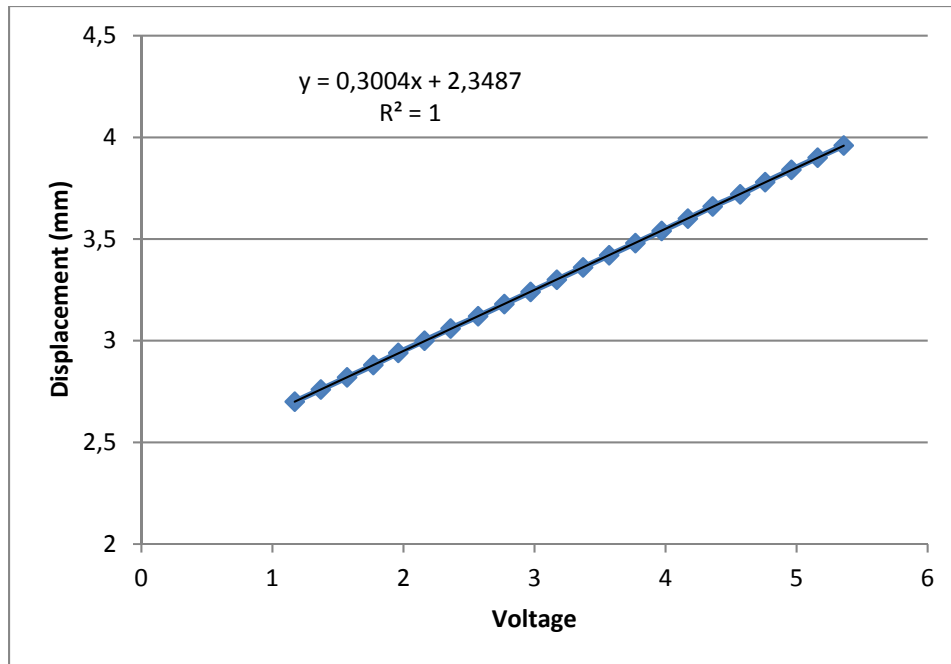
The test machine was originally equipped with a mechanical counter, as shown in Figure 2-1. This counter consists of a set of gears that connects the motor shaft to the counter. This counter controls the system with a countdown rule, where the desired number of cycles must be set at the beginning of the test. When the counter reaches zero, it stops the motor. The biggest disadvantage of this counter is that it can only count every ten cycles and cannot show nor detect each individual cycle. One issue with this system is connecting and matching the output signal of the counter to the data gathering system. This system does not generate any signal until it reaches zero and shuts down the motor.

For the self-loosening test, especially in the beginning of the test (stage I), it is very important to monitor and record cycles accurately as the self-loosening takes place and find a relationship between cycles and other measured parameters. To solve this problem, a magnetic cycle counter was added to the system. This sensor consists of a fixed and a mobile

part. The mobile part is a permanent magnet which when it passes the fixed part after each cycle inducts the internal coil in the fixed part and generates a signal.

The fixed part is installed on the body of the machine, facing the actuator lever, and the mobile part is installed on the actuator (Figure 2-38).
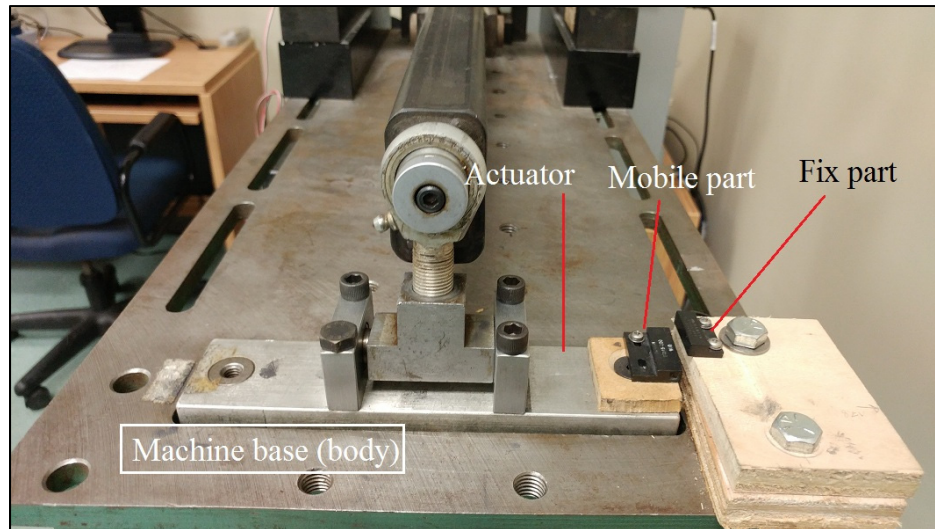

Figure 2-38 Cycle counter position

When the sensor coil enters the magnetic field of the mobile part, it generates a signal; hence their relative position should be set in such a way that the mobile part actuates the coil once per cycle. If not, the number of signals needs to be divided by two by the LabView program. In the current design, the fixed part is installed at an elevation equal to the max displacement that could be applied to ensure that the counter sensor always returns the exact number of cycles.

2.8   Test plates

As shown in Figure 2-39, the joint under study consists of a bolt, nut, washers on both side, and two plates. As mentioned before, the test plates must be designed such that the contact surface is kept in line with the axis of the lateral load sensor and the pivot point. The joint set-up shown in figure 2-39 guarantees the coaxiality of the joint and other parts.

Figure 2-39 Bolted joint set-up

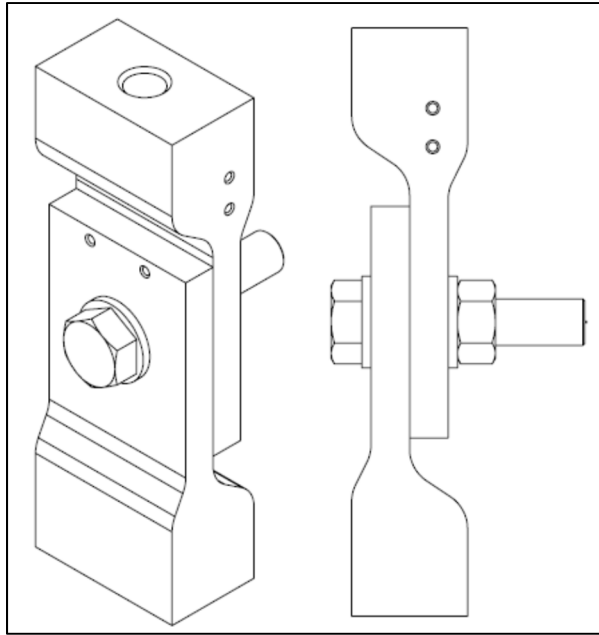The geometry of the test specimen, which has a thickness of 10 mm, is shown in Figure 2-40.The diameter of the bolt hole is dependant on the size of the bolt. In this case, the diameter of the hole is 12.5mm to accommodate the M12 bolt. The test plate and its connections are machined using an automatic CNC machine so as to form a solid part that minimizes the relative displacement between parts.
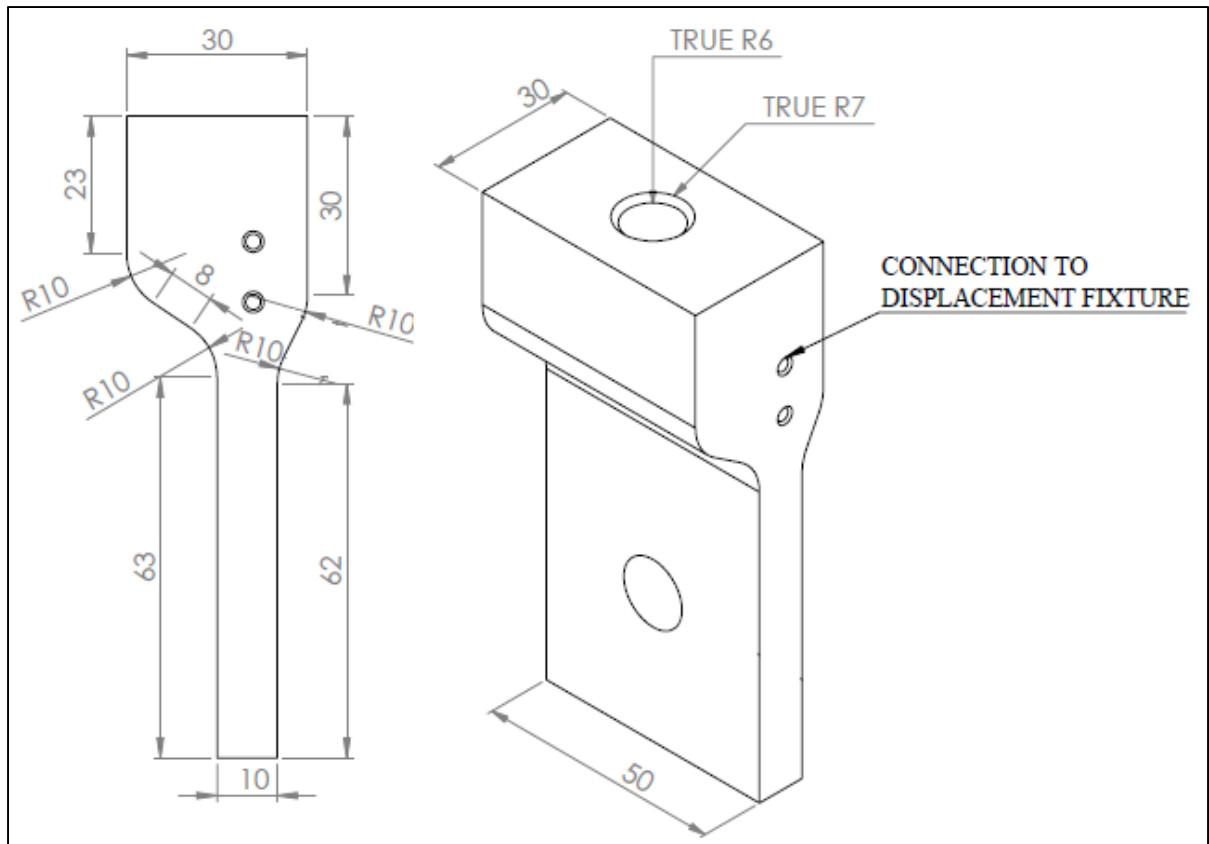
Figure 2-40 Test plate geometry

2.9 Data acquisition system

The data acquisition system consists of a mainboard and electrical kits (Figure 2-2). The main board distributes power and connects all sensors to the computer. LabView software is used to monitor the instrumentation and controls the on and off button. All input data are converted and compiled through the user interface program, which can monitor, control, and record data in real time converted to their relevant units. Figure 2-41 shows the LabView vi of the main program as an example.

Figure 2-41 A part of the main vi program of LabView

The input data in LabView consists of voltages, TC's and frequency from different ports on the main board. The program is used to convert such data to real values or on and off commands.

The final interface of the program is shown in Figure 2-42.:

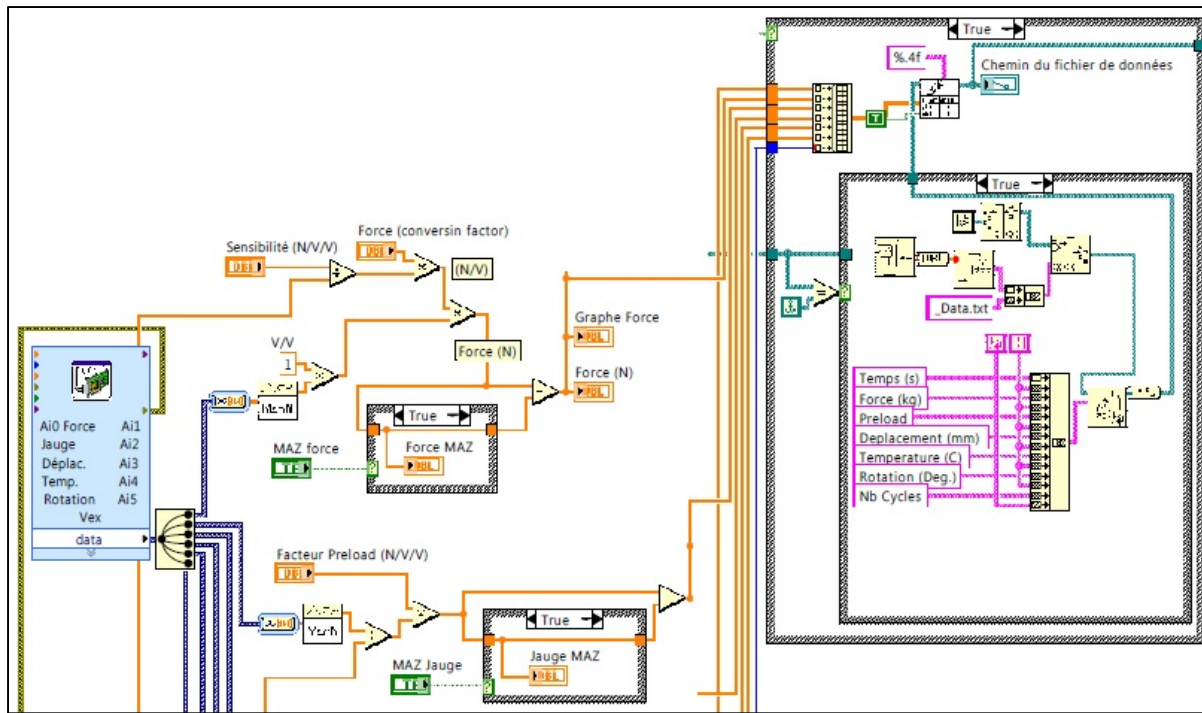- A1, B1, C1 and E1 show the boxes used to input the calibration factors for the lateral force sensor, preload sensor, LVDT, and rotation sensor respectively.
- A2, B2, C2, D, E2 and F2 show the actual reading values of the lateral force, preload, lateral displacement, temperature, and number of cycles respectively.
- M shows the activation and deactivation buttons and motor status (On/Off). For safety reasons, the motor can also be turned on and off via the interface panel.
- N shows the start button.
- P shows the path where the result file will be saved (.txt format). The file location can be set by the user for each test.
- T shows the time.

- S is the emergency shut-off button. This button cuts the main power to the test rig in emergency cases.
- In the chart area, by selecting each tab, a chart for the relevant parameter versus time is shown. Charts can also be exported. To better illustrate each chart, the upper and lower limit of the vertical axis can be set by the user to adjust the chart to the appropriate range of measured parameter.
- MAZ sets the parameters value to zero.
- A3 and F1 are safety values for the lateral force and the number of cycles respectively. When the system reaches one of these limiting value the test stops.
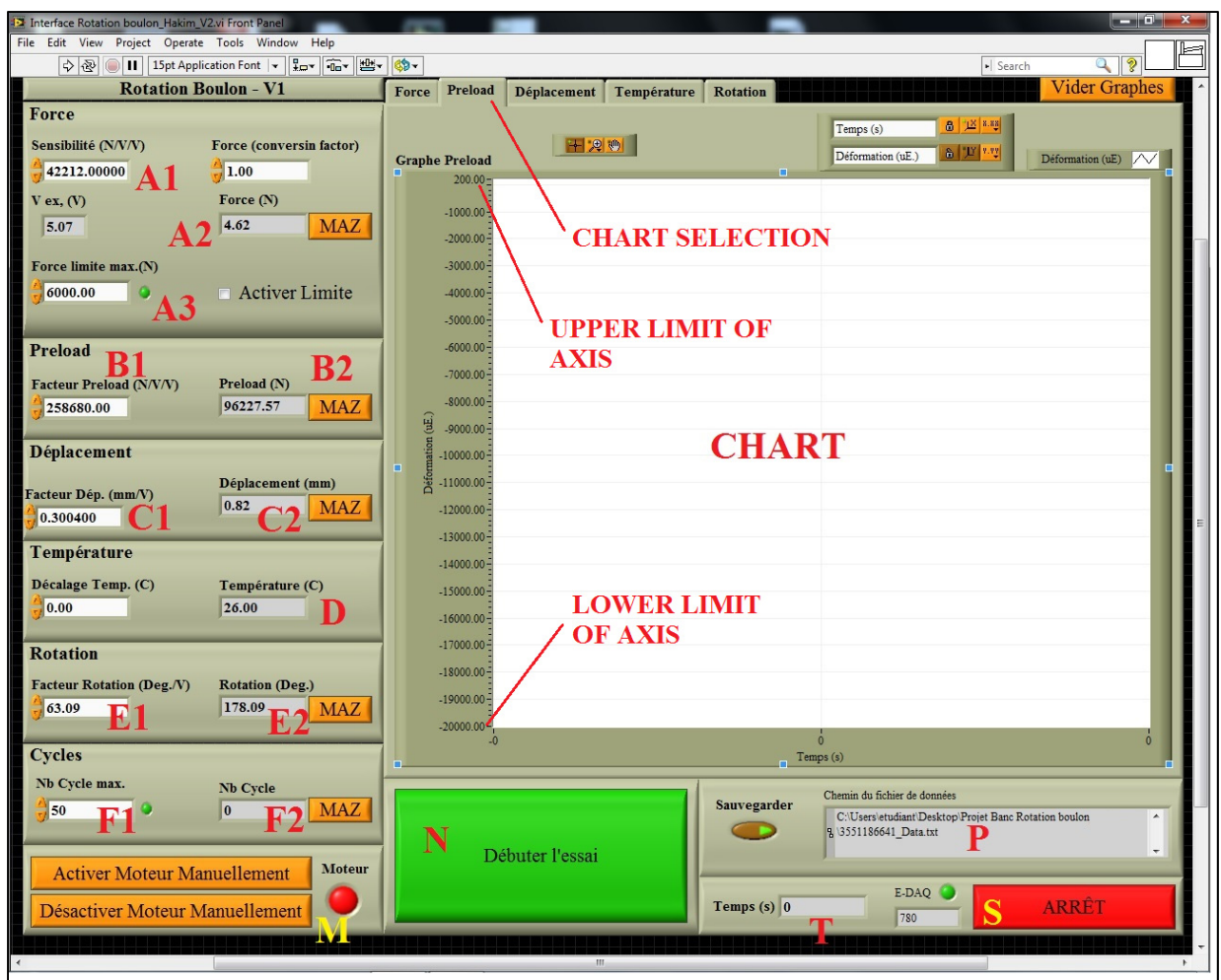

Figure 2-42 Data acquisition user interface

CHAPTER 3

FINITE ELEMENT ANALYSIS

3.1 Description of general model simulation

The F.E analysis of self-loosening in Stage I can be done using a simplified 2D model because there is no displacement or rotation in the third axis. However, when stage II is included in the analysis, rotation around the bolt axis and the helical geometry of the threads necessitates a full 3D finite element analysis. Friction between the threads, contact surfaces of the bolts and nuts with the plates, and friction between plates are important factors that must be included in the F.E. modeling.

The model for this study consists of an M12 (8.8) bolt with an hexagonal cap, an hexagonal nut, two washers, and two plates with a 10mm thickness functioning as the clamping parts. The actual geometry and dimensions of the threads of the bolt and nuts are considered in the 3D model.

The bolt preload is the main parameter to be investigated in this study. To simplify the analysis and reduce the run-time only limited areas around the plates are considered (20 mm on each side). The friction contact elements are used to simulate the contact surfaces of the mating parts, bolt, and nut.

One of the plates is fixed on one end and a lateral displacement is applied to the other plate. The geometry, boundary conditions, and meshing will be explained in further details in the following sections.

3.2 Material description

An Elasto-Plastic material with the following properties is used in the material definition.
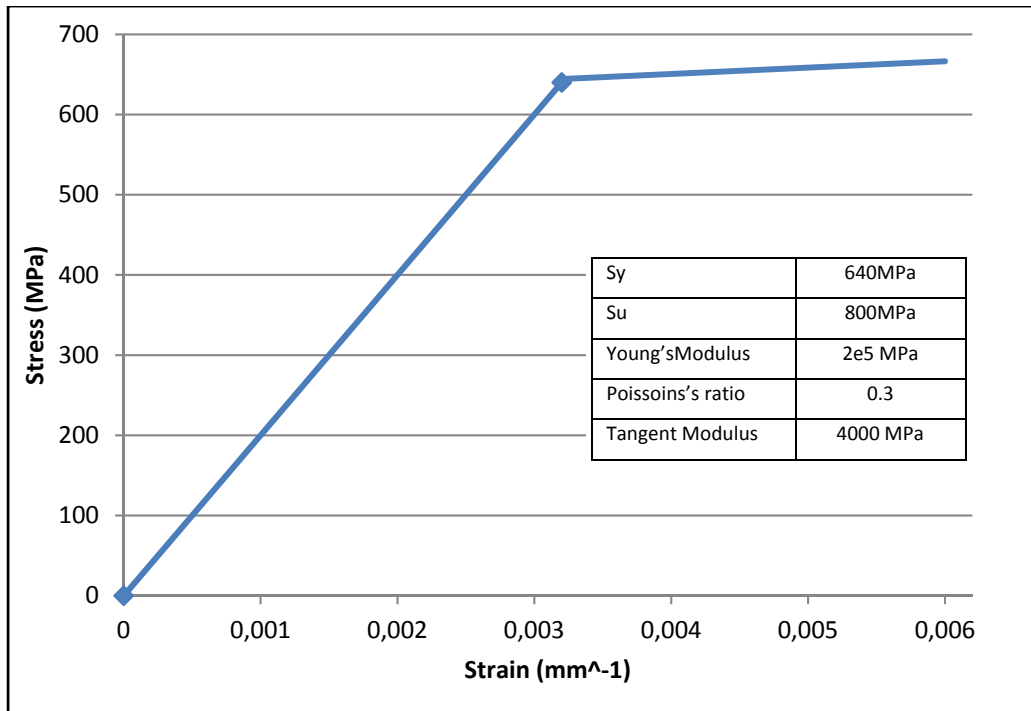
Figure 3-1 Material definition

3.3 Geometry

Generally, using a detailed model for a finite analysis provides more realistic results but subsequently increases the run-time and, in some cases, causes difficulties in convergence. Therefore, accuracy, convergence, and run-time should be balanced for an optimized analysis.

The dimensions of the bolt are based on "ANSI B18.2.3.5M, Metric Hex Bolts" (ASME, 1989a) and its threads are modeled on "ANSI B.1.13M, Metric Screw Threads" (ASME, 2001). The actual geometry of the bolt threads is shown in Figure 3-2. The fillets and chamfers of the threads are not considered in the model to avoid edges with very short length and singularity points and provide a better mesh quality. The final section of the bolt threads is shown in Figure 3-3.
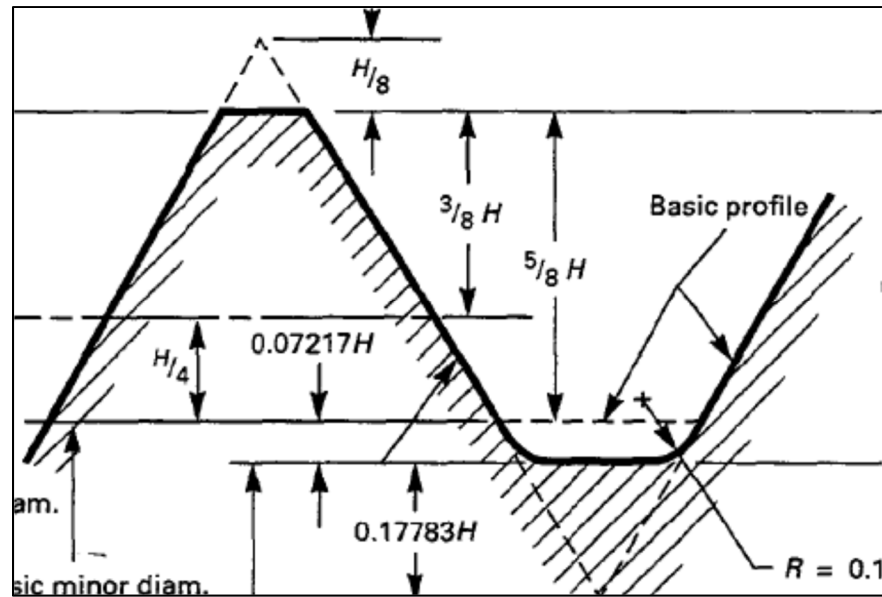
Figure 3-2 Actual geometry of the bolt's thread (ASME, 2001)

The fillets and chamfers of the bolt head (Figure 3-4) are also removed from the model. These details do not have a significant influence on the studied parameters. The details and dimensions of the bolt used in the model are given in Figure 3-5.
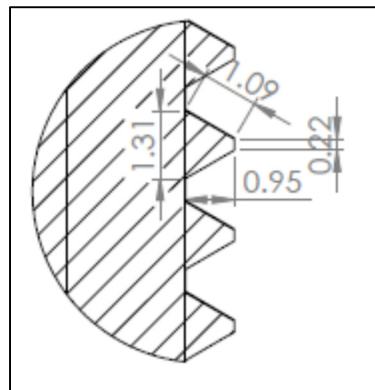
Figure 3-3 Simplified
geometry of the bolt thread.
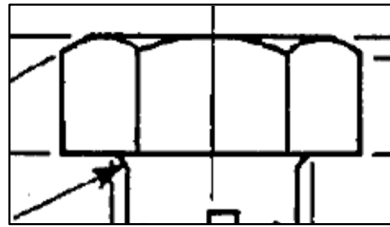
Figure 3-4 Actual geometry
of the bolt head
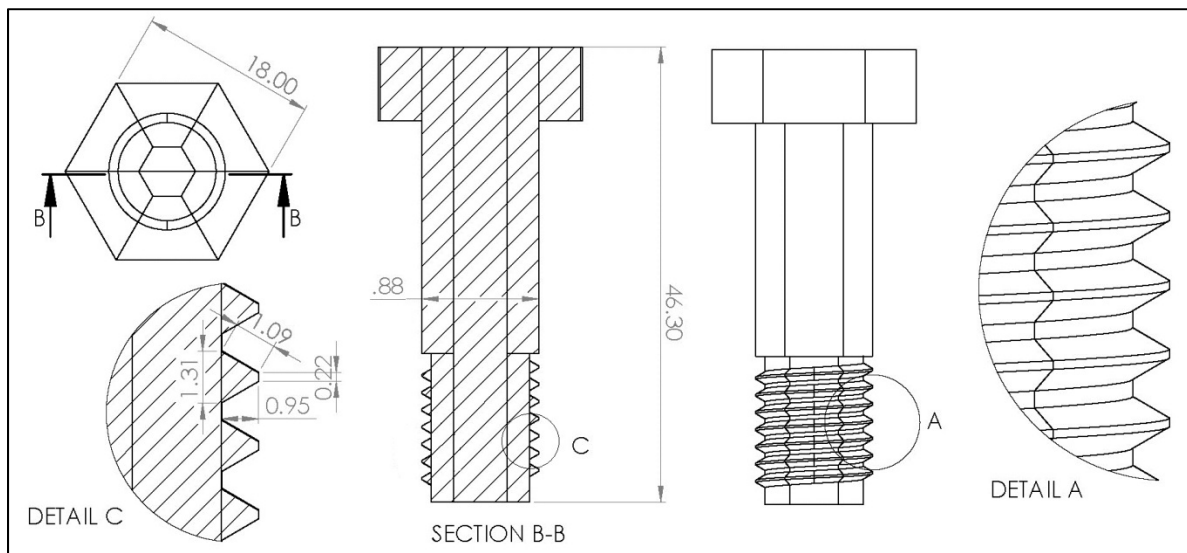
Figure 3-5 Bolt Geometry

The dimensions of the nuts are based on "ANSI B18.2.4.1M-1979 (R1989) Metric Hex Nuts" (ASME, 1989b). In reality, the nut threads merge with its body. However, this geometry leads to a zero-length element meshing; hence, the threads are continued to the point where this section begins to distort. The neglected portion is less than a quarter of a thread and does not affect the results. The same simplification is applied to the nut threads. The geometry and dimensions of the nut are given in Figure 3-6.
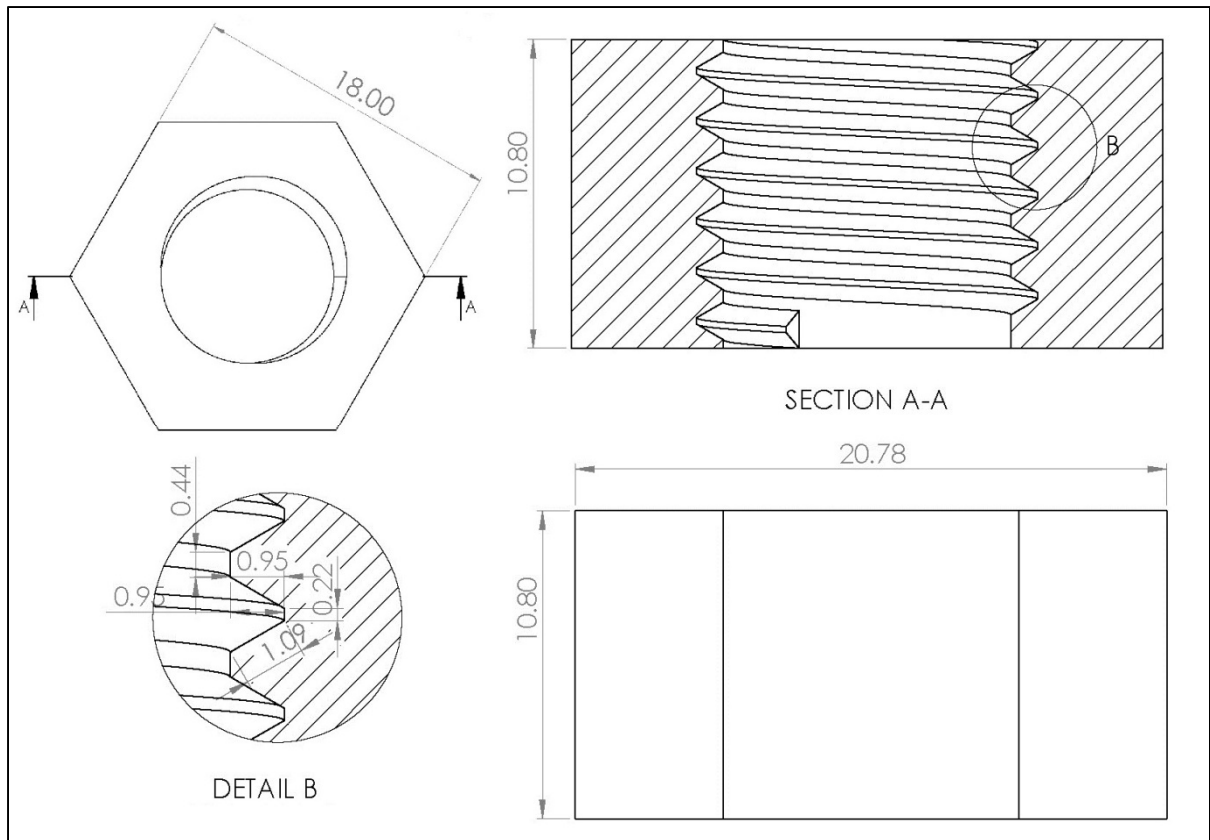
Figure 3-6 Nut's geometry

The dimensions of the washer are based on "ANSI B18.22M-1981 Metric Plain Washer" (ASME, 1981), as illustrated in Figure 3-7. The geometry of the plates is shown in Figure 3-8.

In order to obtain a better mesh quality, the various parts must be cut into smaller pieces. In the Ansys software, a "Part" can consist of one or more "Body". Different mesh type and refinement can be applied to the bodies that make up a part. Ansys automatically adjust the bonds between all bodies and the common nodes in meshing. Dividing a model into appropriate parts and bodies requires both experience and trial-error between the meshing and geometry modeling steps.

Figure 3-7 Washer geometry

Figure 3-8 Plate geometry

3.4   Meshing

The nut is divided into two parts: a cylinder and a thread. The cylinder part consists of six bodies (Figure 3-9). The "Hexagon Dominant" and "Sweep" mesh methods are used for the cylinder and thread, respectively. The thread is divided into 40 bodies to reduce the torsion from "Sweep Section" (Figure 3-9). Images used courtesy of ANSYS, Inc.
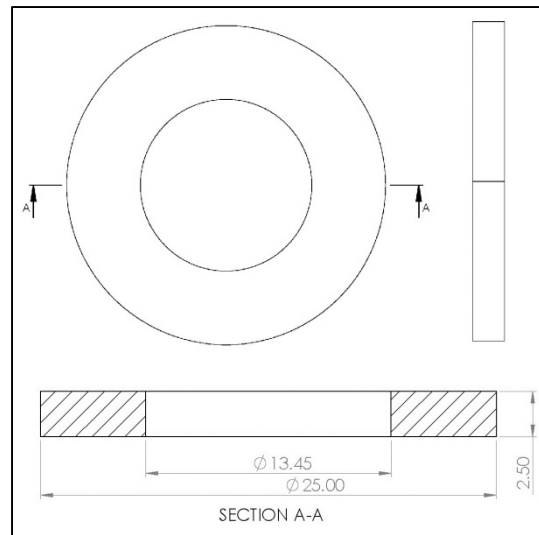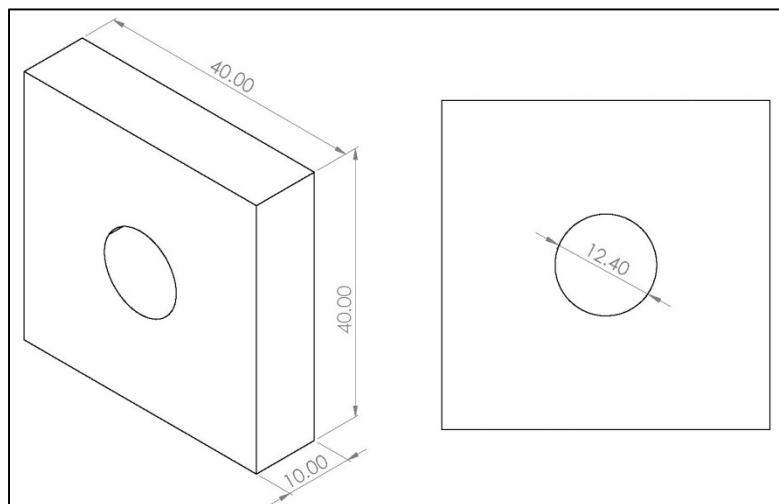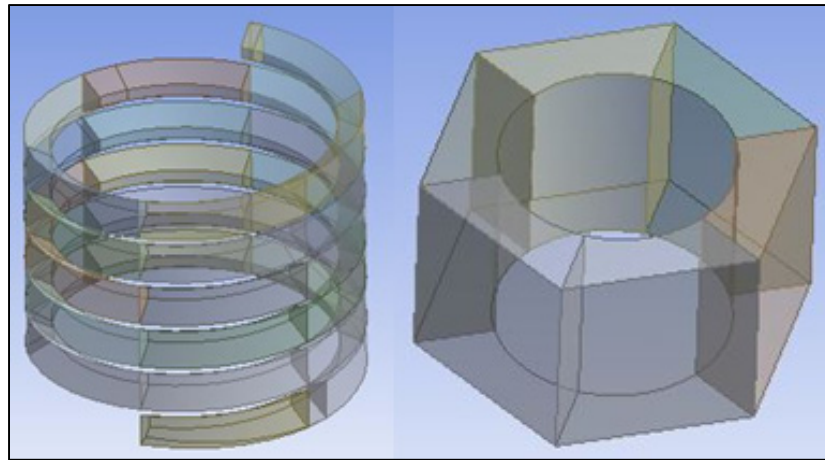
Figure 3-9 Consistant bodies of the nut cylinder and thread

One of the dominant factors in meshing is the ratio between the largest and smallest dimensions of the mesh. The tip of the thread is 0.2mm wide while its length is about 220 mm. This ratio requires a very high number of elements to obtain an acceptable aspect ratio. The nut threads have 5601 elements and 30544 nodes. The threads are bonded to the cylinder to form a single solid part (Figure 3-10). The nut cylinder has 540 elements and 3030 nodes. The meshing of the nut cylinder is shown in Figure 3-11.

The geometry of the plates is simpler than that of other parts and thus is easier to mesh. The hole in the plate does not allow for hexagonal meshing of all areas of the plate. To minimize mesh irregularity caused by the hole, the plates are sliced into eight bodies. Each plate forms a part with 960 elements and 4960 nodes. The "Hexagonal Dominant" method is used for the meshing of the plates.

The washers are located between the plates and bolt cap and nut. In reality, these parts are all affected by the relative displacement. However, if the relative displacement of the bolt, nut, washers, and plates was considered, achieving convergence with finite element analysis would be practically impossible. Therefore, the washers are bonded to the plates to avoid this problem (Figure 3-14). Each washer is divided into 6 bodies and has 240 elements and 1560 nodes. The meshing of the washers is shown in Figure 3-13.
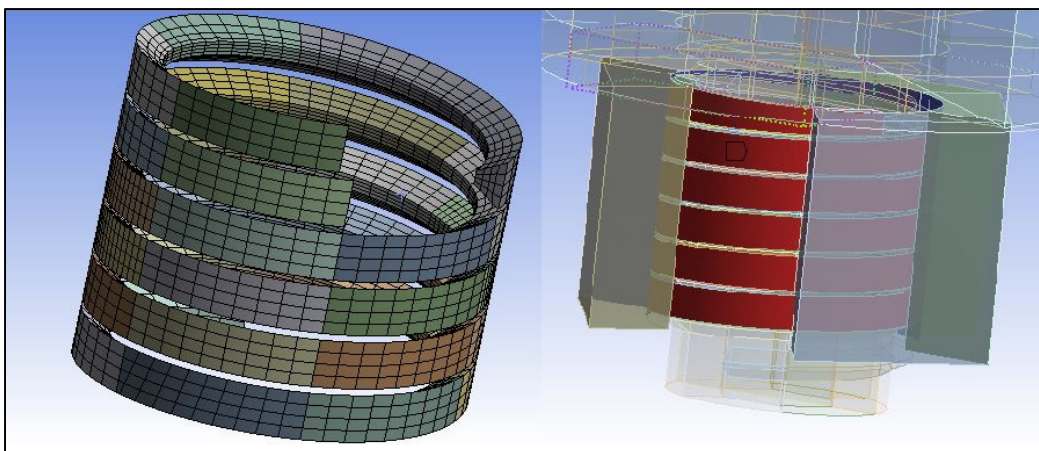
Figure 3-10 Meshing of the nut thread and bonded area
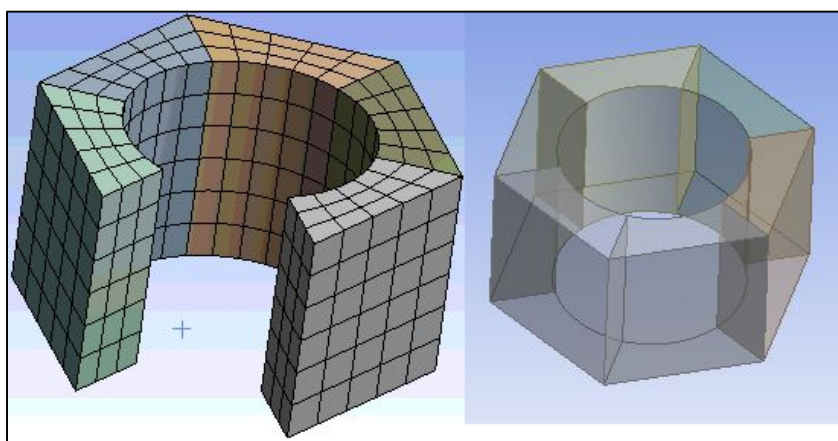
Figure 3-11 Meshing of the nut cylinder
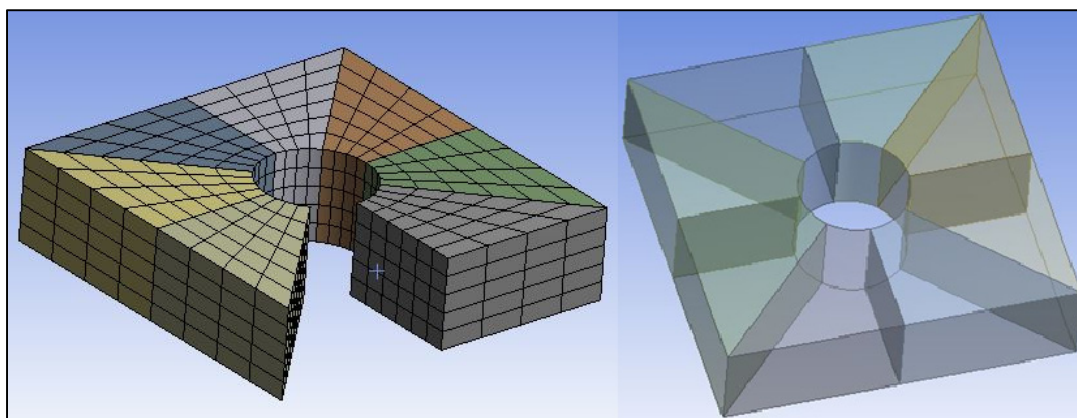
Figure 3-12 Meshing of the plate
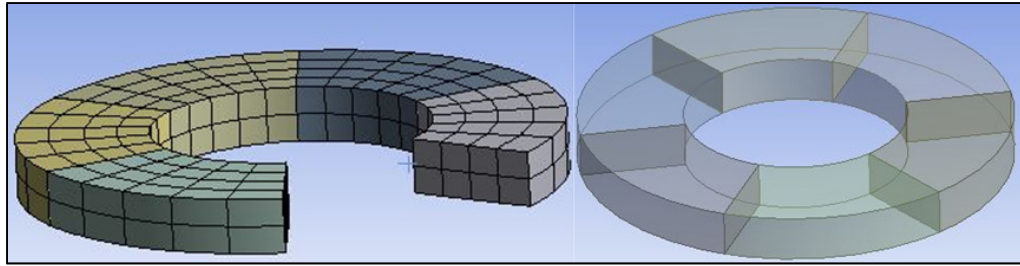
Figure 3-13 Meshing of the washer
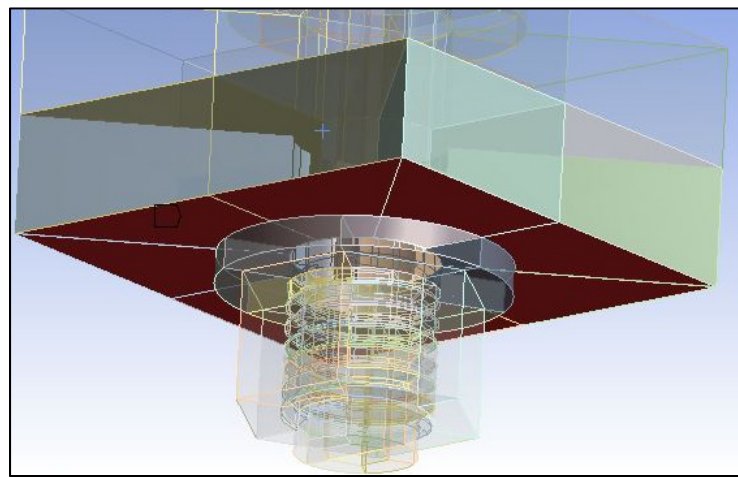
Figure 3-14 Bonded area of the washer to the plate

The bolt is divided into two parts, the body and thread. The body includes the cap and stem. The bolt cap has a hexagonal shape and is connected to the cylindrical stem. Meshing these parts as two different bodies does not result in good quality as the transition from the hexagonal to cylindrical shape causes distortion of the meshes. To solve this problem, the bolt cap is sliced into 14 bodies and the cylindrical stem into 22 bodies (Figure 3-15). These 36 bodies form one part in the model with 4010 elements and 17975 nodes. The "Hexagonal Dominant" and "Sweep" meshing methods are used in the meshing of this part. The meshed part is shown in Figure 3-15.
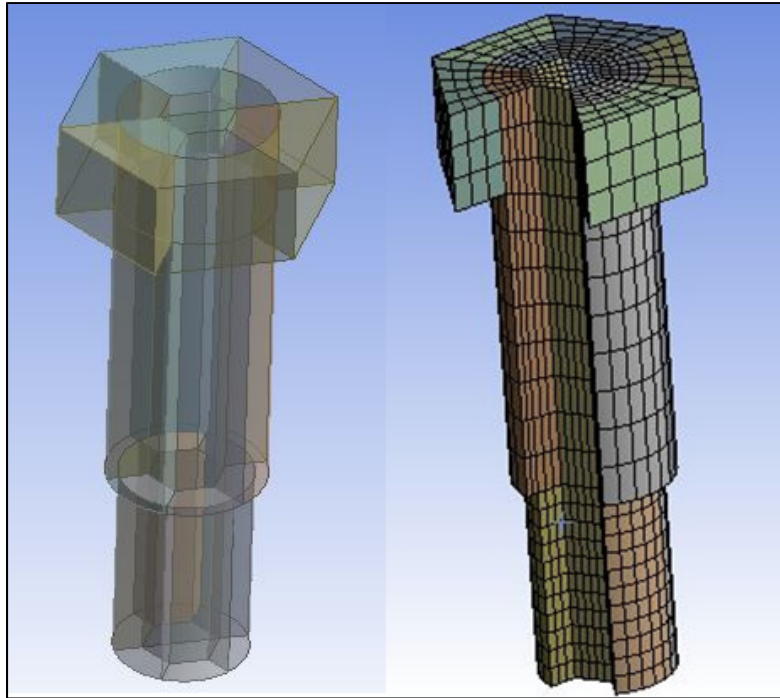
Figure 3-15 Bolt stem, consisting bodies and meshing

Meshing the bolt threads presents a similar problem as the meshing of the nut thread. Because of this, it is divided into 43 bodies and is meshed with the "Sweep" method, resulting in 9612 elements and 56922 nodes. The threads and the stem are bonded at the contact surfaces (Figure 3-17). The washer on the side of the bolt cap is the same as the other washer and both are bonded to the plate.

The model has a total of 22163 elements and 121511 of nodes.

SOLID186 (3-D 20-Node Structural Solid) elements which can support plasticity, large deflection, and large strain are used in this model.
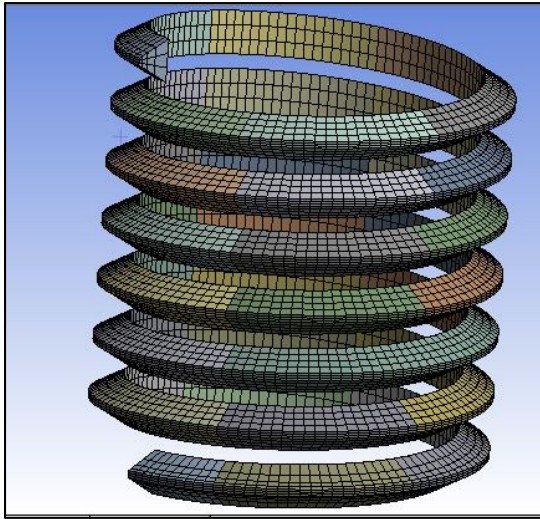
Figure 3-16 Meshing of the bolt threads

Figure 3-17 Bonding surfaces of the

bolt threads and stem

3.5   Mesh convergence criteria

The load in the bolt is used as the mesh convergence criterion. The mesh was refined gradually from 22163 elements and 121511 nodes to 57194 elements and 2913251nodes till the difference on the preload of less than 1% is achieved.

3.6   Boundary conditions

In the real test, one plate is connected to the load cell and is fixed and the other plate is connected to the actuator. Preload keeps the bolt, nut, and washers connected to the plates. To simulate these conditions, the boundary conditions shown in Figure 3-19 are applied.

A: Displacement in Z direction of two points is fixed;

B: Displacement in X and Z direction of two points is fixed;

C: Displacement in Y direction is fixed;

D: Displacement in X direction of two points is fixed;

E: Displacement in X direction of two points is fixed;

F: Applying displacement in Y direction to simulate applied lateral force (Figure 3-18);

G: Bolt pre-tension.

Frictional contact is defined by CONTA174 and TARGE170 for the contact surfaces of the bolt and nut threads respectively (Figure 3-20). The same contact definition is used for the contact surfaces of the bolt cap to the plate (Figure 3-21), nut to plate, (Figure 3-22) and plate-to-plate (Figure 3-23).
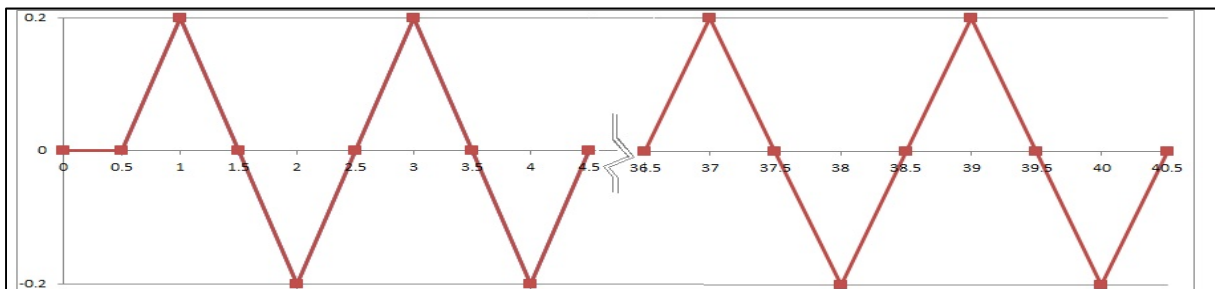
Figure 3-18 Lateral displacement vs. load time

Each quarter of load cycle is defined by 0.5 seconds.
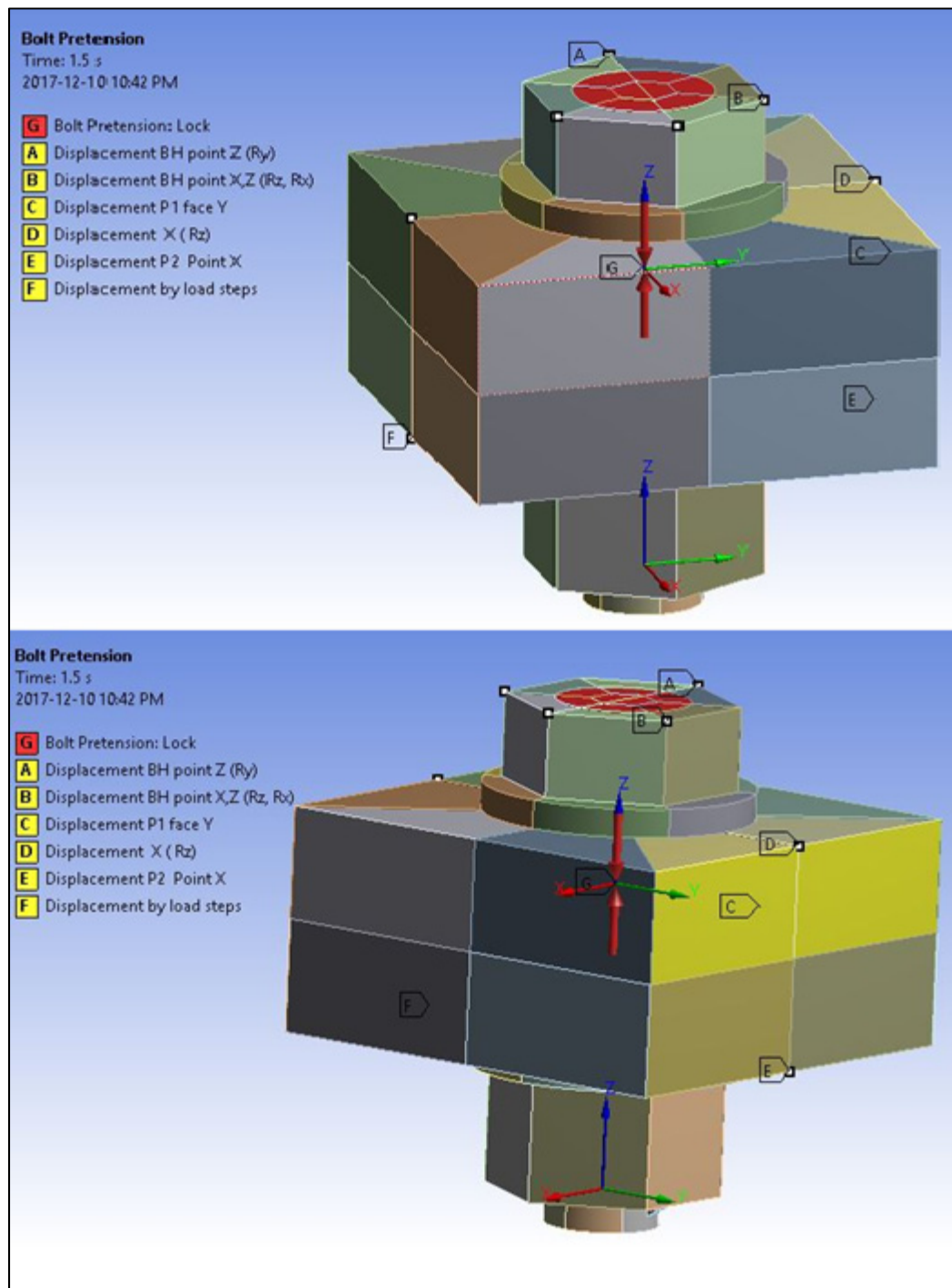
Figure 3-19 Boundary conditions
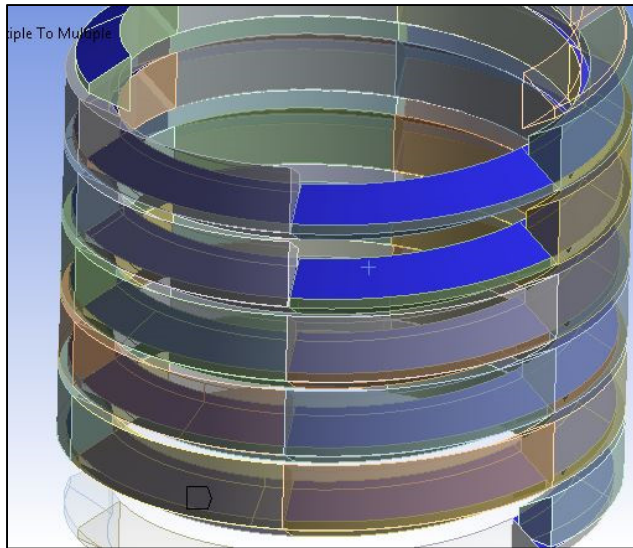
Figure 3-20 Contact between threads
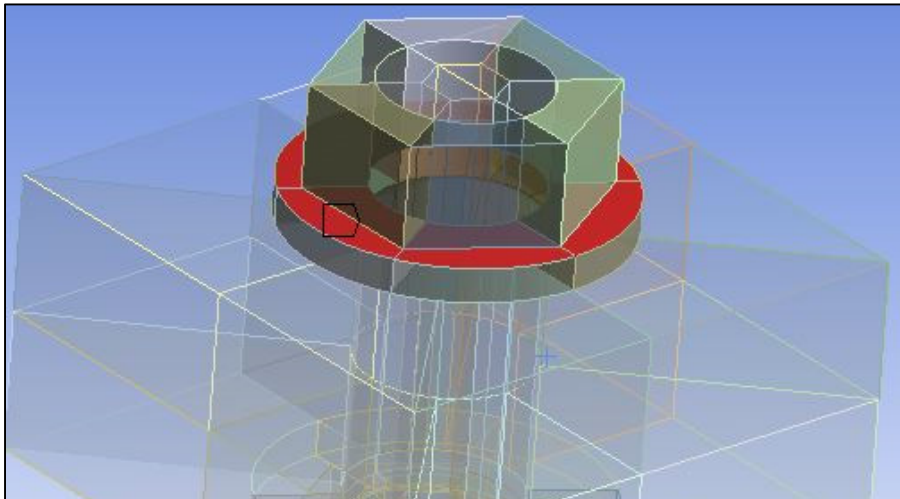
Figure 3-21 Contact surface between the bolt cap and plate

"Bolt Pretension" is used to simulate preload tension in the bolt, a feature which facilitates the modeling of bolts. In previous versions of the Ansys Workbench, the user had to select two nodes inside the bolt on which to apply force or displacement. This was problematic to set up for different load steps. The same concept applies to this simulation feature, but the selection of the nodes and the application of load are done automatically and the user has simply to select a "body" of bolt stem. The user can define a coordinate system within the

selected body to adjust the exact point where pretension is applied. Preload is applied at the origin of the defined coordinate system and in its Z direction. The user then has to define the coordinate system so that the Z-axis is in line with the bolt centerline.
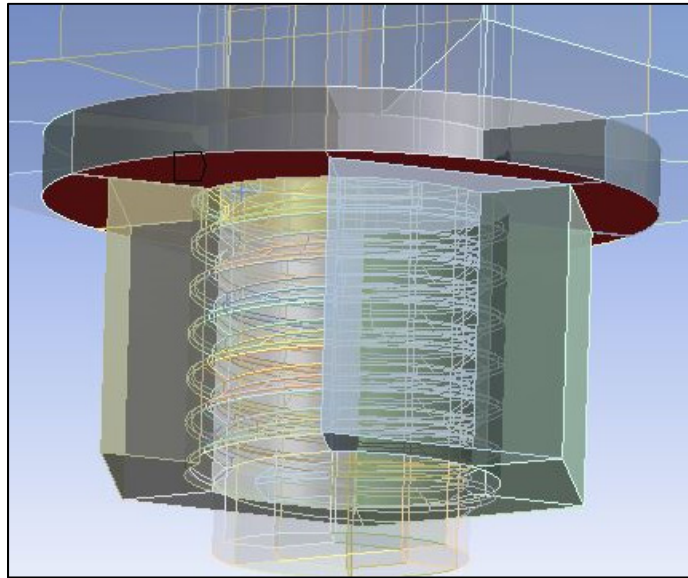
Figure 3-22 Nut to plate contact surface
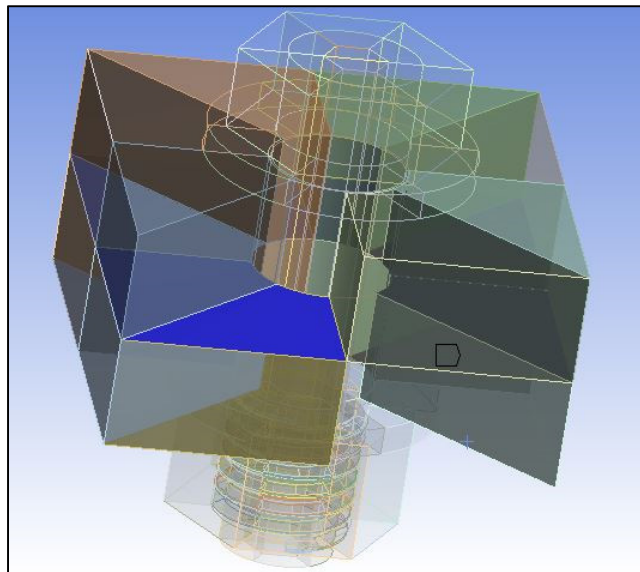
Figure 3-23 Plate-to-plate contact surface

The options available for "Bolt Pretension" are as follow:

- Load, to apply force,

- Adjustment, to apply adjustment in length units,

- Lock, to fix all displacement after tension,

- Open, to remove preload,

- Increment, to apply a length as an incremental adjustment.

Preload is applied in the first load step (0-0.5 s). This preload causes deformation in all joint elements. In load step 2, preload is defined as "Lock," which fixes the deformations caused by the preload and removes the force, allowing the user to combine preload with other loads. The preload definition for all load cases is "lock", except the first load step.

As shown in Figure 3-18, lateral displacement is applied to the mobile plate with amplitude of 0.2 mm. The displacement remains at zero in the first step where preload is applied. The next four steps simulate a full cycle with duration of 2 seconds.

The Ansys Workbench is more user-friendly than the Classic version. The graphical interface for geometry modeling, boundary conditions and others accelerates modeling and post-processing. However not all features and settings are provided in the graphical interface. A "Command Line" can be added to any step of the analysis to solve this problem. APDL commands can be used to make all options used in the Classic version available.

The default value of equilibrium iterations per solution step is 25 in Workbench. The model used in the current study cannot converge with the default settings, so APDL commands are used to change it to the desired value.

3.7   High-Performance Computing of Calcul Quebec.

High Performance Computing (HPC) is a general term used for processing information with aggregate computing power. One of the common methods is parallel processing. In HPC, the main problem is divided into smaller problems which are then assigned to different CPUs,

which solve the equations simultaneously. The software then assembles the results to give the final solution to the problem posed.

For computer performance, the CPU time is a determinant factor in reducing the run-time. The large capacity computing server of Calcul Quebec is used to run the finite element analysis. The Guillimin phase I has 1200 nodes with 12 cores per node, 6 x CPU of 2.67 GHz per core and 24~72 MB of memory per node and phase II has 382 nodes with 16 cores per node, 8 x CPU of 2.67 GHz per core and 64~512 MB of memory per node. The nodes can be reserved and assigned to a specific calculation through specific operating system commands. Like most computing services, Guillimin's server operating system is Linux and therefore users must have basic knowledge of Linux. There is no graphical interface in the installed version of Linux and users must work via the command line.

Two storage spaces are available for users: 50 GB and 2 TB. The 50 GB space has a larger bandwidth and is used to keep the input files. The 2 TB space has a lower bandwidth and is used to keep the result files. To run a file on the Linux server, the ID of the reserved CPUs, the file path, solver path and the destination where the results will be stored, need to be defined.

As mentioned above, the nodes can be reserved via command line and they will be assigned to the user based on the availability of nodes and reservation priority. Once the nodes are assigned to the user the model can be launched. Depending on the number of reserved nodes, the run-time can be reduced from 5 days for local computing to 9 to 12 hours. The results for 20 cycles are about 160 GB in size. Once processing is finished, the files have to be downloaded to a local computer for post-processing.

3.8   Post-Processing

Post-processing is done using the Ansys Workbench and Microsoft Excel. The workbench provides a "User defined" feature, which allows the user to combine Ansys Classic

commands with its geometrical interface. The results are then exported to Excel format to create the desired graphs.

CHAPTER 4

DISCUSSION OF RESULTS

4.1   Introduction

In the following chapter, experimental, finite element, and analytical results will be compared and discussed.

The results of a finite element analysis with 15 kN preload and 0.44 mm lateral displacement are compared with the theory proposed by Zhang et al. and analytical calculations. The experimental tests with different preloads and lateral displacements are performed and the results are also discussed. Finally, the results from finite element analysis and an experimental test with a lateral displacement of 0.02 mm and a preload of 8.1 kN are compared and discussed for the validation of the test bench.

4.2   Experimental results

After conducting a rig shake down preliminary test at different load cases, the first real test is performed with a preload $P_L=8100N$ and a relative lateral displacement between the two plates D=0.025mm for 50 cycles.

As mentioned before, the combination of stage I and II is obtained after few cycles. Therefore, one can expect a substantial drop of load that can occur even after few cycles. As illustrated in Figure 4-1, the preload drop in first step shows the greatest change among all cycles. The rotation in the first and second cycle is 0.04 degrees, but the preload drop in each cycle is 260 N and 40 N respectively. The difference between these two load drops while the rotation is the same is an evidence of the presence of stage I.

As the preload drops, lateral force drops accordingly. The largest lateral force drop also occurs in the first cycle, followed by smaller changes per subsequent cycles.

The trends observed for preload load drop is consistent with the lateral force and rotation trends shown in Figure 4-2 and Figure 4-3. The test rig results are quite logical and match well each other providing evidence that the test rig is working as intended.

As mentioned in the literature, few researchers used Junker test machines with an imposed applied displacement. With the current machine this option is possible to measure imposed displacement and real displacement between plates. The applied displacement on the actuator point was set to 0.2 mm in order to obtain an actual displacement between the plates of 0.025 mm. The displacement setting on the actuator is tuned based on the measured plate relative displacement and is higher because it includes the deformation of the plates, the grips, and the ball joint clearance. This demonstrates the importance of the displacement sensing system installed between the two plates and the advantage of the current design.
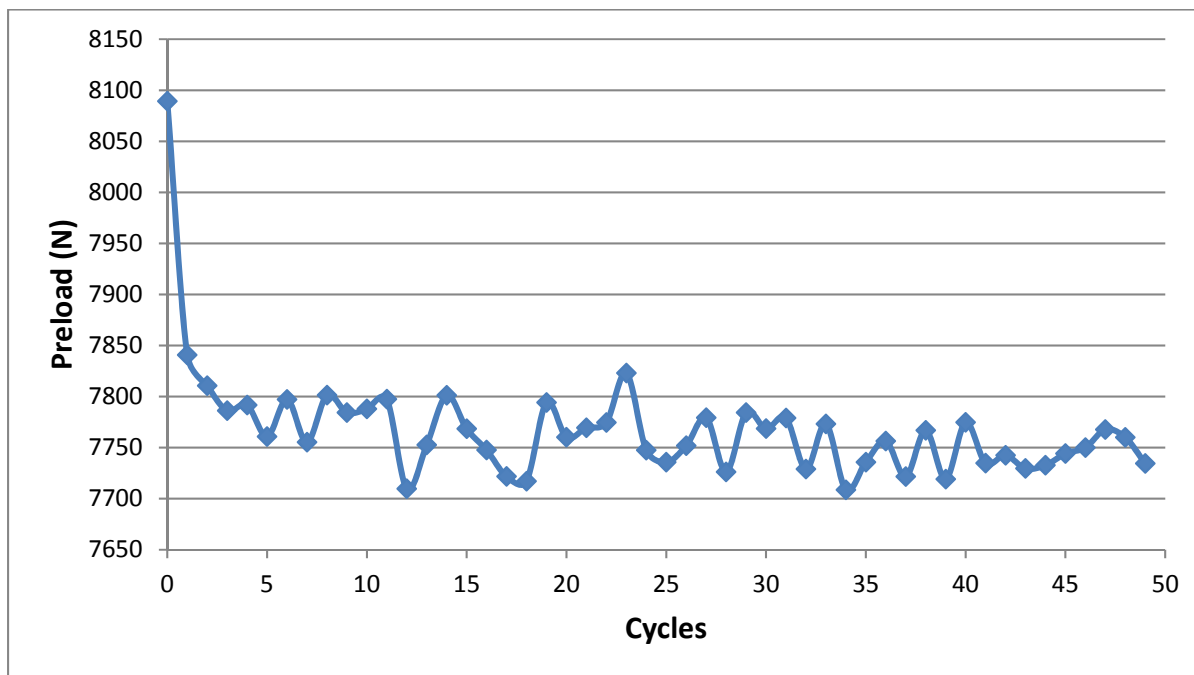

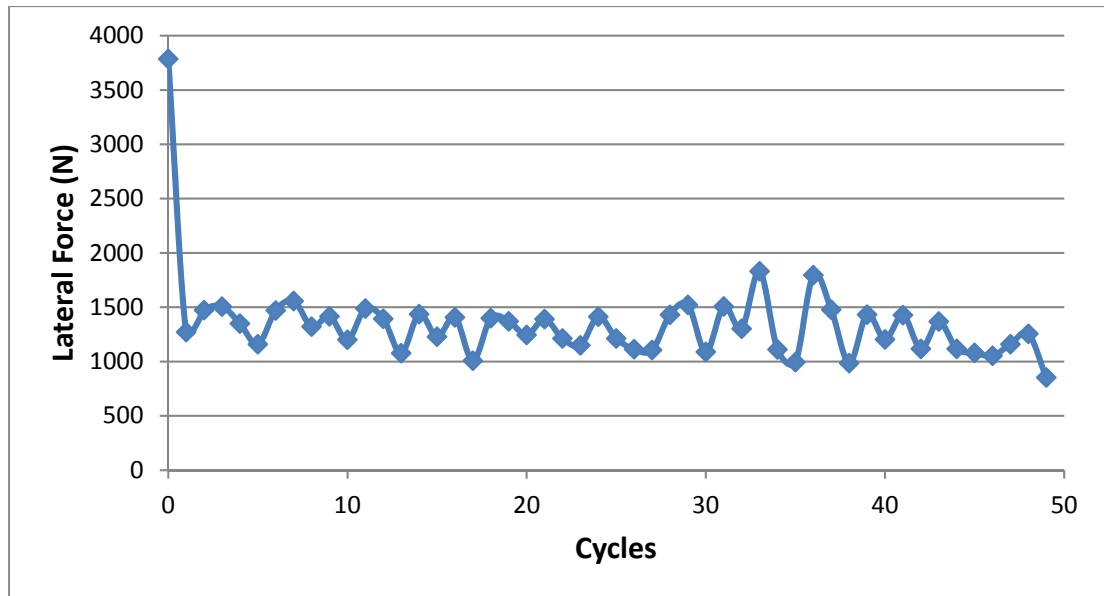Figure 4-1 Preload vs. Cycles (8.1 KN & 0.025mm)

Figure 4-2 Lateral force vs. Cycles (8.1 KN & 0.025mm)
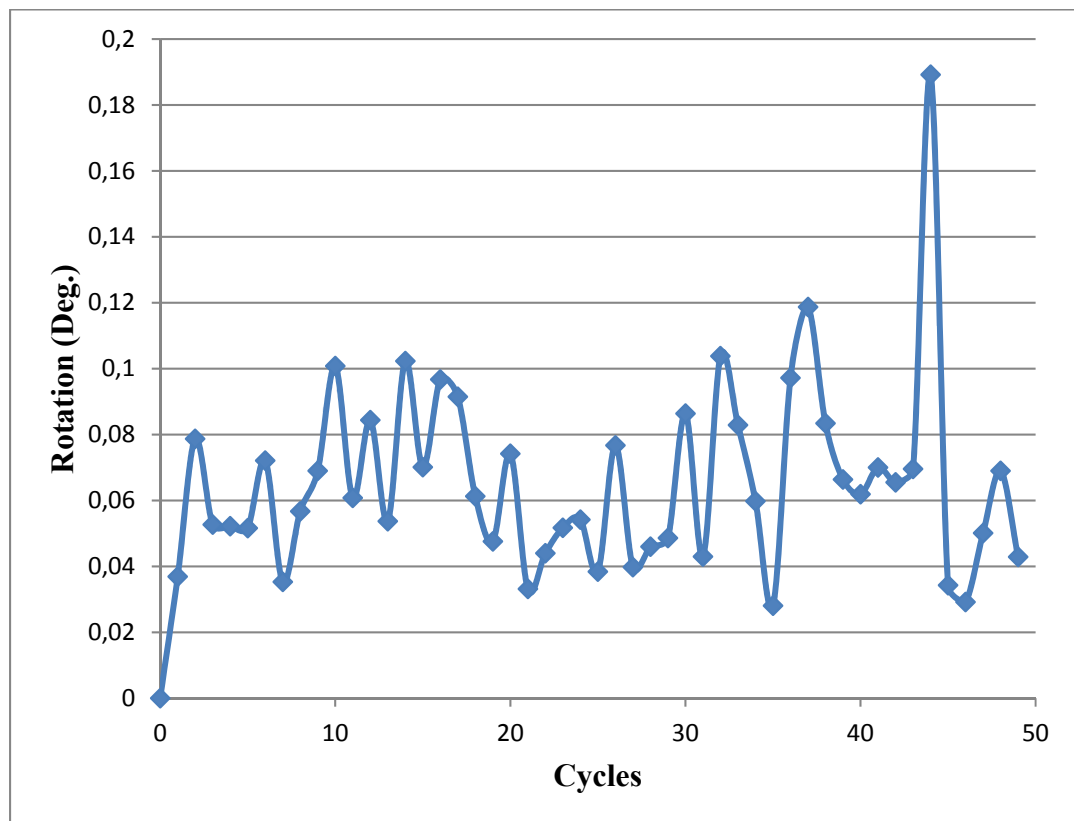
Figure 4-3 Rotation vs. Cycles (8.1 KN & 0.025mm)

86

The second test is performed with P_L=7771 N and D=0.025mm for 50 cycles. The general trends of the preload drop, lateral force, and rotation are the same as the previous test. The results of this test are shown in Figure 4-4 to Figure 4-6.
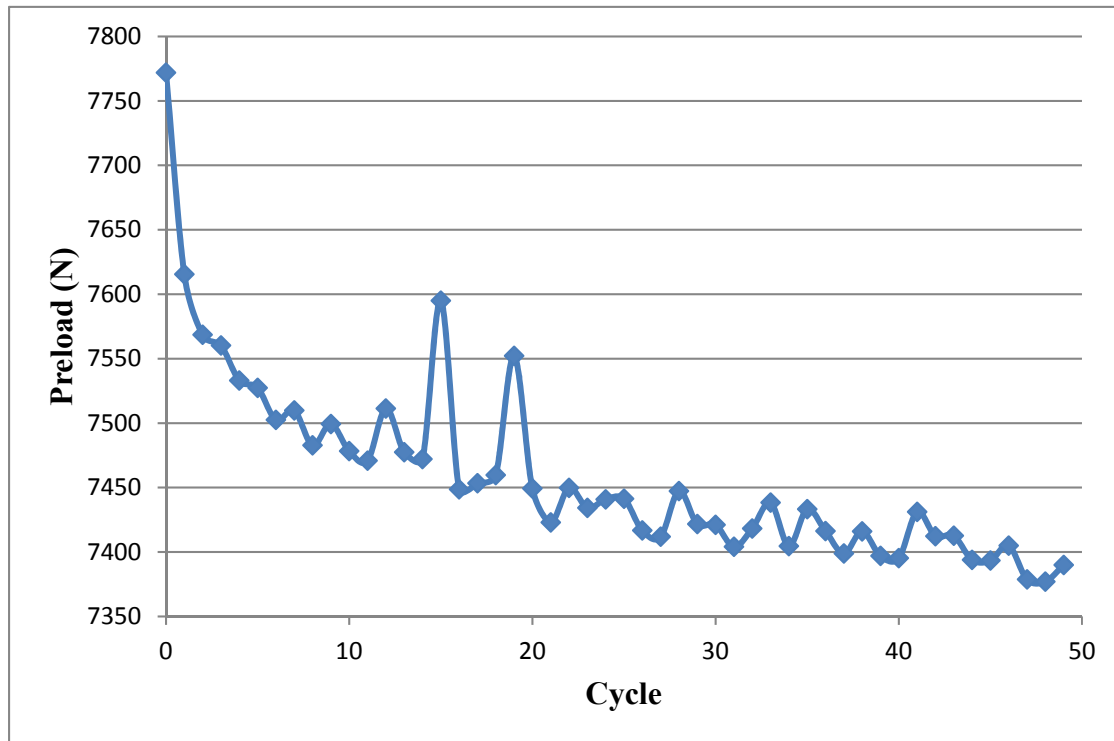
Figure 4-4 Preload vs. Cycles (7.7 KN & 0.025mm)

The third test is performed with P_L=3100N and D=0.075mm for 194 cycles. The preload in this load case is low and accordingly, the stresses on the bolt threads are low. When the stress level is low, the local yield deformation in the thread contact surfaces is less evident and consequently stage I is less likely to occur. In this case the preload drop is caused only by rotation. As it can be observed in Figure 4-7 and Figure 4-10, the preload drop in each cycle is proportional to the corresponding rotation. As previous studies illustrate (Eccles et al., 2010), the preload drop and bolt rotation reaches a plateau and saturate after a certain number of cycles. Such behaviour can be observed in Figure 4-7 and Figure 4-10. The plateau is dependent on various factors such as bolt size, friction, and preload.
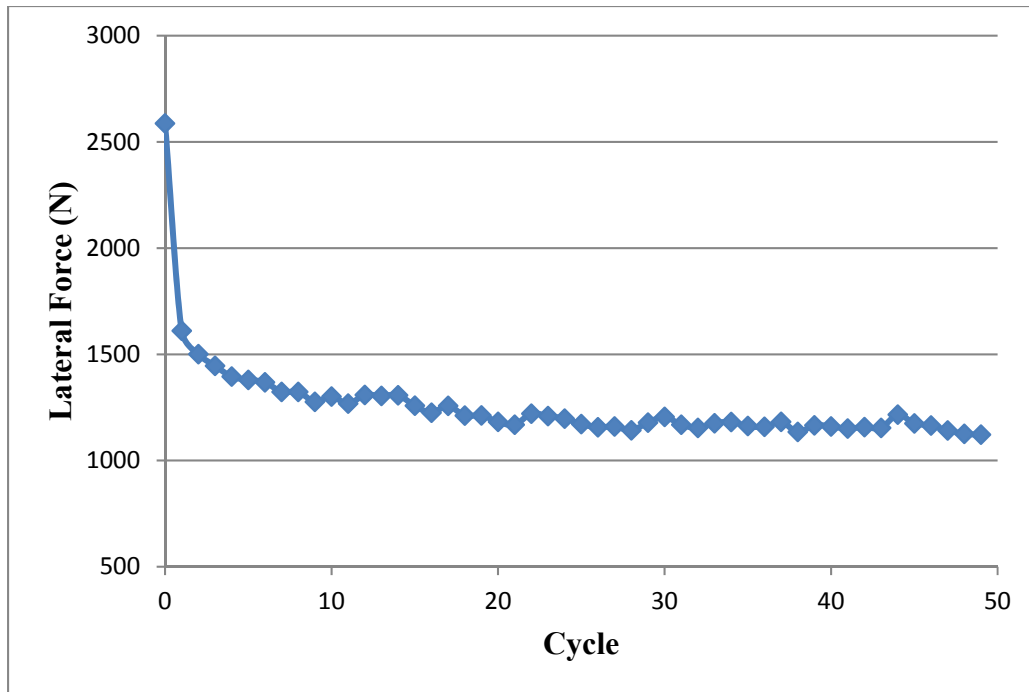
Figure 4-5 Lateral force vs. Cycles (7.7 KN & 0.025mm)
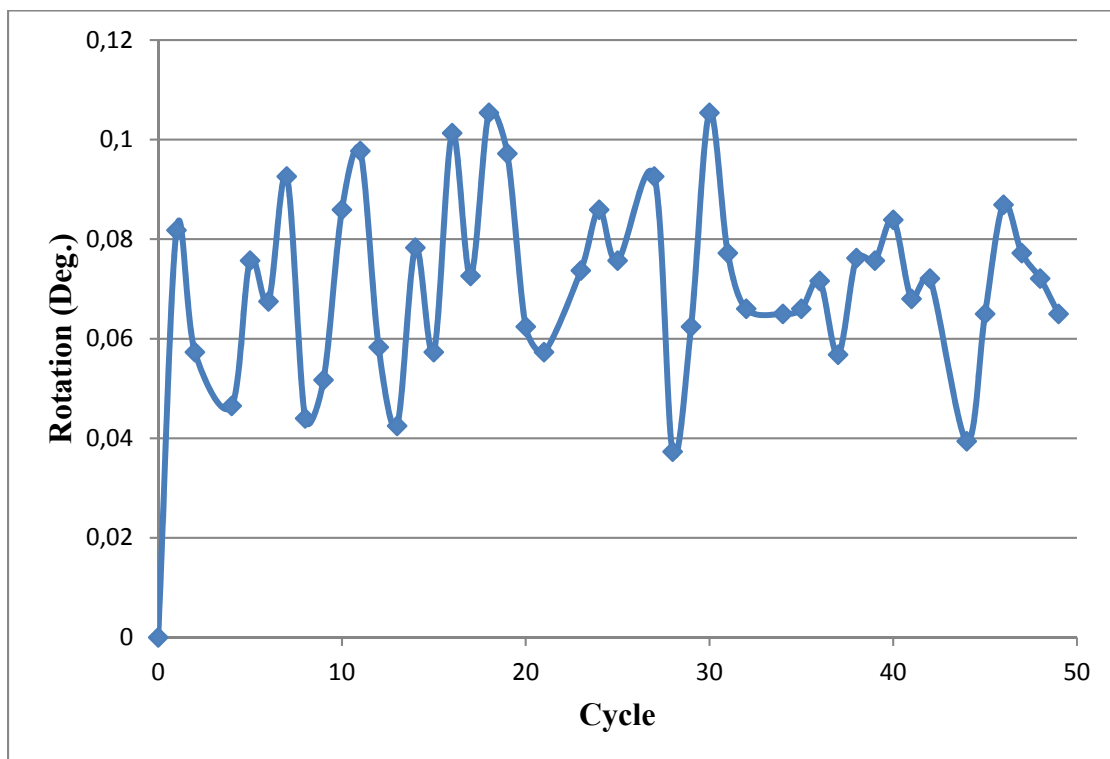
Figure 4-6 Rotation vs. Cycles (7.7 KN & 0.025mm)
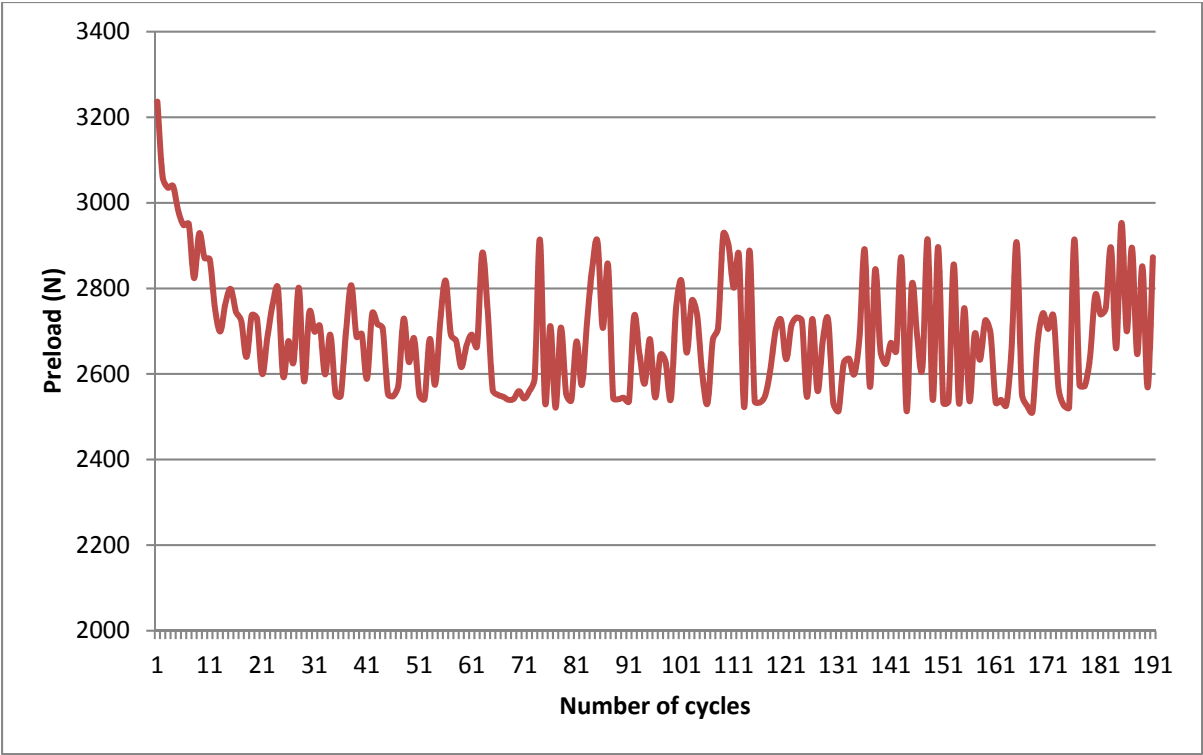
Figure 4-7 Preload vs. Cycles (3.2 KN & 0.075mm)
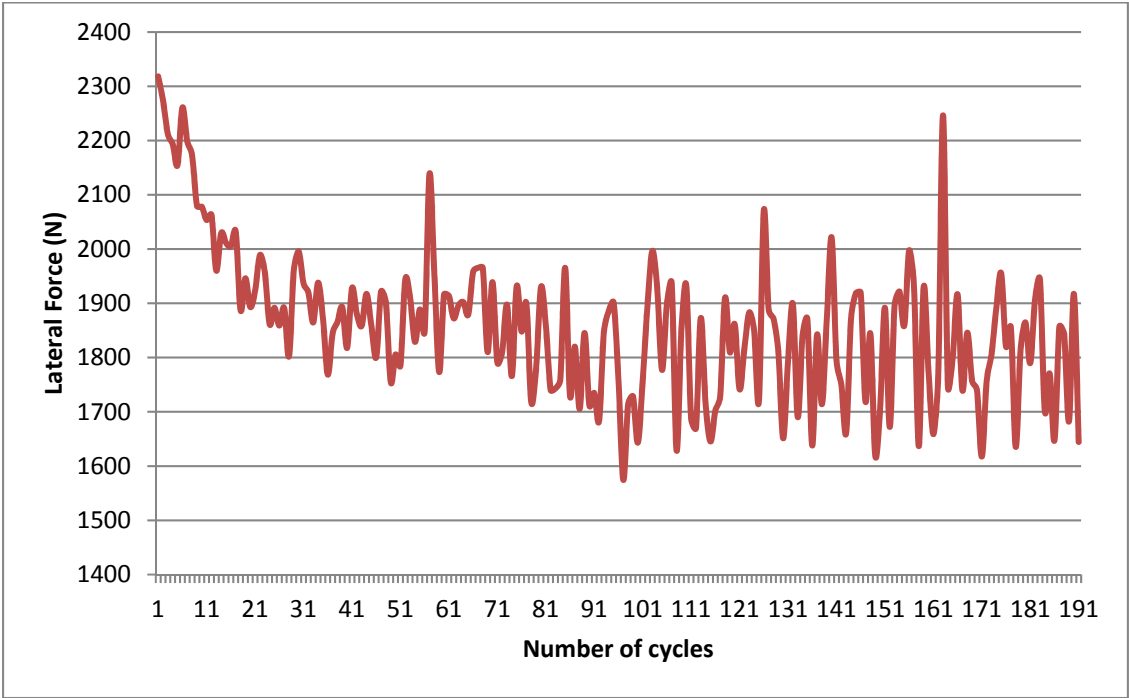
Figure 4-8 Lateral force vs. Cycles (3.2 KN & 0.075mm)
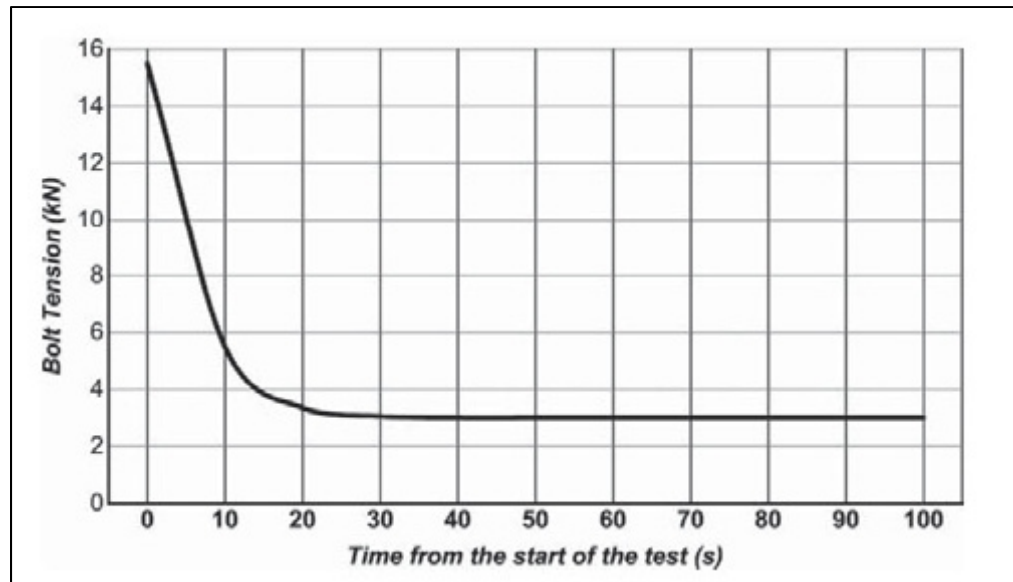
Figure 4-9 Preload vs. time (Eccles et al., 2010)
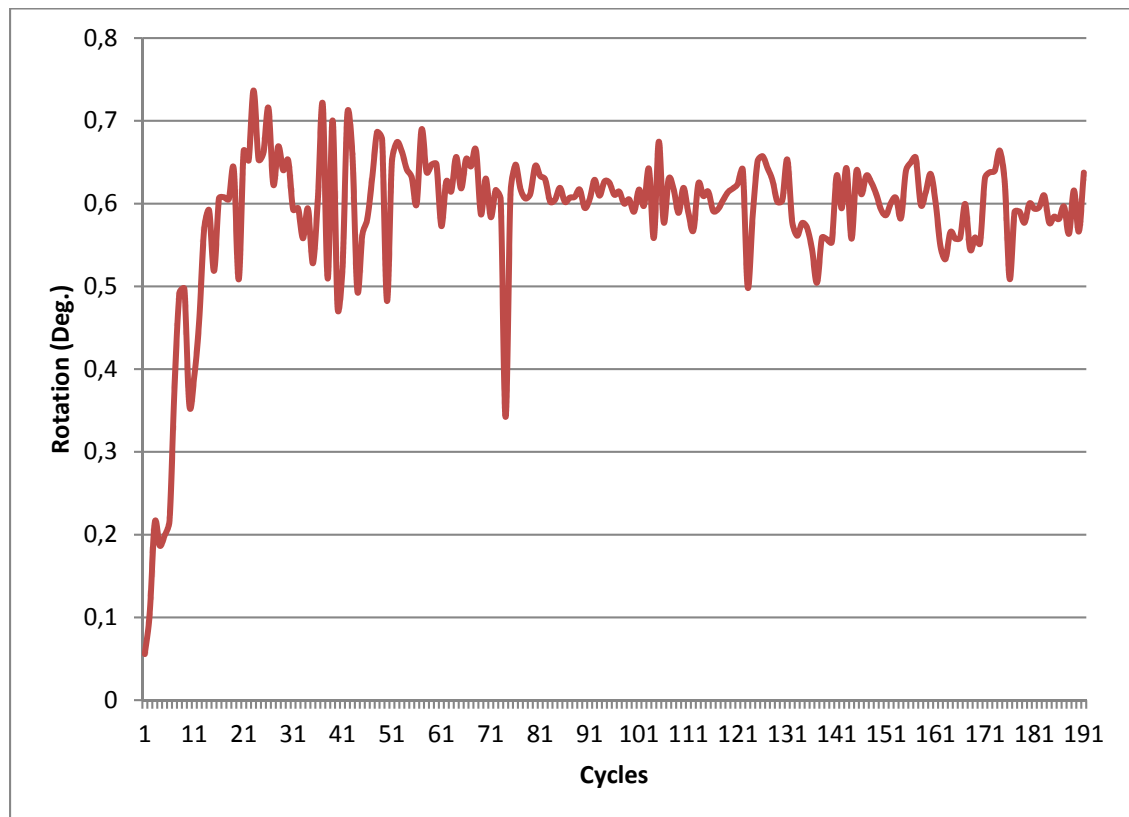
Figure 4-10 Rotation vs. Cycles (3.2 KN & 0.075mm)
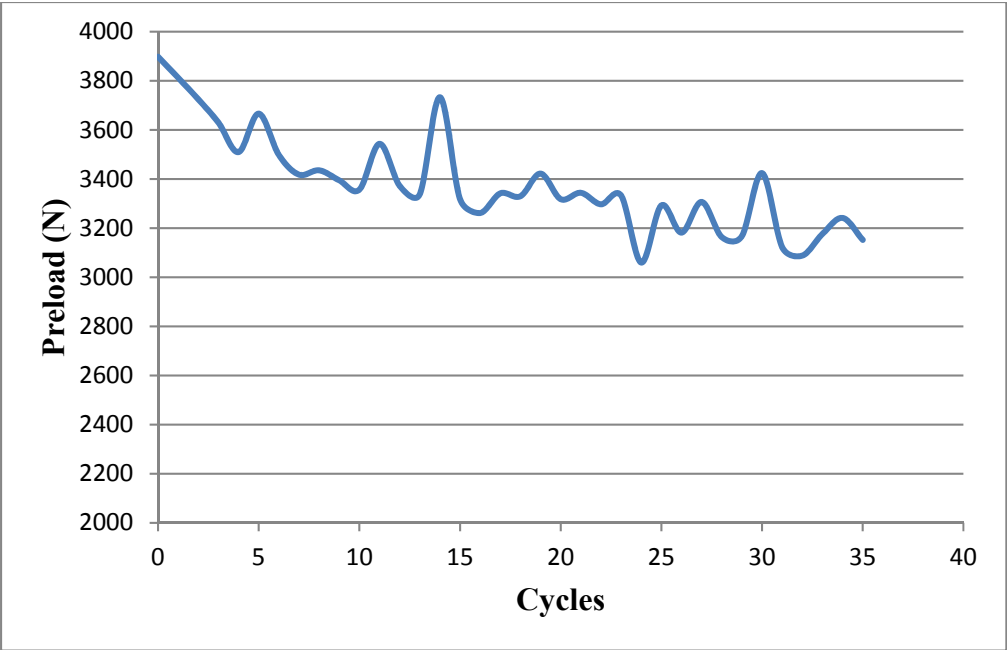
Figure 4-11 Preload vs. Cycles (3.9 KN & 0.06mm)
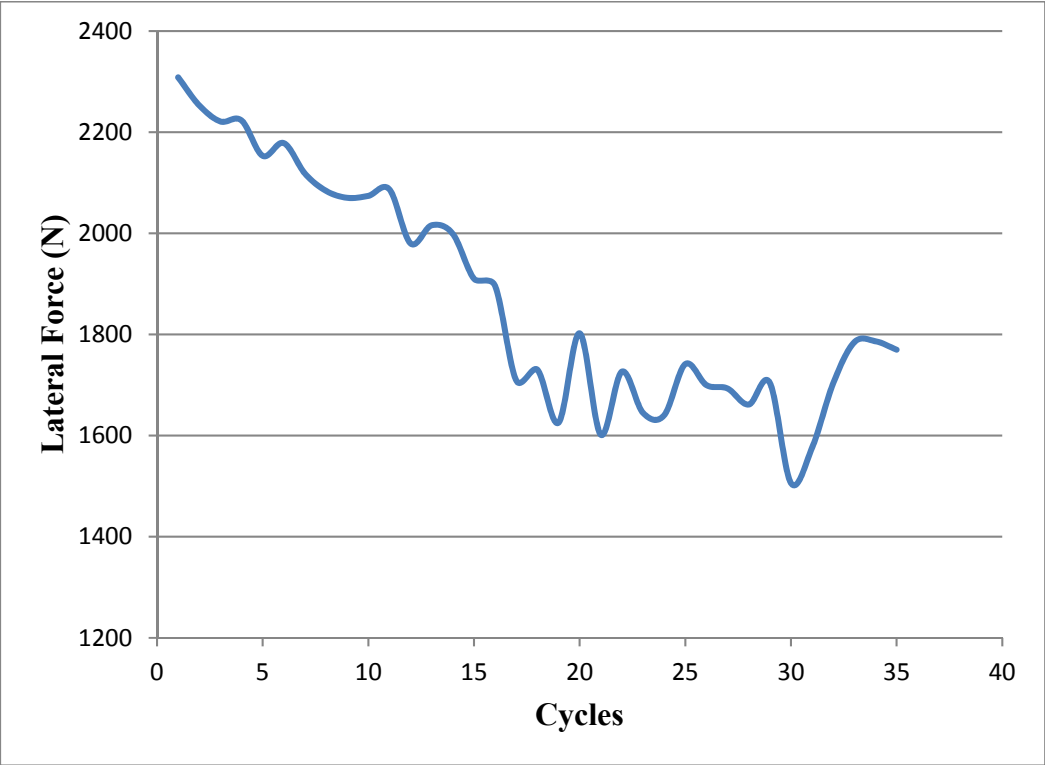
Figure 4-12 Lateral force vs. Cycles (3.9 KN & 0.06mm)
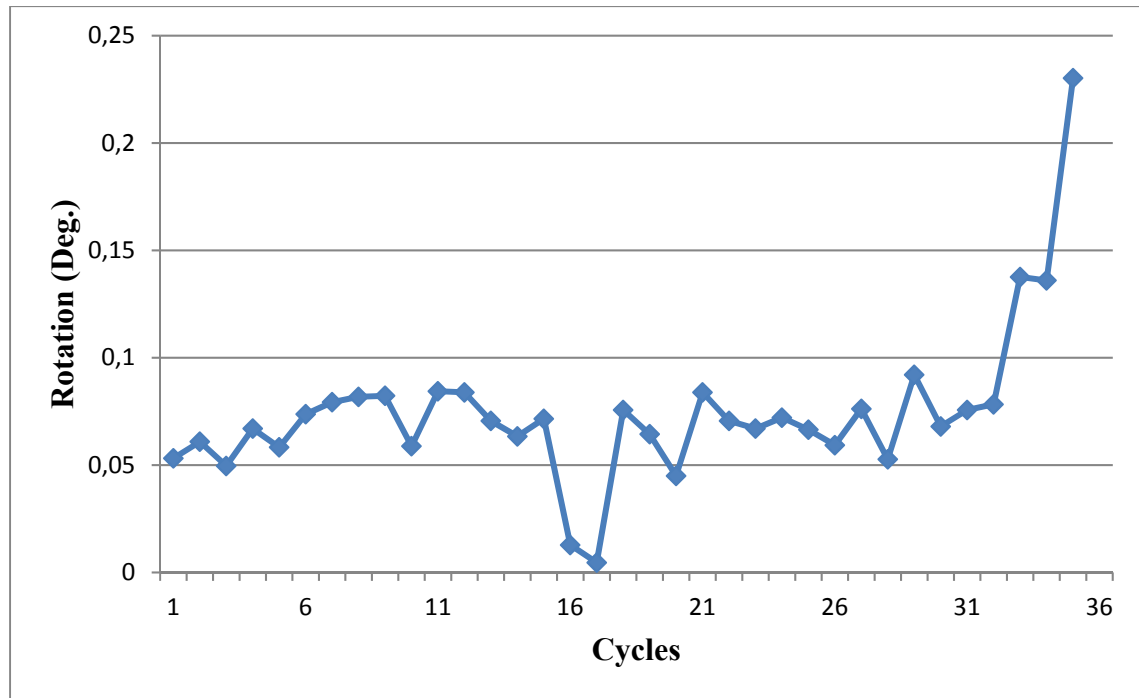
Figure 4-13 Rotation vs. Cycles (3.9 KN & 0.06mm)

Another test is performed with P_L=3900N and D=0.06mm for 35 cycles. The trends for preload drop, lateral force changes, and rotation remain the same as in the previous tests. A comparison of the four tests confirms that the increase of preload has a significant effect on the self-loosening resistance of the bolted joint. The following table illustrates the effect of preload.

Table 4-1 Effect of preload on self-loosening

Preload (KN)	Displacement (mm)	Preload drop after 35 cycles (%)	Preload drop after 50 cycles (%)
8.1	0.025	4.34	4.3
7.7	0.025	4.38	4.9
3.9	0.06	19.13	-
3.2	0.075	21.23	-
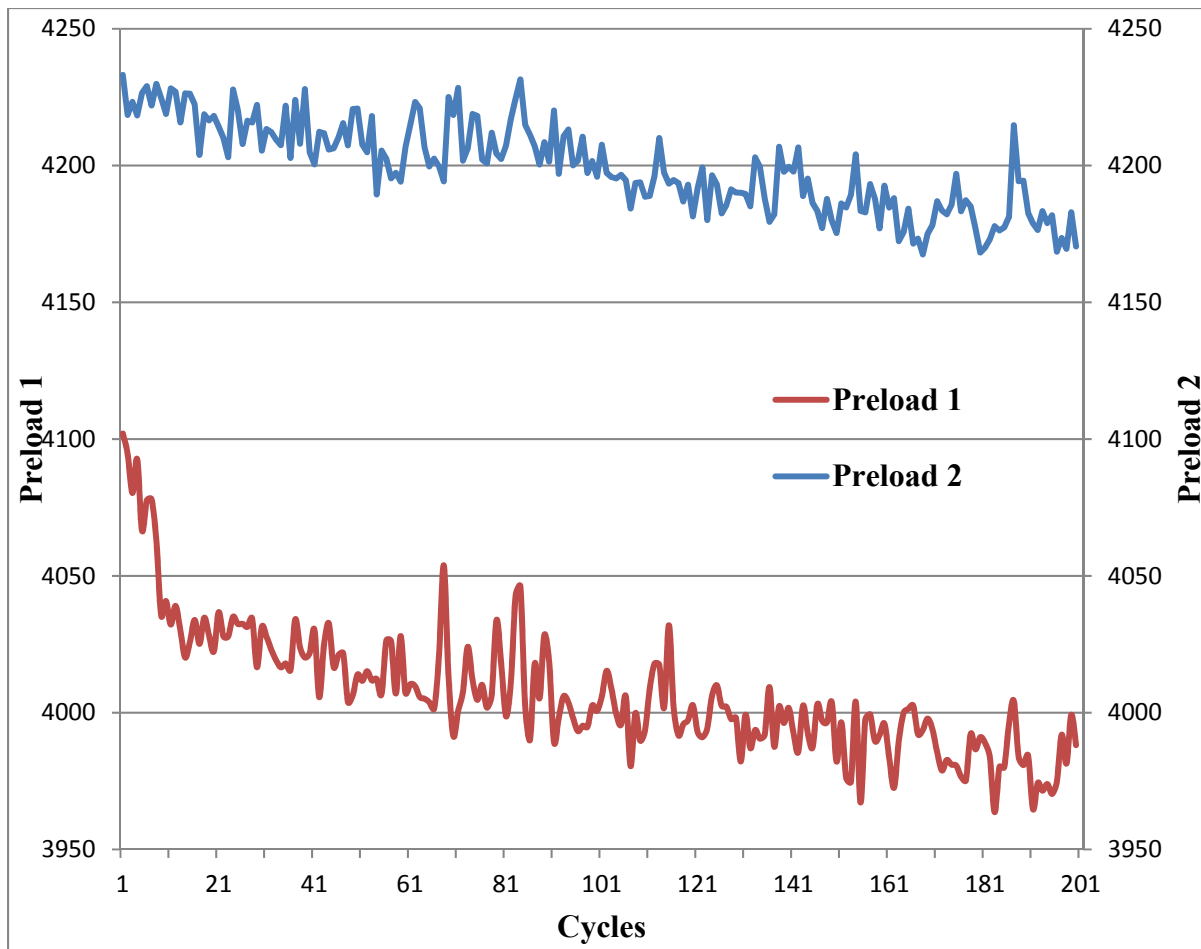
Figure 4-14 Preload vs. Cycles (4.1 & 4.2 KN & 0.005mm)

The effect of preload has been studied in previous research and matches the current results. It was stated that "Clearly, a larger preload enhances the self-loosening resistance of the bolted joint" (Zhang et al., 2007).

Two tests, with near identical preloads, are performed to verify the performance of the test rig and its repeatability of testing. These results are shown in Figure 4-14 through Figure 4-16. The preload drop in cases 1 and 2 is 2.4% and 1.51% respectively. The results are close enough to conclude that the repeatability of the tests is achieved with the current test rig.
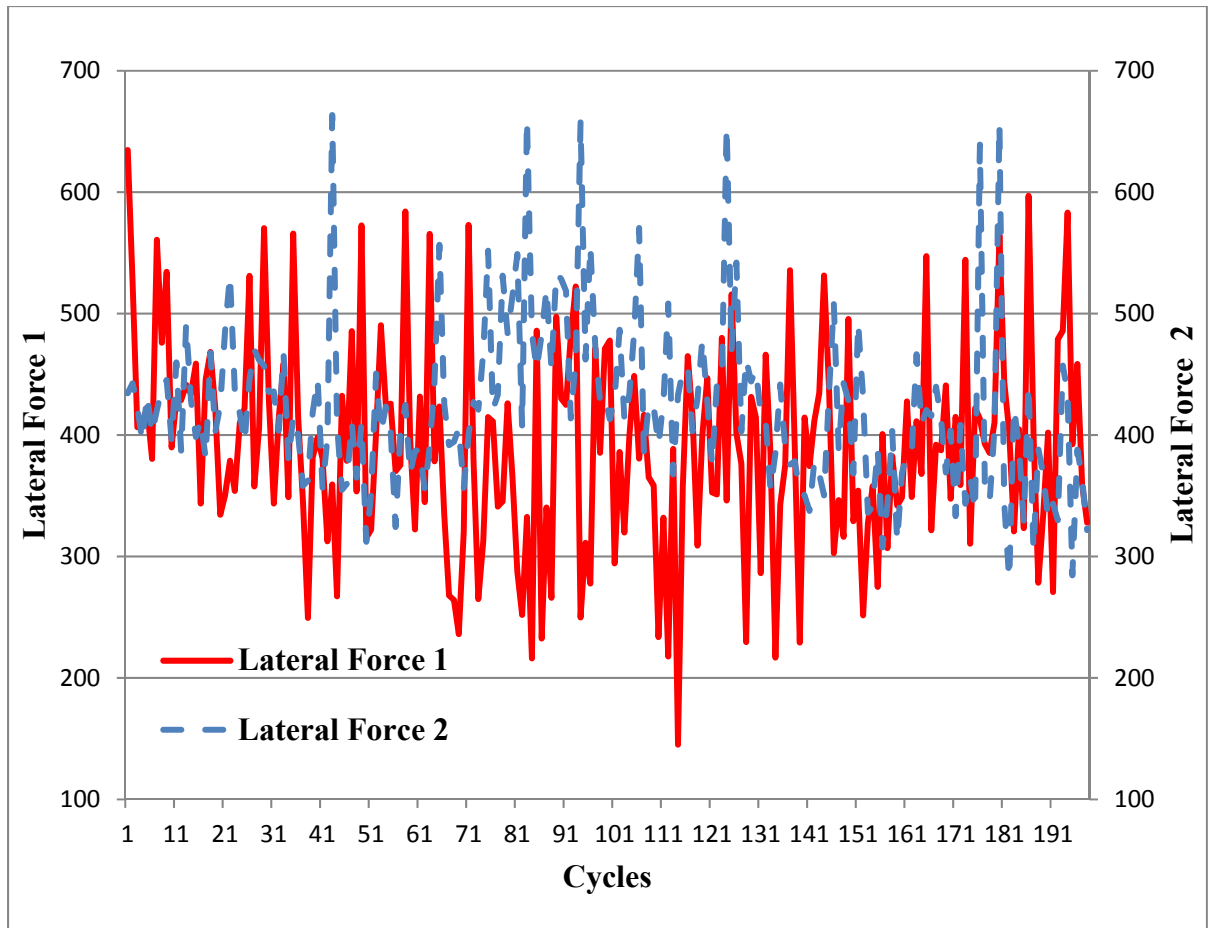
Figure 4-15 Lateral force vs. Cycles (4.1 & 4.2 KN & 0.005mm)
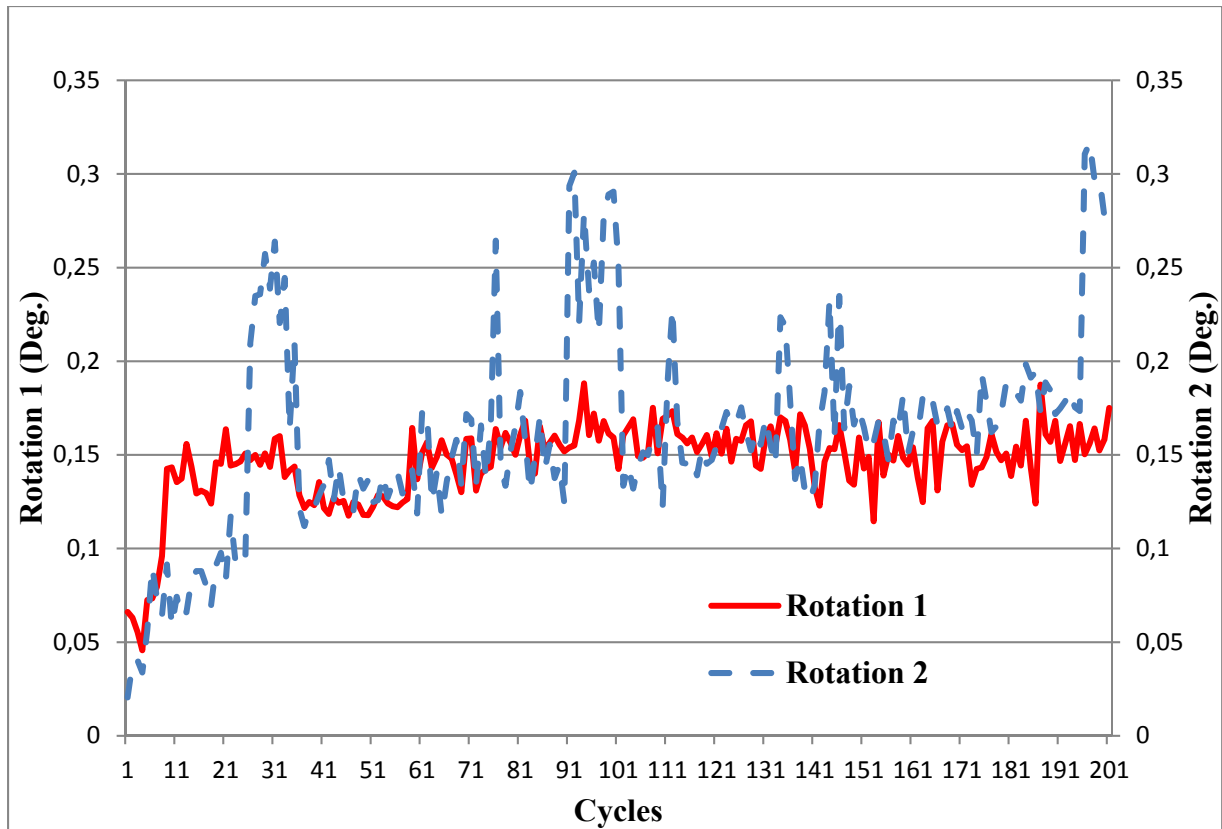
Figure 4-16 Rotation vs. Cycles (4.1 & 4.2 KN & 0.005mm)

4.3 Finite element results

A Finite element run is performed with P_L=15000N and D=0.44mm as the applied displacement on the actuator point.

Preload drop for the different cycles are as shown below:

15000-14380=620, 4.13% equal to 8.7% of total drop (0-1).

14380-13982=398, 2.65% equal to 5.6% of total drop (1-2).

10861-10528=333, 2.2% equal to 4.6% of total drop (10-11).

8168-7904=264, 1.76% equal to 3.7% of total drop (19-20).

Total preload drop 7096N = 48%.
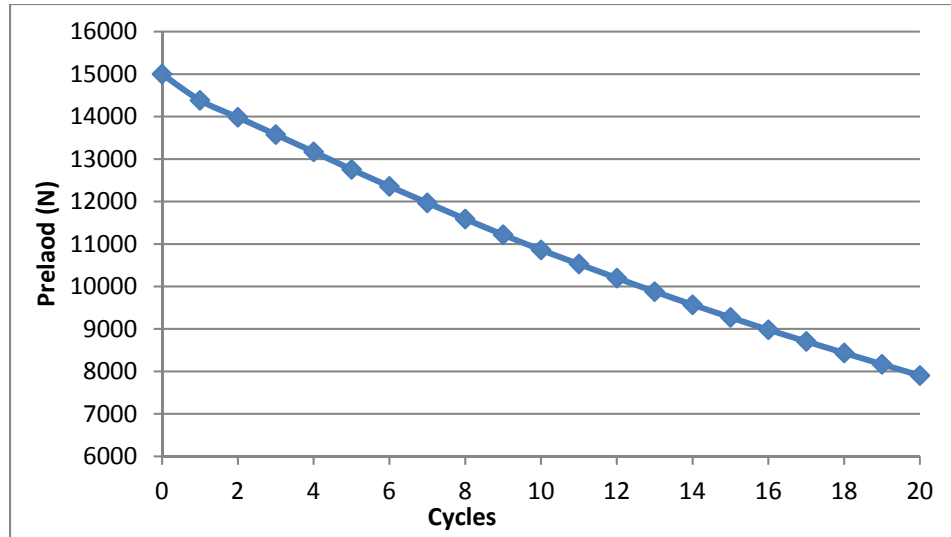
Figure 4-17 Preload (15 KN and 0.44mm)

The preload drop and the nut rotation in the first and second cycles are 620N - 0.12 degree and 398N – 0.264 degree, respectively. The preload drop in the first cycle is greater than in the second cycle even though it has a smaller rotation. As mentioned previously, the main mechanism for preload drop in stage I is plastic deformation without rotation between threads. This theory can be clearly justified through the results of this FEA.

As it is illustrated in Figure 4-18, the decrease in lateral force is proportional to the consequent preload drop.

Zhang et al. propose a theory to justify the rotation mechanism. They conclude that the displacement in the circumferential direction can be calculated with the relative radial (transverse) displacement of the bolt and nut, thread angle, and pitch angle. Equation (4-1) shows the proposed equation where d is the circumferential displacement, β is the pitch angle, μ is the friction coefficient, and t is transverse displacement. (Taken from (Zhang et al., 2007)):

$$d = \frac{\tan \beta}{\mu} t \qquad (4\text{-}1).$$
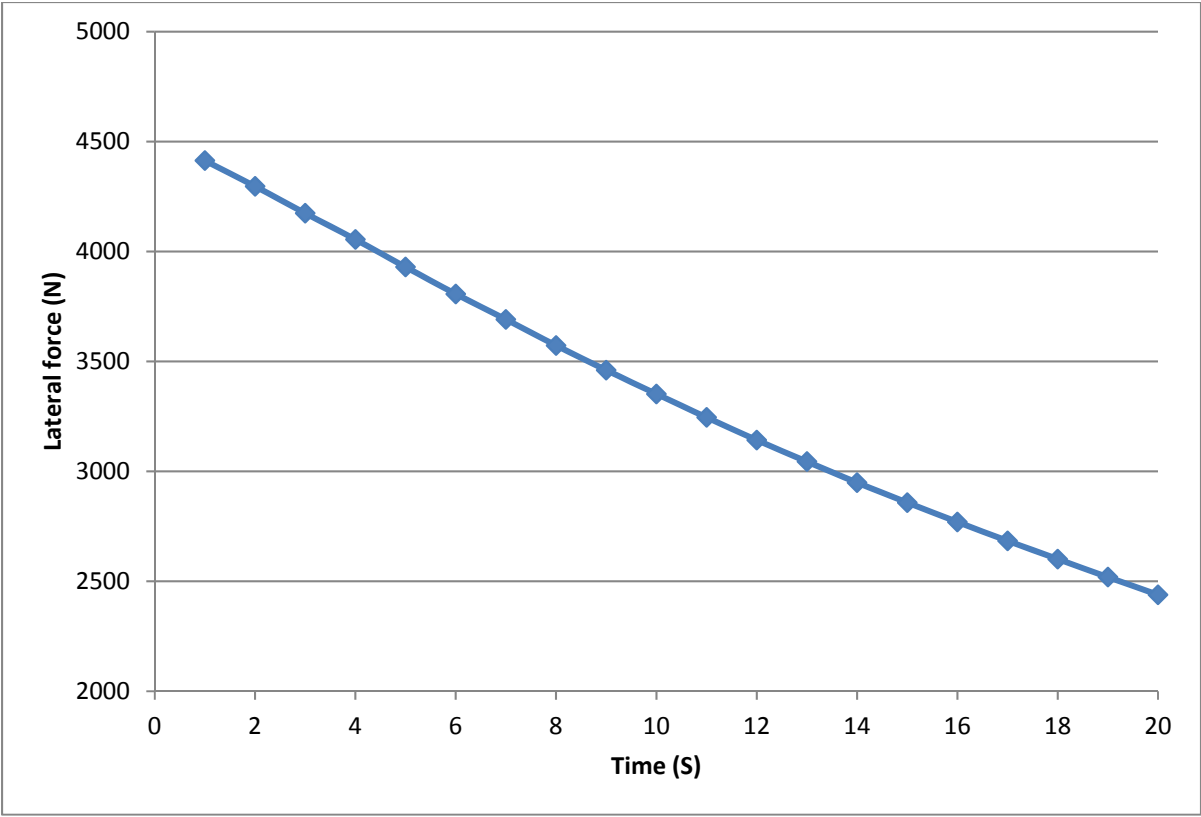
Figure 4-18 Lateral force (15 KN and 0.44mm)
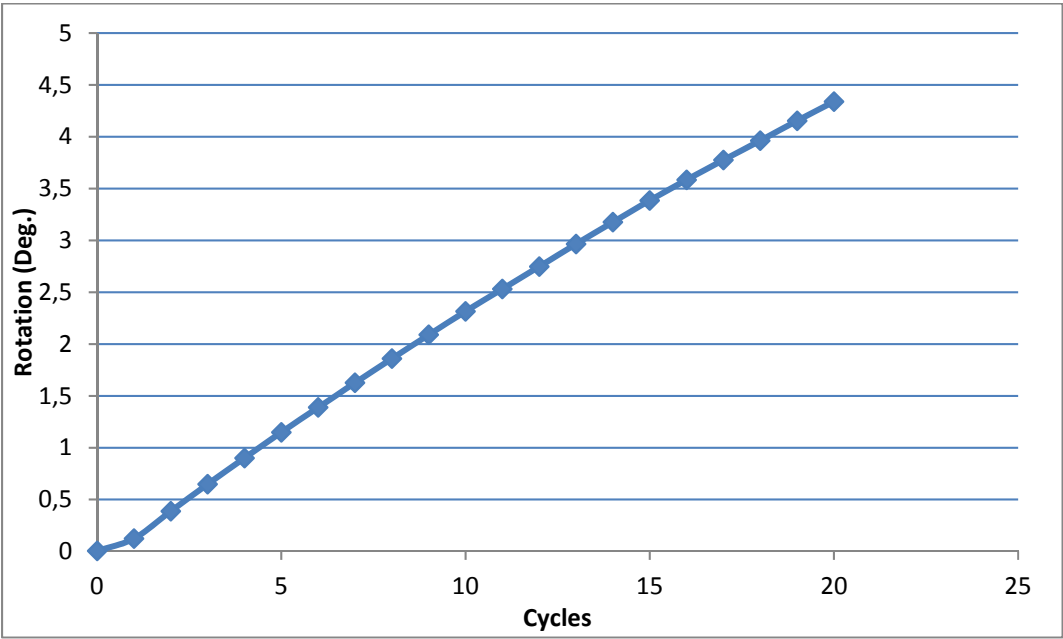
Figure 4-19 Rotation (accumulated) (15 KN and 0.44mm)
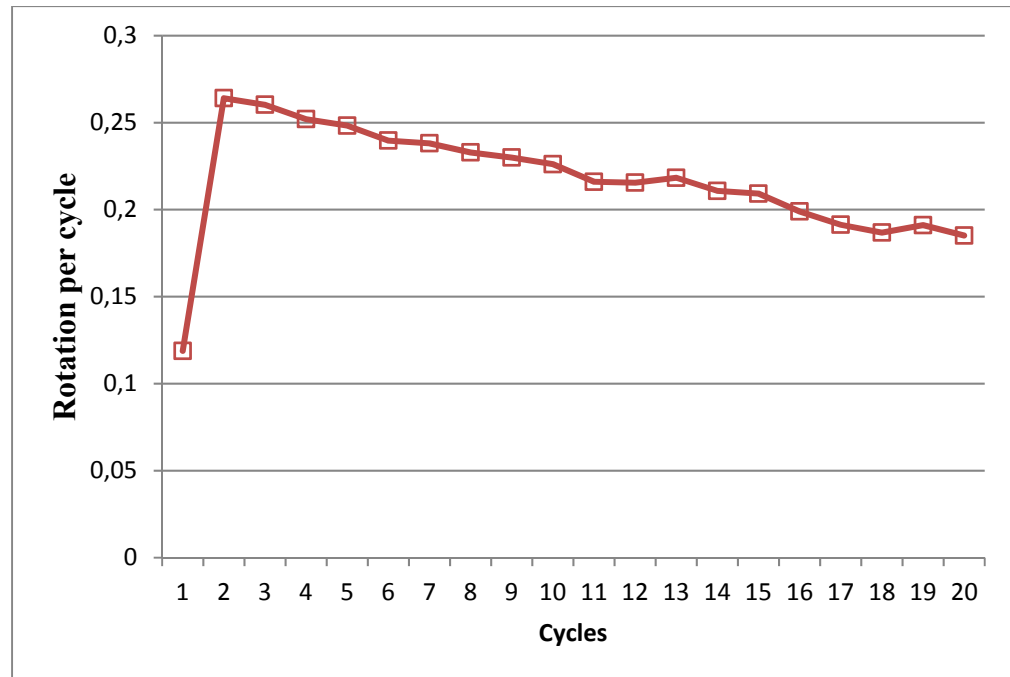
Figure 4-20 Rotation per cycle (15 KN and 0.44mm)
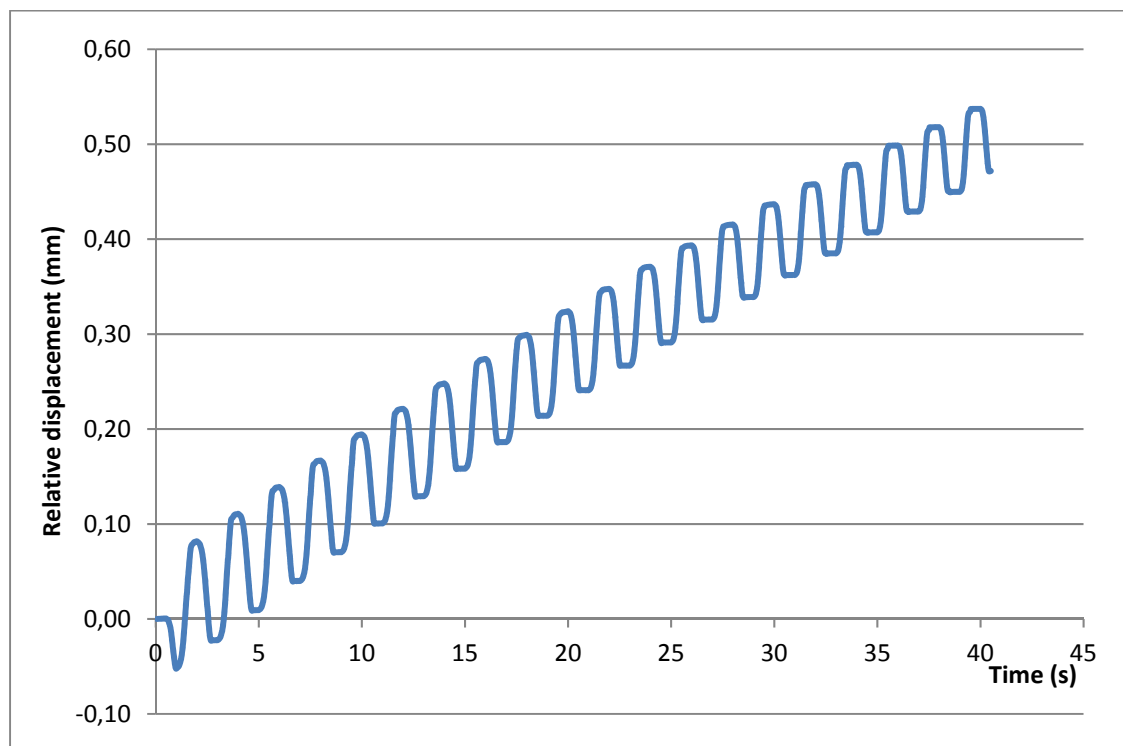
Figure 4-21 Transverse displacement between threads (15 KN and 0.44mm)
in actuation direction

Figure 4-21 shows the transverse displacement of the bolt and nut thread which is used to calculate rotation as per the equation suggested by Zhang et al. Figure 4-22 shows the result of that rotation versus the rotation from the FE analysis, which are in agreement.

Figure 4-23 shows the transverse displacement and rotation in each cycle. The reduction of transverse displacement and rotation from second cycle to the last cycle results in a descending trend. The first cycle has the highest transverse displacement with the lowest rotation. The transverse displacement in the first cycle causes plastic deformation in the threads, which is the major mechanism for load drop in first cycle.
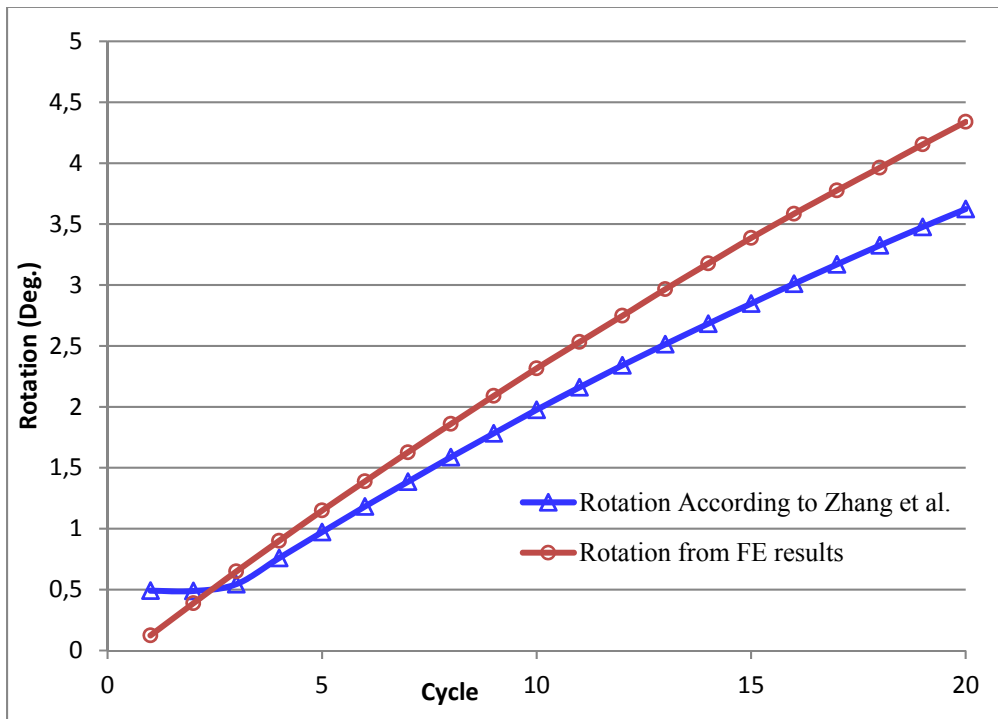
Figure 4-22 FE Rotation vs. rotation proposed by (Zhang et al., 2007)
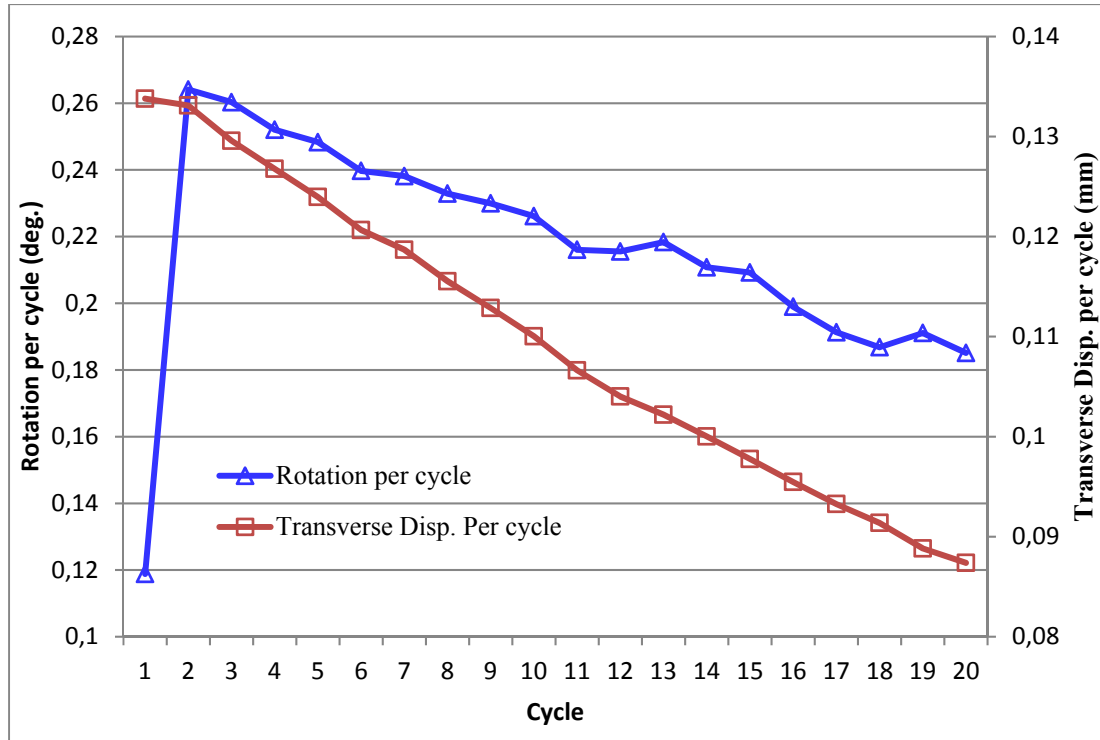
Figure 4-23 Transverse displacement and rotation per cycle

The FE results are verified with theoretical calculations and compared with proposed calculation method by Zhang et al.

For the theoretical evaluation, the rotation from the FE is used to calculate the axial displacement of the bolt and its relevant load drop. The stiffness of the joint is calculated according the following equations:

$$K_b = \frac{A_d A_t E}{A_d l_t + A_t l_d}$$

4-2

Where K_b, A_d, A_t, E, l_t and l_d are bolt stiffness, major-diameter area of the bolt, tensile-stress area, Young's modulus, length of threaded portion of the bolt, and length of unthreaded portion of the bolt, respectively. (Taken from (Budynas & Nisbett, 2008) page 413.)

$$K_m = \frac{0.5774\,\pi\,E\,d}{2\,\ln\left(5\frac{0.5774l+0.5d}{0.5774l+2.5d}\right)}$$

4-3

Where K_m, E, l and d are members stiffness, Young's modulus, grip length, and hole diameter in the plate, respectively. The frustum is considered as a cone with a half-apex angle of 30°. (Taken from (Budynas & Nisbett, 2008) page 415.

$$\frac{1}{K_j} = \frac{1}{K_b} + \frac{1}{K_m}$$

4-4

Where K_j is the joint stiffness.

Then load drop can be obtained as:

$$\text{Preload drop} = K_j \times d_x$$

4-5

$$d_x = \frac{Rotation}{360} \times \text{Bolts pitch}$$

4-6

FE results are compared with theoretical calculations and Zhang's method in Figure 4-24.

The difference between the theoretical results and the FE results can be attributed to the fact that the calculation of stiffness is an approximation given by Budyna and Nisbett 2008. The theory based on a frustum with a 30° angle is used in the theoretical method, which considers the stiffness of the part in the cone area whereas FE considers the parts beyond this area which affects the results considerably. This comparison validates the FE results.

Another finite element analysis is performed with the loading conditions of one of the experimental tests. In this analysis, the preload and the lateral displacement are 8.1 kN and 0.12 mm, respectively. The applied lateral displacement results with a relative displacement of 0.02 mm between the rigid plates is close enough to the previous experimental test conducted with 8.1 kN of preload and 0.025 mm of relative displacement.
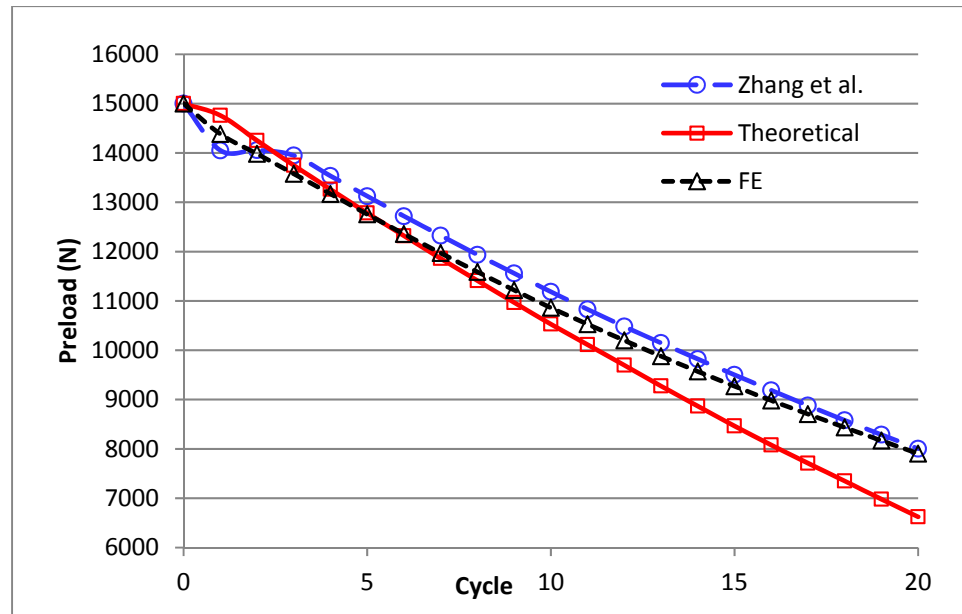
Figure 4-24 Preload drop comparison

As shown in Figure 4-25, the load drop trend is similar in both the experimental and FE results. These curves indicate a good agreement between the finite element analysis and the test rig results. Figure 4-26 compares the lateral force from both methods. In the experimental test, the initial lateral force is rather high compared to other cycles. This is caused by the misalignment of the bolted joint fixation assembly.

Figure 4-27 shows the comparison of the rotation between the FE and experimental tests. An increase in the rotation is very clear in both cases. In the first five cycles the values are close to each other. The difference in further cycles can be explained by the lateral movement of the rotation sensor and bolt end notch; as the bolt gradually loosens during the test. An adjustment of the end notch may be required in order to avoid any loosening.
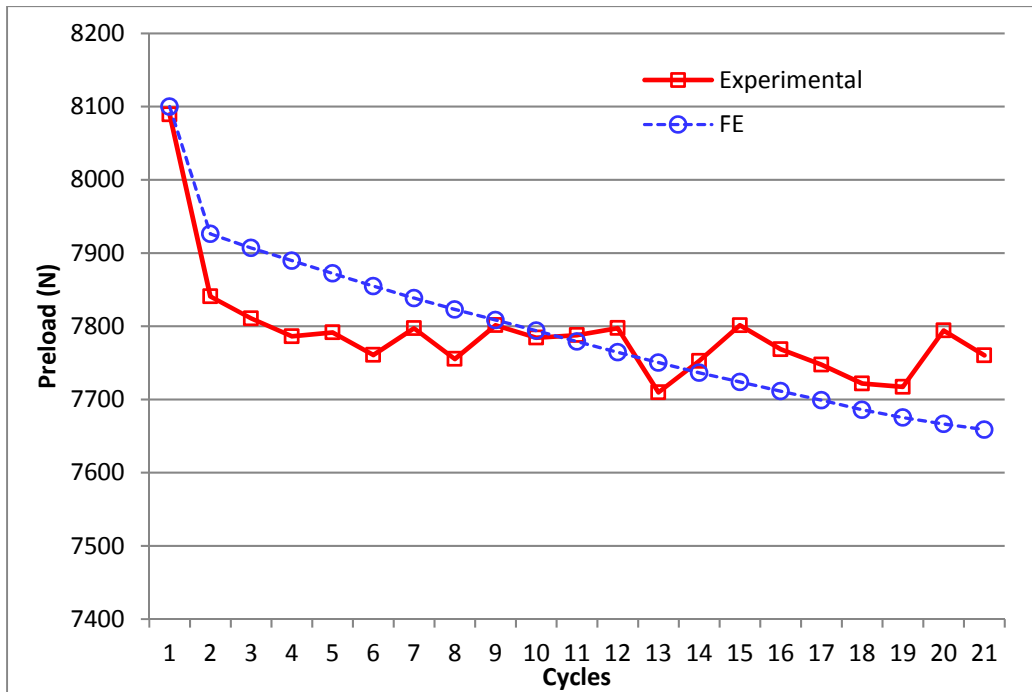
Figure 4-25 Preload drop in 20 cycles (8.1kN and 0.02mm displacement)
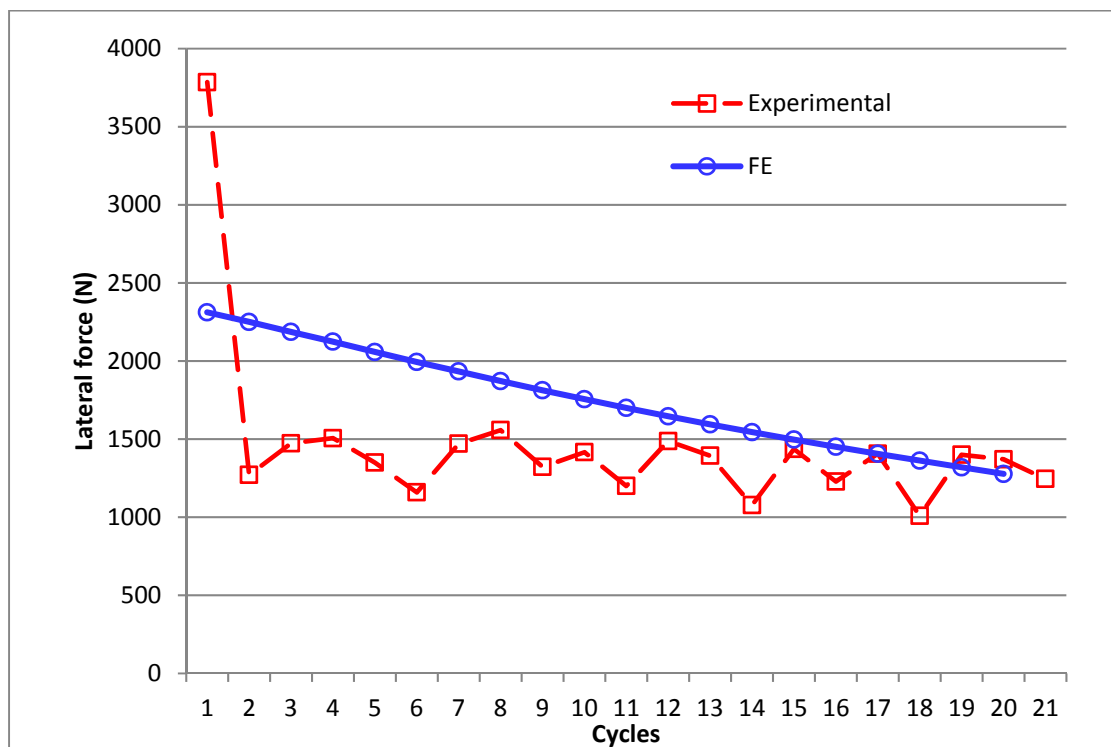
Figure 4-26 Lateral force in 20 cycles (8.1kN and 0.02mm displacement)
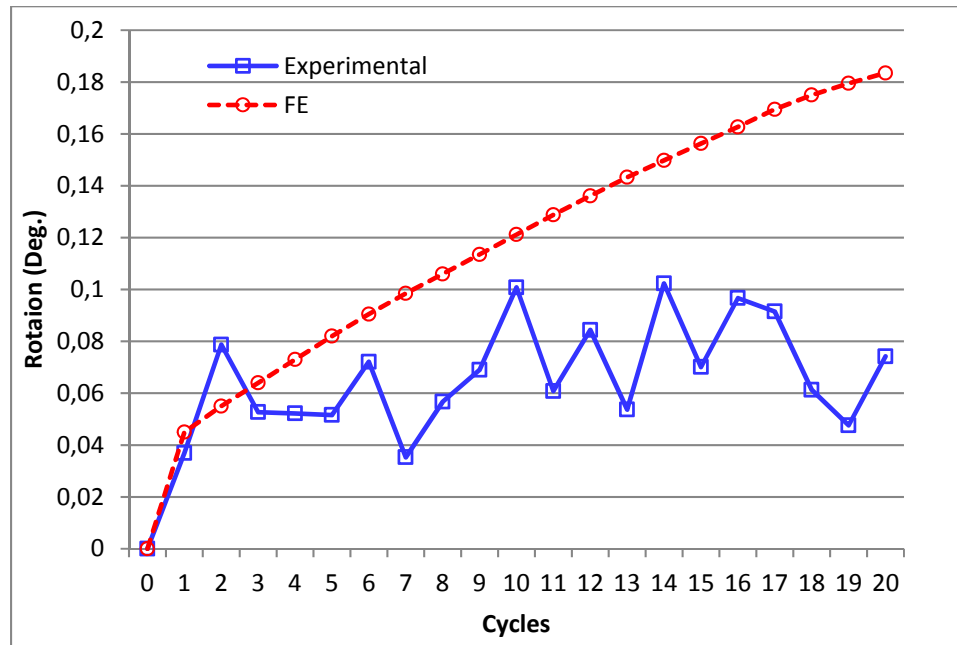
Figure 4-27 Rotation in 20 cycles (8.1kN and 0.02mm displacement)

In general, the FE and experimental results show good agreement. Some adjustments are needed in order to have reliable results. The data acquisition system is not appropriate for this kind of study. Due to the dynamic nature of the problem and the presence of cyclic displacement, the frequency of sampling must be higher in order to pick up all the measurements during a displacement or load cycle. The recorded data is not taken at the same point during the cycle and therefore fluctuations are shown in all recorded data.

In addition, the rig requires some adjustment at the attachments level in order to avoid clearance and loosening. The shake down of the test rig needs to be pursued further for the purpose of consolidating the test results and produce accurate and reliable performance of the test rig.

CONCLUSION

Performance of the test rig

To ensure the integrity of a structure, it is crucial to retain preload in its bolted joints. The first step in doing this requires knowing and quantifying the determinant factors for self-loosening. Experimental tests are widely used to study bolted joints and validate analytical and finite element studies. The basic requirement for any experimental test is a reliable test machine. In the current study, a fatigue test machine is used in conjunction with a bolted joint clamping fixture to study the effects of geometry, material and stiffness on the self-loosening of clamped joints. Test machines used in previous studies are reviewed to find disadvantages of different measurement methods to develop a high-performing test rig.

Inserting a load cell into the bolt joint, which is a very common measurement method, directly affects the stiffness of the joint (see paragraph 2.3). In the current study, the load cell is replaced by a strain gauge inside the bolt, which does not alter the grip length and the stiffness of the joint. A strain gauge is calibrated to directly measure the force. The conclusion related to the success of the test rig to reproduce the results are very promising. Indeed, the preload measured in the load case with 8.1 kN and 0.02 mm displacement shows 6.5% load drop in the experimental test the finite element gives 4.4% which give confidence in the test rig and accuracy of measurement system.

Based on the FEM results, to capture the real relative displacement of the plates, it is important to do the measurement as closer as possible near the bolt location. As presented in chapter 4, measuring lateral displacement at vicinity of bolt location is quite different from measured displacement at the actuator point, as is the case in other studies. In previous experimental studies described in the literature, the displacement of the actuator of the Junker machine is considered to be as the relative displacement that causes self-loosening, which have led to unrealistic results in some cases. This is because the displacement at the actuation point includes the resultant deformations of the connecting parts including the clamping

parts. Therefore, the comparison with the actual industrial applications are not realistic and the self-loosening and its time duration in bolted joints become unpredictable. To overcome this difficulty, the displacement sensor is installed on the test plate adjacent to the bolt hole with a rigid support to measure the actual relative displacement of the clamped plates. The displacement ratio at the actuator to the plate hole location in the first experimental test was found to be 8 which justifies the design system location.

As demonstrated in previous studies, the rotation in stage I is ignored, while stage II shows considerable rotation. This fact is used to indicate the transition point between two stages during the experiment. Hence, to study accurately both stages of self-loosening in bolted joints, it is essential to measure rotation continuously. While most test machines are not equipped with rotation sensor, the proposed test rig measures rotation continuously. In addition, rotation measurement can be linked to the drop of load when stage II takes place.

Bearing in mind that temperature changes joint dimensions and material properties when it is important, its effect on self-loosening of bolted joints could shed some light. Hence, the proposed test rig set-up is equipped with a thermocouple to give an indication on the variation of the room temperature. Nevertheless, the effect of high temperature is not part of the objectives of the short-term research plan.

In order to simulate the real behaviour of a bolted joint, it is essential to model both stages, while most of previous studies simulate the second stage only. This rig offers the possibility to study both stages I and II. The FE simulation led to accurate numerical results which are close to experimental findings as presented in chapter 4.

To study the real behavior of bolted joints, it is important to use 3D model which considers rotation, instead of 2D modelling. A 2D simulation can be used to model stage I of self-loosening which is due to an elasto-plastic deformation of the threads and the local deformation at the asperity level. As presented in chapter 3, the current study uses a full 3D

model with the real 3D bolted joint geometry to simulate the real behavior giving results close to experimental findings.

Contribution

The main contributions of the current study are as the followings:

1- Proposing a new flexible test set-up to be installed on a tensile compression machine to study the self-loosening of bolted joints. This set-up measures rotation, lateral displacement, axial force, lateral force and temperature while capturing the real bolted joint behaviour. This contribution meets the objectives one to four of the current study.

2- Developing a 3D FE model using an elastic-plastic material behavior that simulates the real behaviour of bolted joint. It serves as a mean to validate the overall design and the test rig ability to experimentally reproduce the self-loosening mechanism. This model can be used in future studies to investigate parameters that cannot be measured experimentally such as contact pressure, stresses and deformations at critical locations. This contribution meets the last objective of the current study.

FUTURE STUDIES

Test rig improvement

The performance of few instruments is questionable. The calibration of few instruments is conducted with elementary means and proper calibration tools are needed. The rotation sensor is calibrated with an angle indicator A more precise calibration device is needed. In addition, the rotation sensor fixation can be improved by finding a solution that will eliminate or account for the relative lateral displacement of the nut and the bolt which causes self-loosening. The reducing of the variation in the captured rotation during each cycle would increase the accuracy of the system.

Frequency of the test in the first and second cycles is lower than the rest. Coefficient of static friction is higher than kinematic, so bigger force is required to start the cyclic motion. The test rig motor is not powerful enough to overcome start-up inertia and static friction. Using a motor with higher starting torque would be an excellent improvement to do to the current rig.

Preload should be measured at the start of the test however its variation and the cyclic lateral force should be recorded at all time and in particular when the displacement is at its maximum. The current control program requires higher sampling frequency to pick up the maximum and the minimum values of the measured cyclic parameters. The Labview vi could be modified to take more data points during each cycle to solve this problem.

A circular oven around the test plates could be added to the test rig to study the effect of temperature on the self-loosening of bolted joint. A temperature sensor is already installed and is connected to the data acquisition system, although the temperature of the joint due to friction generated by the speed of transverse load or displacement cycling cannot be controlled. However, a temperature PID controller would be required. Studying the effect of temperature is very important for high temperature applications, especially in power and oil and gas industries where many clamped plates and bolted joints are exposed to self-loosening

at high temperature. Quantifying the effects of initial load, materials, joint stiffness, temperature and creep are few research challenges that could be the subject of future studies to be conducted with the designed rig.

FE model to study self-loosening

The developed finite element model is validated and can be used to study the effects of different parameters on the self-loosening of bolted joints. The stiffness of the joint, initial load, lateral displacement and force, temperature, friction, materials and threads geometry and clearance are to name a few. Performing FE analysis with different geometry, materials and loading conditions can be done quite easily. The effects of stiffness and grip length along with other parameters could show interesting results. Experimental tests with a possible variation of certain of the above-mentioned parameters conducted on the present designed test rig can be performed to validate some aspects of FE modeling.

APPENDIX I

Strain gage catalog, KYOWA

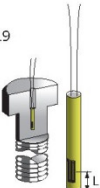## Strain Gages for Measuring Axial Tension of Bolts

Patterns Gage Resistance, Gage Factors	Models	Dimensions (mm)				Remarks
		Grid		Base		
		Length	Width	Length	Width	

●KFG Series Foil Strain Gages for Measuring Axial Tension of Bolts

Uniaxial
Resistance: 120 Ω
Gage factor: Approx. 1.9

If it is difficult to bond a strain gage to the surface of a bolt for measuring the tightening stress, these gages enable the measurement by embedding into a hole, 2 mm diameter, bored from the top head of the bolt. They are applicable to materials having a linear expansion coefficient of 11μm/m per °C.

ϕ0.14 Polyester-coated copper cable 5 mm long

Applicable Adhesives and Operating Temperature Range after Curing

Adhesives	Operating Temp. after Gluing the Gages
EP-180	Normal Temp. to 50°C

5 gages/pkg

Options Dedicated gage terminal

Model	Dimensions	Base material	Conductor material	Remarks
T-F29	Outer: ϕ6 Inner: ϕ2.5	Glass epoxy	Copper foil	For bolt gages

T-F29

Length from the tip of base to the center of grid

L
KFG-3: 2.7 mm
KFG-1.5: 1.75 mm

KFG-3-120-C20-11	3	app. 6	11.5	ϕ1.9	Bore diameter 2
KFG-1.5-120-C20-11	1.5	app. 6	5	ϕ1.9	Bore diameter 2

General-purpose Foil Strain Gages KFGT

Patterns Gage Resistance, Gage Factors	Models	Dimensions (mm)				Remarks
		Grid		Base		
		Length	Width	Length	Width	

●KFGT Series Foil Strain Gages with a Temperature Sensor

Uniaxial 3-wire system
Polyester-coated copper lead wire
1 m long each
Resistance: 120 Ω
Gage factor: Approx. 2.1
Temperature sensor: T-type thermocouple
Accuracy: Within 1.5 °C

The KFGT gages are foil strain gages incorporating a T-type thermocouple for simultaneous measurement of strain and temperature. They ensure not only efficient strain measurement under environments where temperature change or temperature gradient requires simultaneous measurement of strain and temperature but also highly precise compensation of thermally-induced apparent strain. It is recommended to use Kyowa data logger UCAM-60B as a mating instrument.

Applicable Adhesives and Operating Temperature Range after Curing

Adhesives	Operating temp. after Gluing the Gages
CC-33A	−10 to 120°C
CC-36	−10 to 100°C
CC-35	−10 to 120°C
EP-340	−10 to 120°C

KFGT-5-120-C1-11 N1M3	5	2.1	10	4.5	Standard accessories: lead-wire stopper to prevent the gage from damaging
KFGT-5-120-C1-16 N1M3					
KFGT-5-120-C1-23 N1M3					
KFGT-5-120-C1-27 N1M3					Pre attached lead wire 1-m long
KFGT-2-120-C1-11 N1M3	2	1.8	7	4.5	Extension lead wires are optionally available.
KFGT-2-120-C1-16 N1M3					
KFGT-2-120-C1-23 N1M3					5 gages/ pkg.
KFGT-2-120-C1-27 N1M3					

Gage lead 1 connected
Lead stopper
T-type thermocouple Cu ⊕(Brown)
T-type thermocouple CuNi ⊖(Gold)
Gage lead 2' (Green)
Gage lead 2 (Green)
Gage lead 1 (Red)
Sensing point of T-type thermocouple
Gage leads 2 and 2' connected
Soldered

*Figure is KFGT-5-120-C1-11 N1M3

Options Extension Lead-wire Cables

Models	Dimensions (mm)			Remarks
	Length	Width	Thickness	
NT-1M	1000			With gage terminal T-F25
NT-2M	2000	7.2	1.2	
NT-4M	4000			

5 gages/pkg

STRAIN GAGE FOR STRESS MEASUREMENT ON TIGHTENED BOLTS

OPERATION MANUAL

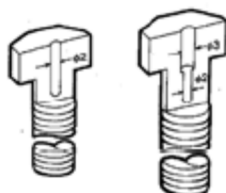### 1. Necessary tools and expendables
- Adhesive ... EP-18 or EP-34
- Balance .... 100 to 200g capacity
- Solvent ..... Acetone • Solvent container • Toothpick

2. Boring a hole in the bolt
Bore a ϕ2.0 hole in the bolt subjected to measurement. If the bolt is large in diameter, it requires a deep hole. In this case, bore a hole in two (ϕ3 and ϕ2) stages to facilitate adhesive pouring.

3. Cleaning and drying the hole
(1) Insert the accessory tube into the bolt hole, and squeeze it about 20 times in the solvent so that fats and metal powders are moved from the hole.
(2) Remove the solvent from the hole by shaking the bolt. Then sufficiently dry the hole. Dry it for over 1 hour at a room temperature or for over 30 minutes at 50 to 70°C.

4.
Fix the bolt upright by using a cardboard box or other, on the top of which a hole is provied to hold the bolt top.

5. Pouring of the adhesive and insertion of the strain gage into the hole
(1) Compound the adhesive (referring to the operation manual of the adhesive).
Once compounded, the viscosity of the adhesive comes to grow in next 15 minutes or so. Therefore, quickly proceed and finish insertion of the gage. If the adhesive's viscosity is high, it will not smoothly go into the bolt hole. If so, compound the adhesive anew.

(2) Take the adhesive on the top of the accessory tube. Insert the tube into the bolt hole, then push and pull the tube about 10 times so that the adhesive spreads over the wall surface of the hole.
Next, take a small amount of the adhesive with a toothpick. Insert the toothpick into the hole. At this time, tilt the bolt slightly. Fill the hole with the adhesive which flows down the hole wall, taking care to avoid air bubbles.
(Once formed, an air bubble checks flowing of the adhesive. If it occurs, remove the bubble using a toothpick.)
All this work decides the quality of subsequent gage installation.
(3) Form a thin coat of the adhesive over the outside of the gage. Gradually insert the gage into the bolt hole which has been filled with the adhesive.
(One time of compounding of the adhesive allows to handle 3 to 5 bolts. A skilled operator can handle about 10 bolts.)

6. Hardening of the adhesive
Keep the bolt upright during hardening of the adhesive. A required hardening time is:
24 hours or more at a room temperature, or
3 hours at 50 to 60°C (and subsequent 1 hour or more at a room temperature)

7. Connection of the leadwires
Solder the L-6 or L-7 vinyl leadwires to the gage-leads. If the strength of the gage-leads is insufficient, cement the exclusive gage terminal to the bolt head, then connect the leadwires to the terminal. In this case, a release agent is necessary, which is to be used to peel off the coat from the gage-leads (polyester-coated copper wires).

8. Calibration of a tensile load
Perform load calibration to evalue the adhesion of the gage. (Accuracy is rated at about 0.5 to 1%R0.)
(Inferior adhesion results in an extremely low output or large creep.)

LIST OF BIBLIOGRAPHICAL REFERENCES

ASME. (1981). *B18.22M Metric Plain Washer*. New York: ASME.

ASME. (1989a). *B18.2.3.5M Metric Hex Bolts* New York: ASME.

ASME. (1989b). *B18.2.4.1M Metric Hex Nuts* New York: ASME.

ASME. (2001). *B1.13M Metric Screw Threads* New York: ASME.

Bickford, J. H. (2008). *Introduction to the Design and Behavior of Bolted Joints* (4 éd.). Boca Raton: CRC Press.

Budynas, R. G., & Nisbett, J. K. (2008). *Shigley's mechanical engineering design* (Vol. 9). McGraw-Hill New York.

Eccles, W., Sherrington, I., & Arnell, R. D. (2010). Towards an understanding of the loosening characteristics of prevailing torque nuts. *Proceedings of the Institution of Mechanical Engineers, Part C: Journal of Mechanical Engineering Science, 224*(2), 483-495.

Jiang, Y., Zhang, M., & Lee, C.-H. (2003). A study of early stage self-loosening of bolted joints. *Journal of Mechanical Design, 125*(3), 518-526.

Jiang, Y., Zhang, M., & Lee, C.-H. (2006). An experimental investigation of the effects of clamped length and loading direction on self-loosening of bolted joints. *Journal of pressure vessel technology, 128*(3), 388-393.

Junker, G. H. (1969). *New Criteria for Self-Loosening of Fasteners Under Vibration*. doi: 10.4271/690055. Repéré à http://dx.doi.org/10.4271/690055

MIDORI_PRECISIONS. (2009). CP-2UN/CP-2UTN Repéré à http://www.midori.co.jp/cp-2un-e.html

Nassar, S. A., & Housari, B. A. (2007). Study of the effect of hole clearance and thread fit on the self-loosening of threaded fasteners. *Journal of Mechanical Design, 129*(6), 586-594.

OSHA. (2013). Hydrogen Sulfide. Repéré à https://www.osha.gov/SLTC/hydrogensulfide/hazards.html

Sawa, T., Ishimura, M., & Karami, A. (2010). A Bolt-nut Loosening Mechanism in Bolted Connections under Repeated Transverse Loadings (Effect of inclined bearing surfaces

on the loosening). Dans *ASME 2010 Pressure Vessels and Piping Division/K-PVP Conference* (pp. 397-403). American Society of Mechanical Engineers.

Sawa, T., Ishimura, M., & Nagao, T. (2012). A Loosening Mechanism of Bolted Joints under Repeated Transverse Displacements. Dans *ASME 2012 Pressure Vessels and Piping Conference* (pp. 333-341). American Society of Mechanical Engineers.

Shih, T. (2015, May/June). Global Automative Fastener Import & Export Statistics & Trend Analysis. *Fastener World, 152*, 182-192.

Systems Integrators LLC. (2011). LFE 150 Owner's Manual (pp. 23). 23630 N 35th Drive, Suite one
Glendale, AZ 85310: Systems Integrators LLC.

TE_Connectivity_Corporation. (2017). LVDT Tutorial. Repéré à http://www.te.com/usa-en/industries/sensor-solutions/insights/lvdt-tutorial.html

Yang, X., Nassar, S., & Wu, Z. (2010). Formulation of a Criterion for Preventing Self-Loosening of Threaded Fasteners Due to Cyclic Transverse Loading. Dans *ASME 2010 Pressure Vessels and Piping Division/K-PVP Conference* (pp. 415-425). American Society of Mechanical Engineers.

Yang, X., & Nassar, S. A. (2011a). Effect of Non-Parallel Wedged Surface Contact on Loosening Performance of Preloaded Bolts Under Transverse Excitation. Dans *ASME 2011 Pressure Vessels and Piping Conference* (pp. 405-415). American Society of Mechanical Engineers.

Yang, X., & Nassar, S. A. (2011b). Effect of thread profile angle and geometry clearance on the loosening performance of a preloaded bolt-nut system under harmonic transverse excitation. Dans *ASME 2011 Pressure Vessels and Piping Conference* (pp. 393-404). American Society of Mechanical Engineers.

Yang, X., & Nassar, S. A. (2012). Deformation and Slippage Modeling for Investigating Bolt Loosening Under Harmonic Transverse Excitation. Dans *ASME 2012 Pressure Vessels and Piping Conference* (pp. 321-332). American Society of Mechanical Engineers.

Zaki, A., Nassar, S., & Yang, X. (2010). Vibration Loosening Model for Preloaded Countersunk-Head Bolts. Dans *ASME 2010 Pressure Vessels and Piping Division/K-PVP Conference* (pp. 361-371). American Society of Mechanical Engineers.

Zaki, A. M., Nassar, S. A., & Yang, X. (2011). Criterion for Preventing Self-Loosening of Preloaded Countersunk Head Threaded Fasteners. Dans *ASME 2011 Pressure Vessels and Piping Conference* (pp. 369-380). American Society of Mechanical Engineers.

Zaki, A. M., Nassar, S. A., & Yang, X. (2012). Effect of conical angle and thread pitch on the self-loosening performance of preloaded countersunk-head bolts. *Journal of pressure vessel technology, 134*(2), 021210.

Zhang, M., Jiang, Y., & Lee, C.-H. (2007). Finite element modeling of self-loosening of bolted joints. *Journal of Mechanical Design, 129*(2), 218-226.

Ansys Inc. (2015), Ansys Academic Research Mechanical (Version 15) [Computer software]. Canonsburg, Pennsylvania: Ansys Inc.